2005

Continuous-time block-oriented nonlinear modeling with complex input noise structure

Dongmei Zhai
Iowa State University

Continuous-time block-oriented nonlinear modeling with complex input noise structure

by

Dongmei Zhai

A dissertation submitted to the graduate faculty

in partial fulfillment of the requirements for the degree of

DOCTOR OF PHILOSOPHY

Co-majors: Statistics; Chemical Engineering

Program of Study Committee:
Huaiqing Wu, Co-major Professor
Derrick K. Rollins, Co-major Professor
Max Morris
Ramon Gonzalez
Gerald M. Colver

Iowa State University

Ames, Iowa

2005

Graduate College
Iowa State University

This is to certify that the doctoral dissertation of

Dongmei Zhai

has met the dissertation requirements of Iowa State University

Signature was redacted for privacy.

Co-major Professor

Signature was redacted for privacy.

Co-major Professor

Signature was redacted for privacy.

For the Co-major Program

Signature was redacted for privacy.

For the Co-major Program

Table of Contents

List of Figures

List of Tables

Abstract

The continuous-time closed-form algorithms to sinusoidal input changes are proposed and presented for single-input, single-output (SISO) Hammerstein and Wiener systems with the first-order, second-order, and second-order plus lead dynamics. By simulation on theoretical Hammerstein and Wiener systems, the predicted responses agree exactly with the true process values. They depend on only the most recent input change. The algorithms to SISO Hammerstein and Wiener systems can be conveniently extended to the multiple-input, multiple-output (MIMO) systems as shown by the two-input, two-output examples and demonstrated by the simulated seven-input, five-output continuous stirred tank reactor (CSTR). The predictions and the simulated theoretical responses agree exactly and the predicted multiple CSTR outputs are close to the true process outputs. The proposed algorithms can predict the responses closer to the true values when comparing with the piece-wise step input approximation of the sinusoidal input changes on a simulated MIMO CSTR. In addition, as the noisy process input could be decomposed as summation of sinusoidal signals imposed on a step input change; the proposed algorithms can be employed to predict outputs for the noisy process inputs once the decomposition is done and the predicted noisy process outputs are shown to be close to the true ones, and are much better than the predictions based on the perfect filtering of the input signals.

The estimating equations based on the moment method are proposed for the Wiener dynamic process with stochastically correlated process input disturbances or noises and they work well for the parameter estimation. No one has ever proposed such method before. This approach has led to stable and robust estimators that have reasonable estimation errors and there is no need to measure the input disturbances or noises, or to calculate the time derivative of the observed output variable. Only the original process output observations over time are needed. The original model can be shifted to an approximate model under some conditions. This approximation is acceptable based on some analysis and derivation. The estimating equation methodology was shown to work well for the approximate model, while other existing methods do not work at all.

Chapter 1. Introduction and Literature Review

1.1 General background and organization

In industry, it is desired to have safe operation of processes with chemical processes, such as chemical reactors, distillation columns, or heat exchangers, while meeting specified production rates and product quality. Process control is the key to achieving these objectives for chemical processes, which by nature are usually dynamic and nonlinear. A process control system is in charge of monitoring the process output, and implementing input changes based on the current conditions (Ogunnaike and Ray, 1994). In order to set up an effective control scheme, we first need to understand the behavior of the process. A process model is a good way to describe the real process. The model allows us to carry out an efficient process analysis and to predict how the process responds for certain type of input change. This is crucial in model-based control, especially in model predictive control.

Model predictive control (MPC) is a class of computer control schemes that utilize a dynamic model and available measurements to explicitly calculate and predict the future outputs and also control these output responses as close as possible to the desired responses (Ogunnaike and Ray, 1994). In the late 1970s, MPC schemes began to be applied to chemical engineering processes, including distillation columns and batch processes. Earliest MPC applications were in oil and paper industries. For a nonlinear multi-variable process with constraints and complicated dynamics, MPC would have more advantages, though it can be challenging to get an accurate predictive model for the process. Process output prediction by using some appropriate model is one of the four basic elements of MPC schemes. It is obvious that having an appropriate model is critical in MPC.

Many predictive control schemes have been proposed based on the direct use of nonlinear models. Although a lot of efforts have been put on nonlinear MPC and many papers have

been published, the nonlinear MPC is basically still an academic concept rather than a practical control strategy (Lee, 2000). Nonlinear model development, state estimation, and rapid, reliable solution of the control algorithm were said to be the three most significant difficulties in nonlinear MPC applications.

This research concentrates on continuous-time modeling and prediction of nonlinear dynamic systems. Two important block-oriented models, the Hammerstein and Wiener models, which can approximate the nonlinear dynamic systems efficiently, are chosen particularly. The continuous-time prediction algorithms for these two models with different dynamic characteristics under sinusoidal input sequences are derived and proved to be able to predict the process responses exactly for theoretical Hammerstein and Wiener systems. These algorithms do not depend on all past input changes, but only the most recent input change. This makes the prediction feasible. These algorithms are then extended to multiple-input, multiple-output (MIMO) systems and applied on a simulated MIMO continuous stirred tank reactor (CSTR), which has been identified as a nonlinear Wiener system. The proposed continuous-time algorithm for sinusoidal input sequences is compared with the piece-wise step input approximation. Also, noting that the noisy process input can be decomposed as summation of sinusoidal sequences, the proposed algorithms can be employed to predict the outputs for noisy input signals. These algorithms are critical when designing the nonlinear model predictive controller. The dynamics investigated in this work includes the first order, the second order and the second order plus lead (single zero, two poles) dynamics, the three typical candidates for the process dynamics. These dynamic models and their corresponding models with time delay can approximate the dynamics of most real systems adequately.

Noting that the error term has to be treated as stochastically continuous in time when the continuous-time method is used, this work then considers the parameter estimation of the continuous-time block-oriented Wiener system with stochastic input errors, where the

stochastic differential equation plays a critical role. Two different models, the original one and the approximate one, are considered. The corresponding estimating equations are established for each model to estimate the dynamic parameter of the system and covariance structure parameters of the input errors. Simulations are carried out to test the proposed estimating equations and some suggestions are made for the estimation procedures. Comparisons with the methods proposed by other researchers are also done based on the second approach with the approximate model.

This dissertation first reviewed the literatures on block-oriented models, particularly the Hammerstein and Wiener models, including their application and parameter identification in nonlinear systems modeling. The progress of the continuous-time approach made by Dr. Rollins' group is then reviewed in details. The Hammerstein and the Wiener Block-oriented Exact Solution Techniques (H-BEST and W-BEST) are introduced, as well as the continuous-time classical, restricted and unrestricted algorithms for the step input change sequences. Some considerations of the statistical experimental design when implementing the BEST technique are also summarized. Then, in Chapters 2 and 3, the closed-form compact algorithms are developed and simulation studies are carried out for the single-input, single-output (SISO) Hammerstein and Wiener systems with first order, second order dynamics, and second order plus lead dynamics when they are forced by sinusoidal input changes. These algorithms are verified by simulation on theoretical Hammerstein and Wiener systems, and they can be extended to MIMO systems as demonstrated in Chapter 2 on two-input, two-output theoretical systems. Application of the proposed algorithms to a simulated CSTR in Chapter 3 further illustrates the ability of the algorithms. Chapter 4 and 5 presents the parameter estimation of the Wiener system with the stochastic input errors by using estimating equations, but with two different modeling approaches. Chapter 6 gives the

general conclusions of this work and presents future works. The mathematical derivations of the closed-form compact algorithms provided in Chapters 2 and 3 are given in the Appendix.

1.2 The nonlinear system and model building

Most physical processes in reality behave nonlinearly to some extent. Examples of such processes are: higher-order reaction, distillation, pH neutralization, heat exchange, and incomplete mixing. Since many processes exhibit only mildly nonlinear dynamic behavior, linear models, which are simple and convenient, can be employed to approximate them reasonably. Also with effective regulatory control, deviations from steady state will be small. Thus it is often reasonable to treat such systems as approximately linear. However, this is not adequate for systems that have strong nonlinear behavior or that deviate significantly from normal operating conditions. For these systems, nonlinear models, which can incorporate the complex dynamics, nonlinearity and interactions, should be adopted though they are less simple. During the past decade, more and more researchers have been working on developing nonlinear models instead of approximate linear models. This is motivated by the need for improving the product quality and reducing the energy and material consumption.

As the heart of MPC, a proper model is needed to ensure accurate prediction. The model should match the requirements of control — harmonious in structure and complexity, and approximate the true process closely. It can be challenging to determine the model for a process, especially a nonlinear process. Basically, there are two approaches to build the model. The first approach is to set up physical models for each operation unit based on some simplified assumptions. The first-principles, including the fundamental laws of mass, energy, momentum, and the dynamic behavior of the system etc. have to be well known. And a combination of these models gives an overall model that describes the whole process.

This model might not be able to represent the process well due to limited knowledge of the physical systems. Furthermore, such a model often employs many differential and algebraic equations, which complicate the model and limit its usefulness in control.

The second approach, which is called system identification, is to build an empirical model from the input and output data gathered from experiments on the process. The principles or internal mechanism in the process can be unknown. The process is treated as a "black box." After selecting a model structure, the model parameters are estimated based on the input and output data. The model obtained needs to be checked to ensure its validity. This requires extensive measurements of process behavior though no detailed process knowledge is required. Such approaches as Nonlinear Auto-Regressive Moving Average with eXogeneous inputs (NARMAX) (Holcomb et al., 1995), Artificial Neural Network (ANN) (Normandin et al., 1994), and Volterra series (Pearson, et al., 1996) belong to the class of empirical modeling. They usually have no physical meaning related to the real processes, and are all discrete-time models.

Rollins et al. (1998) proposed a semi-empirical modeling technique lying between the extremes of theoretical and empirical modeling, which was originally called "SET." It can be considered as "gray-box" modeling. The input/output data are used to determine the parameters in the model that is phenomenologically based. These parameters have some physical meaning. The advantages of SET were demonstrated on a simulated highly nonlinear single-input, single-output (SISO) CSTR. The development of a SET model needed only few input changes with outputs measured off-line. SET does not require the on-line output data and can handle mild extrapolation beyond the conditions used in fitting the model. SET also worked well for cases with large time delay and substantial noise. Later, this algorithm was enhanced and the model was identified as a Hammerstein model (Rollins et al., 2003). The Wiener model, which is highly related to the Hammerstein model, was also

investigated (Bhandari and Rollins, 2003). These block-oriented modeling methodologies belong to the semi-empirical approach.

1.3 Block-oriented nonlinear model structures

The block-oriented models are series or parallel combinations of linear dynamics blocks and static nonlinear mappings. The block-oriented models and the structure identification for nonlinear dynamic systems based on input/output data were reviewed by Billings (1980) and Haber and Unbehauen (1990) in details. Later, Chen (1995) gave a review on modeling and identification of parallel nonlinear systems of the block-structured network models. Here, some basic types of block-oriented model structures that could be used for the nonlinear dynamic processes are introduced.

1.3.1 The Hammerstein model

Narendra and Gallman (1966) were the researchers who dealt with the Hammerstein model at early time. A Hammerstein system consists of a static nonlinear mapping or gain followed by a linear dynamic block, as shown in Figure 1.1, where $\boldsymbol{u(t)}$ is the input vector, $\boldsymbol{v(t)}$ is intermediate vector, which is usually not measurable, and $\boldsymbol{y(t)}$ is the output vector. $\boldsymbol{f(u(t))}$ is the nonlinear static gain functions and $\boldsymbol{g(t)}$ is the block transform function for the linear dynamics. Note that, $\boldsymbol{v(t)} = \boldsymbol{f(u(t))}$ and each element of $\boldsymbol{y(t)}$ can be obtained by employing $y_i(t) = \int_0^t v_i(\xi) \cdot g_i(t-\xi) \cdot \mathrm{d}\xi$.

The Hammerstein model has a simple structure with relatively few parameters, and is one of the simplest and most popular block-oriented nonlinear models. It has been shown to represent many processes with nonlinear characteristics well. Much work has been done to investigate the applications of this model. Many chemical processes, such as distillation column (Eskinat et al., 1991), polymerization process (Su and McAvoy, 1993), and pH

neutralization process (Zhu and Seborg, 1994), and bioreactors (Jyothi and Chidambaram, 2000, 2001), have been modeled as a Hammerstein system efficiently. The Hammerstein model is also popular for modeling biological phenomena, such as lung mechanics and electrically stimulated muscle. The big advantages of the Hammerstein model include its simple structure and its efficient parameterization. However, almost all of the work involves use of discrete-time models (Eskinat et al., 1991; Su and McAvoy, 1993; Zhu and Seborg, 1994; Doyle et al., 2002; etc.) except for Greblicki (2000) and Rollins et al. (2003), who employed a continuous-time approach. The method proposed by Greblicki (2000) was nonparametric and the dynamic block was identified using impulse responses methods. The approach of Rollins et al., which is parametric, will be introduced in details in Section 1.4.

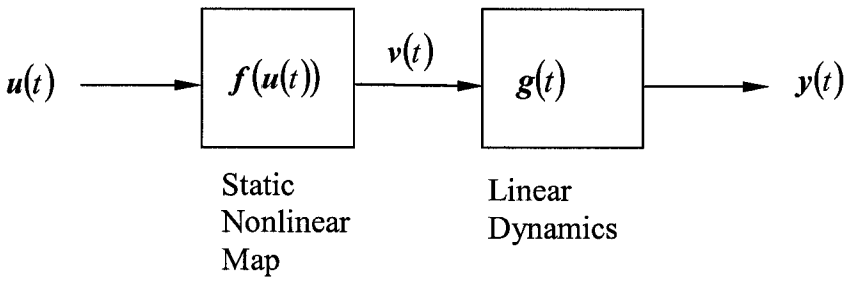

Figure 1.1. A general Hammerstein model structure. Here, $u(t)$, $v(t)$ and $y(t)$ are all vectors, and $f(u(t))$ and $g(t)$ could be several different nonlinear mappings and linear dynamic relations respectively.

Either parametric or nonparametric method can be applied to identify the two subsystems of the Hammerstein model, the static nonlinearity and the linear dynamics. Typically, the static nonlinear part is approximated by a polynomial function, and the linear dynamics is fitted by methods such as ARMAX model (Eskinat et al., 1991), neural network dynamic model (Su and McAvoy, 1993), and continuous model (Rollins et al., 2003). A polynomial is chosen to approximate the static nonlinear part because "it is simple and satisfies the condition for control by means of its roots" (Norquay et al., 1999a). However, this is not

always a good choice, especially when the process is highly nonlinear. Eskinat et al. (1991) concluded that a low-order (e.g. $n \leq 4$) polynomial was not adequate for a high-purity distillation column process when modeled by a Hammerstein model. This is partially because polynomials cannot present the saturated behavior of the ultimate limits of product purity. Norquay et al. (1999a) suggested a piecewise polynomial approximation such as cubic splines.

Pearson and Ogunnaike (1997) pointed out that using nonparametric estimation for the nonlinearity could make it possible to see whether the Hammerstein model is adequate for a high-purity distillation column process, which is one advantage of nonparametric approaches.

Several other identification methods for the Hammerstein model have been proposed (Al-Duwaish and Karim, 1997; Bai, 1998; Zhu, 1999; etc.). More recently, Jyothi and Chidambaram (2000, 2001) used the Hammerstein model to represent bioreactors with multiple inputs and incorporated it in feed forward control after identifying the model. Pearson and Pottmann (2000a, 2000b) gave a gray-box identification approach to three classes of block-oriented models, including the Hammerstein, Wiener and feedback block-oriented models and then they used a distillation column as an example to illustrate their approach. Various identification methods proposed for Hammerstein model with nonlinear biological systems were reviewed by Hunter and Korenberg (1985).

1.3.2 The Wiener model

The Wiener model has the same two elements as the Hammerstein model, but in the reverse order. As shown in Figure 1.2, in the Wiener model structure, the input vector $\boldsymbol{u}(t)$ goes through the linear dynamics block to get the intermediate vector $\boldsymbol{v}(t)$, and then $\boldsymbol{v}(t)$ is transformed by the static nonlinear functions $\boldsymbol{f}(\boldsymbol{v}(t))$ to get the output vector $\boldsymbol{y}(t)$. Again, $\boldsymbol{v}(t)$ is not observable. Mathematically, each element of $\boldsymbol{v}(t)$ is $v_i(t) = \int_0^t u_i(\xi) \cdot g_i(t-\xi) \cdot d\xi$ and

the output $y(t) = f(v(t))$.

Wiener models, though simple, can be employed to model some nonlinear chemical processes, such as pH neutralization and high purity distillation. It seems that almost all the papers (Greblicki, 1992, 1997; Wigren, 1993; Kalafatis et al., 1995; Huang et al., 1998; etc.) about the Wiener model use a discrete-time approach except for Greblicki (1999) and Bhandari and Rollins (2003). Greblicki (1999) used the nonparametric kernel regression method to estimate the nonlinear part and a correlation method to estimate the impulse response of the linear dynamics. These methods are quite different from that proposed by Bhandari and Rollins (2003), which is parametric and will be introduced later in Section 1.4.

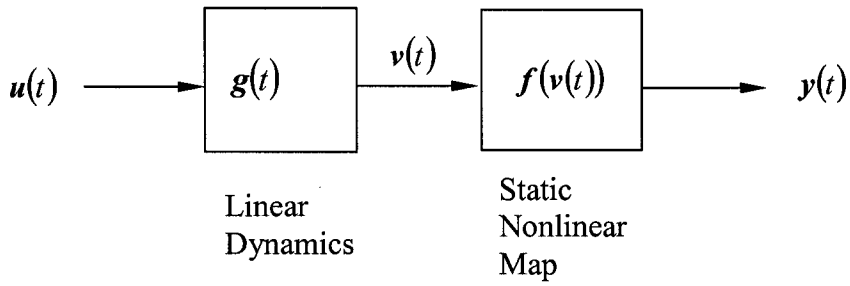

Figure 1.2. A general Wiener model structure. Here, $u(t)$, $v(t)$ and $y(t)$ are all vectors, and $g(t)$ and $f(v(t))$ could be several different linear dynamic relations and nonlinear mappings respectively.

The discrete-time approaches have been widely investigated. Kalafatis et al. (1995) used a frequency sampling filter (FSF) model to describe the linear dynamics and a simple least-squares algorithm to estimate the parameters of the linear system and the inverse static nonlinearity at the same time when they identified the Wiener model structure for a pH process by taking advantage of the invertibility of the static nonlinear part. They clarified that the Wiener model could be used to model a pH process only under certain conditions depending on the ratio of control reagent flow rate to feed rate and on the dynamic behavior of the pH probe. The advantage of their approach is that the estimate of the pH titration

curve can be obtained in significantly less time. However, this method requires that the inverse of the static nonlinear part be expressed as a power series, which could be difficult and may restrict its usefulness.

A piecewise linear model for the static part and a linear transfer function model for the dynamics were used in the method proposed by Wigren (1993). He used a recursive prediction error method for parameter estimation. He set the gain of the static part to a predetermined value to solve the redundancy in gains, but this made the identification of static part complicated.

In the approach of Greblicki (1992, 1997), a nonlinear kernel regression estimator was employed for both the nonlinear static part and the linear dynamics. This kernel approach had no constraints on the functional form of the nonlinearity, except that the function has to be invertible. It is hard to apply this approach to multiple-input, single-output (MISO) systems and processes with unknown dead time.

Huang et al. (1998) used a relay feedback test to identify model structure. They then employed simple transfer functions, for example, first or second order plus dead time to represent the linear dynamics, and an invertible algebraic function defined on an operation domain to represent the static nonlinear part. Identification of the Wiener model was done in two steps. They did not consider dynamics higher than second order because of the limitation of this proposed method and also because higher order dynamics are seldom used for control. They gave some simulation results to show the ability of this method.

Various nonlinear parameterized black-box and gray-box structures can be chosen in the method proposed by Ikonen and Najim (2001). A finite step response and a transfer function with a feedback polynomial were used to represent the linear dynamics and these two were compared. A pneumatic valve model, a distillation column model, and a pilot pump-valve system were used to illustrate the ability of this approach.

There are some problems in various discrete-time approaches as pointed out by Ikonen and Najim (2001). Above all, there are always a large number of parameters in the model and parameter redundancy exists in gains of dynamic and static parts. Whether the inverse of the nonlinear part can be obtained is a key in achieving the control objective. Since the inverse of the nonlinear static part may not exist, there are only restricted forms that can be used to approximate the nonlinear part. In addition, usually complicated two-step identification is needed.

1.3.3 Other related model structures

A. The sandwich and reversed-sandwich models

The sandwich model (LNL) and reversed-sandwich model (NLN) are shown in Figure 1.3, where the notations are the same as those in Figures 1.1 and 1.2. Here "N" denotes the static nonlinearity and "L" denotes the linear dynamics, and these notations were introduced by Chen (1995) in his review on block-oriented nonlinear models. These two models are in fact general forms of Hammerstein (NL) and Wiener (LN) models.

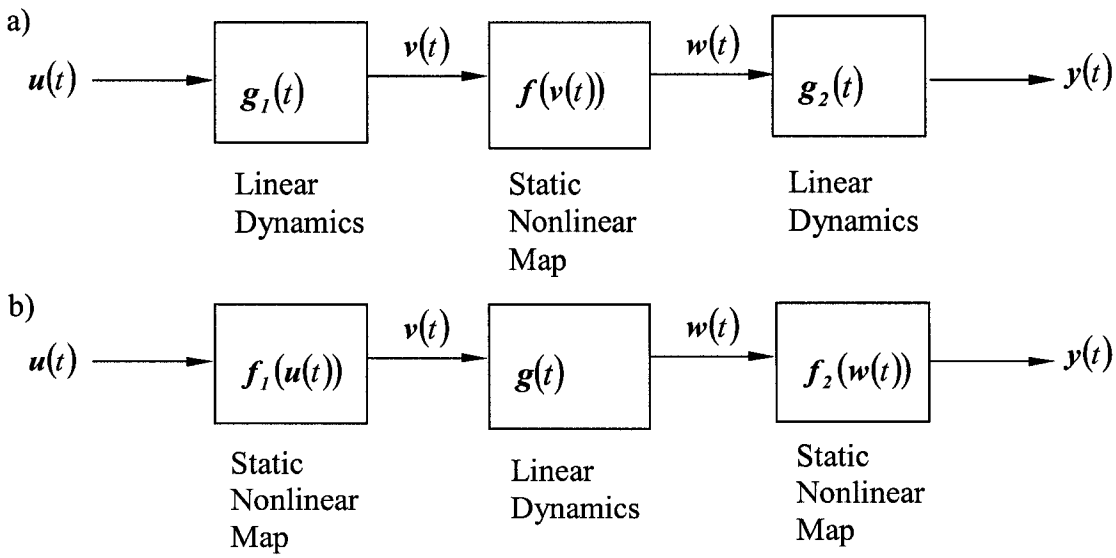

Figure 1.3. a) Sandwich model structure; b) reversed-sandwich model structure.

An LNL model with two linear subsystems and a quadratic polynomial was proposed by Emerson et al. (1992) to examine the relationship between luminance inputs and neural impulse outputs. French et al. (1993) considered using an NLN model to refine their Hammerstein model for the fly photoreceptor response to wide range light stimuli. Actually, an LNLN structure proposed by Segal and Outerbridge (1982) generalized both the LNL and NLN model structures. They proposed LNLN model as an alternative of the Wiener model for the response of the primary afferent neurons in the semicircular canal in bullfrog to large-amplitude sinusoidal and triangular motion.

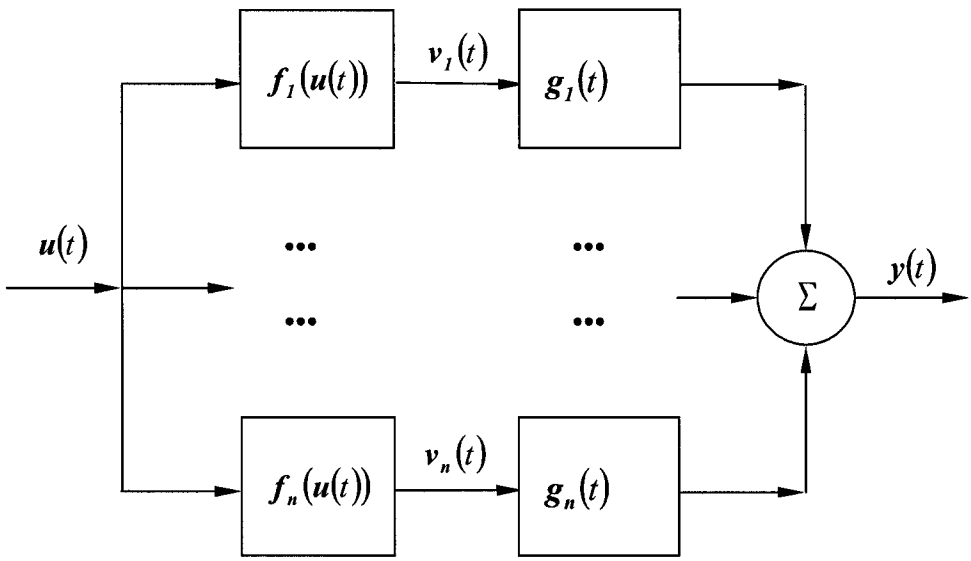

Figure 1.4. n-channel Uryson model structure.

B. The Uryson model and projection-pursuit model

The Uryson model and the projection-pursuit model are also members of the general class of block-oriented nonlinear models, corresponding to the Hammerstein and the Wiener model respectively. The Uryson model consists of n Hammerstein models in parallel, as shown in Figure 1.4. The notations are the same as before. The projection-pursuit model,

which is named from the statistical regression literature by Fan and Gijbels (1996), consists of n parallel Wiener models (Billings, 1980; Doyle et al. 2002) and can be obtained by replacing the Hammerstein models in Figure 1.4 with Wiener models. Both Uryson and projection-pursuit models have only one common input $\boldsymbol{u(t)}$.

1.3.4 MPC with Hammerstein and Wiener models

Many efforts have been put in designing the MPC scheme with Hammerstein and Wiener models. Fruzzetti et al. (1997) proposed a nonlinear MPC scheme with the Hammerstein model and demonstrated the scheme on a pH neutralization process and a binary distillation column. Patwardhan et al. (1998) presented a method for a nonlinear MPC scheme using partial-least-squares (PLS) based on Hammerstein and Wiener structures and demonstrated the scheme on a simulated pH-level control of an acid-base neutralization process. Norquay et al. applied Wiener model predictive control to a pH neutralization process (1998, 1999a) and also to an industrial C2-splitter (1999b). Jeong et al. (2001) incorporated the Wiener model into MPC of a continuous methyl methacrylate polymerization reactor. Bloemen et al. (2001) also proposed an MPC scheme with the Wiener model for dual composition control of a distillation column. However, as said before, all these are still academic concepts.

1.4 The continuous-time parametric approach

In this section, the development of the continuous-time parametric approach made by Dr. Rollins's group on Hammerstein and Wiener models will be reviewed particularly. First, the Hammerstein and the Wiener Block-oriented Exact Solution Techniques (H-BEST and W-BEST) (Rollins et al., 2003; Bhandari and Rollins, 2003) are introduced, and then the continuous-time classical, restricted and unrestricted algorithms for the step input change sequences (Chin et al., 2004) are presented. As Chen and Rollins (2000) have shown, the

discrete-time models can have critical drawbacks when sampling is infrequent, non-constant, or not online, while the continuous-time methods, like H-BEST and W-BEST, do not suffer from these limitations. All the discussion below assumes that the model structure is known so that we can concentrate on the model parameter identification and process prediction.

1.4.1 H-BEST

Rollins et al. (1998) proposed a continuous-time dynamic modeling method for the non-linear process behavior based on intuition. In their approach, called the Semi-Empirical Technique (SET), they presented the first explicit continuous-time predictive algorithm of the output for a simulated SISO CSTR with step input changes. This methodology is based on an underlying Hammerstein structure. The predictive equations for the outputs are written as a combination of linear dynamics with nonlinear steady-state gains. Rietz and Rollins (1998) showed that this method was accurate for modeling both open- and closed-loop SISO processes and also for a real process operated by a distributed control system. Rollins et al. (1999) also applied this method to more complex SISO processes, including a second order response with underdamped and inverse response behavior, and the method gave accurate prediction. Walker (1999) used this method to model a surrogate human's thermoregulatory response to changes in the ambient conditions successfully. Further, Rollins and Bhandari (2000) showed that the method worked well without using past response data. Loveland (2002) applied this methodology to real industrial data for the first time, and demonstrated its ability to handle system nonlinearity. In addition, Rollins et al. (2003) demonstrated its ability of accurately modeling a nonlinear MIMO system on a household dryer, and it was also demonstrated that this method had the ability to address interactions between inputs. Until then, the methodology had been demonstrated on both real and simulated processes. This methodology for system identification and prediction is named as H-BEST and is

presented on a SISO Hammerstein system as below (Rollins et al., 2003).

Consider a Hammerstein system with a second-order overdamp plus lead dynamic system described by Eqs. 1.1, and nonlinear static mapping shown by Eq. 1.2.

$$\tau_1\tau_2\frac{d^2y(t)}{dt^2}+(\tau_1+\tau_2)\frac{dy(t)}{dt}+y(t)=\tau_a\frac{dv(t)}{dt}+v(t) \tag{1.1}$$

$$v(t)=f(\boldsymbol{u}(t),\boldsymbol{\beta})=\beta_1u_1(t)+\beta_2u_2(t)+\beta_3u_1(t)u_2(t)+\beta_4u_1(t)^2+\beta_5u_2(t)^2 \tag{1.2}$$

Taking the Laplace transform of Eq. 1.1 gives

$$G(s)=\frac{Y(s)}{V(s)}=\frac{\tau_as+1}{\tau_1\tau_2s^2+(\tau_1+\tau_2)s+1} \tag{1.3}$$

where, $Y(s)=\mathscr{L}[y(t)]=\int_0^\infty y(t)\cdot e^{-st}dt$, $V(s)=\mathscr{L}[v(t)]=\int_0^\infty v(t)\cdot e^{-st}dt$, and inputs $u_i(t)$ and outputs $y(t)$ are both deviation variables as defined as in Figure 1.1. It is assumed that the system is at steady state at $t=0$ with $u_i(0)=0$, $i=1,2$.

For a single step input change at $t=0$, the solution is given by Rollins et al. (2003) as

$$y(t)=f(\boldsymbol{u}(t=0);\boldsymbol{\beta})\cdot g(t;\tau) \qquad \text{for } t>0 \tag{1.4}$$

where $f(\boldsymbol{u}(t);\boldsymbol{\beta})$ can be any nonlinear function of $\boldsymbol{u}(t)$, $\boldsymbol{\beta}$ is the parameter vector for the static nonlinear mapping, and the linear dynamics is described by $g(t;\tau)$, defined by Eq. 1.5.

$$g(t;\tau)=\mathscr{L}^{-1}\left[G(s)\cdot\frac{1}{s}\right] \tag{1.5}$$

where $\mathscr{L}^{-1}$ is the inverse Laplace transform operator.

For a series of step input changes, given by Eq. 1.6

$$\boldsymbol{u}(t)=\begin{cases}\boldsymbol{u}(0) & 0\le t<t_1\\ \boldsymbol{u}(t_1) & t_1\le t<t_2\\ \boldsymbol{u}(t_2) & t_2\le t<t_3\\ \vdots & \vdots\\ \boldsymbol{u}(t_i) & t_i\le t\end{cases} \tag{1.6}$$

the algorithm developed (Rollins et al., 2003) is

$$y(t)=\begin{cases} f(\boldsymbol{u}(t=0);\boldsymbol{\beta})\cdot g(t;\boldsymbol{\tau}) & 0\le t<t_1 \\ y(t_1)+[f(\boldsymbol{u}(t=t_1);\boldsymbol{\beta})-y(t_1)]\cdot g(t-t_1;\boldsymbol{\tau}) & t_1\le t<t_2 \\ y(t_2)+[f(\boldsymbol{u}(t=t_2);\boldsymbol{\beta})-y(t_2)]\cdot g(t-t_2;\boldsymbol{\tau}) & t_2\le t<t_3 \\ \vdots & \vdots \\ y(t_{i-1})+[f(\boldsymbol{u}(t=t_i);\boldsymbol{\beta})-y(t_{i-1})]\cdot g(t-t_i;\boldsymbol{\tau}) & t_i\le t \end{cases} \tag{1.7}$$

This algorithm gives an exact mathematical solution to a theoretical Hammerstein process as shown by Rollins et al. (2003). For a real process, the coefficient vector $\boldsymbol{\beta}$ can be determined by the steady state data and the dynamic parameter vector $\boldsymbol{\tau}$ can be determined by the dynamic data after step changes. It is clear that the model identification relies heavily on data. This necessitates statistical consideration of experimental designs that will give reliable data and ensure accurate parameter estimation, which will be discussed later.

To apply the H-BEST to a real system, firstly one needs to obtain the model of the process, which includes specifying the model forms for $f(\boldsymbol{u}(t);\boldsymbol{\beta})$ and $g(t;\boldsymbol{\tau})$, and obtaining parameter estimates for these functions. Steps to identify the process described by Rollins et al. (2003) are as follows:

1. Determine the statistical experimental design to be used.
2. Run the experimental design as a series of step tests, allowing steady state to occur after each change and collecting the data dynamically over time.
3. Use the steady-state data to determine the ultimate response function, $f(\Delta\boldsymbol{u}(t);\boldsymbol{\beta})$, where $\Delta\boldsymbol{u}(t)=\boldsymbol{u}(t)-\boldsymbol{u}_{ss}$ is a deviation variable.
4. Use the dynamic data to determine the dynamic response function, $g(t;\boldsymbol{\tau})$ for each output.

The predictions can be obtained by incorporating $f(\boldsymbol{u}(t);\boldsymbol{\beta})$ and $g(t;\boldsymbol{\tau})$ functions into the algorithm given by Eq. 1.7. They also demonstrated that this technique was successfully applied to a theoretical Hammerstein process and a household dryer.

Hulting et al. (2002a) applied H-BEST in modeling the human thermoregulatory system with three inputs and two outputs. For this MIMO system, they concluded that H-BEST could accurately predict the responses of skin temperature and sweat rate for changes in the environment with changes in ambient temperature, relative humidity, and wind speed. They also indicated that this methodology was able to make full use of statistical design of experiments (SDOE) for optimal data collection and accurate parameter estimation.

Bhandari and Rollins (2004) applied the continuous-time nonlinear modeling technique, H-BEST, to the high purity distillation column investigated by Eskinat et al. (1991) and compared the continuous-time H-BEST to the discrete-time approach of Eskinat. H-BEST gave more accurate predictions than Eskinat's model when comparing the sum of squared prediction error.

1.4.2 W-BEST

W-BEST was first proposed by Bhandari and Rollins (2003). They showed that W-BEST is an exact solution for a theoretical Wiener model and applied W-BEST to a simulated CSTR to show its predictive ability. The W-BEST algorithm is given below (Bhandari and Rollins, 2003).

For changes in the input vector $\boldsymbol{u}^{p\times 1}(t)$, a general, unrestricted solution to the Wiener system can be written as

$$y_i(t) = f_i(\boldsymbol{v}_i(t); \boldsymbol{\beta}),\ i = 1,\ldots,q \tag{1.8}$$

$$v_{ij}(t) = \mathscr{L}^{-1}\left\{G_{ij}(s)\cdot U_j(s)\right\},\ j = 1,\ldots,p \tag{1.9}$$

where $f_i(\boldsymbol{v}_i(t))$ can be any nonlinear function of $v_{ij}(t)$'s, $\boldsymbol{v}_i(t)$ is a $p\times 1$ vector with the rth element equal to $v_{ir}(t)$ and $\boldsymbol{\beta}$ is the parameter vector for the static nonlinear mapping.

$U_j(s) = \mathscr{L}\{u_j(t)\}$ and $G(s)$ is the linear dynamic transfer function in Laplace domain. With the restriction that the process response reaches steady state between input changes, they obtained the exact solution that depends only on recent input changes for a series of step input changes occurring at times t_k, t_{k+1}, etc.. The solution to the Wiener system is

$$v_{ij}(t) = v_{ij}(t_k) + \left[u_j(t_k) - v_{ij}(t_k)\right] \cdot g_{ij}(t - t_k; \tau) \tag{1.10}$$

where

$$g_{ij}(t;\tau) = \mathscr{L}^{-1}\left\{G_{ij}(s) \cdot \frac{1}{s}\right\} \tag{1.11}$$

τ is a vector of continuous-time dynamic parameters. This solution is called the W-BEST solution. The procedure to apply W-BEST is as follows:

1. Determine the statistical experimental design to be used.
2. Run the experimental design as a series of step tests, allowing steady state to occur after each change while collecting the data dynamically over time.
3. Use the steady-state data to determine the ultimate response function, $f_i(v_i(t); \beta)$, by noting that $v_{ij}(t) = u_j(t)$ at steady state.
4. Use the dynamic data to determine the dynamic response function, $g(t; \tau)$ for each output by trial and error.

The predictions of process outputs can then be obtained by incorporating $f(v(t);\beta)$ and $g(t;\tau)$ functions into the W-BEST algorithm given in Eq. 1.10.

Bhandari and Rollins (2003) applied the W-BEST algorithm to a theoretical Wiener system and a simulated seven-input, five-output CSTR to demonstrate the ability of the W-BEST modeling methodology. A second-order plus dead time with lead dynamics was employed to model the CSTR process dynamics. They used an arbitrary step input sequence to test the obtained model. It was shown that the W-BEST prediction is adequate for the output responses of the CSTR. W-BEST is able to identify the nonlinear static gain functions

of the intermediate variables efficiently from the ultimate response modeling, which is a challenge when modeling a Wiener system.

1.4.3 The classical, restricted and unrestricted algorithms

Later on, the algorithms for the MIMO Wiener processes were further investigated by Chin et al. (2004). They defined the classical, restricted and unrestricted algorithm for a MIMO Wiener system clearly for the first time. For a step input change sequence shown in Eq. 1.12,

$$\boldsymbol{u}(t)=\begin{cases}\boldsymbol{u}_0=0 & 0<t\le t_1\\ \boldsymbol{u}_1 & t_1<t\le t_2\\ \boldsymbol{u}_2 & t_2<t\le t_3\\ \vdots & \vdots\\ \boldsymbol{u}_K & t_{K-1}<t\end{cases} \tag{1.12}$$

where $\boldsymbol{u}_k=\left[u_{1,k},u_{2,k},...,u_{p,k}\right]^T$, $u_{j,k}$ is the value of the jth input in the kth interval, and $j=1,2,...,p$; $k=1,2,...,K$, the classical algorithm is given by Eq. 1.13.

$$v_{ij}(t)=\sum_{l=1}^{K}\left(u_{j,l}-u_{j,l-1}\right)\cdot g_{ij}\left(t-t_{l-1}\right)\cdot \boldsymbol{S}\left(t-t_{l-1}\right) \tag{1.13}$$

where, $\boldsymbol{S}\left(t-t_{l-1}\right)$ is the shifted unit step function and $g_{ij}(t)$ is defined as before in Eq. 1.11. This algorithm depends on all previous input changes. It is hard to use this algorithm in practice without a fading memory treatment to reduce the dependence on the number of past inputs. Still, there are lots of parameters involved.

The W-BEST algorithm (Bhandari and Rollins, 2003), shown in Eq. 1.10, was classified as the restricted algorithm. It depends on only the most recent input change, $u_{j,k+1}$, and is defined as "compact." It is useful when predicting output responses for Wiener process. However, it has the requirement that the process has to reach its steady state between step input changes. The accuracy of the algorithm is not satisfactory when the process does not

meet this requirement.

To overcome this limitation, an unrestricted algorithm was proposed by Chin et al. (2004). Assume that the linear dynamic function is with *n* poles and *m* zeros and can be written as

$$G_{ij} = \frac{V_{ij}(s)}{U_j(s)} = \frac{b_{ij,m}s^m + b_{ij,m-1}s^{m-1} + \ldots + b_{ij,1}s + 1}{a_{ij,n}s^n + a_{ij,n-1}s^{n-1} + \ldots + a_{ij,1}s + 1} \tag{1.14}$$

With step input changes given in Eq. 1.12, the proposed unrestricted W-BEST algorithm in the interval $t_k < t \le t_{k+1}$ is

$$v_{ij}(t) = u_{j,k+1} \cdot g_{ij,1}(t - t_k) - u_{j,k} \cdot g_{ij,2}(t - t_k) + \sum_{l=1}^{n} v_{ij}^{(l-1)}(t_k) \cdot g_{ij,l+2}(t - t_k) \tag{1.15}$$

where, $v_{ij}^{(r)}(t_k)$ is the *r*th derivative of v_{ij} at time t_k. Totally *(n+2)* dynamic functions $g_{ij,k}$, $k = 1,2,\ldots,n+2$, are defined (See the paper for details.). This algorithm only requires the two most recent input changes, and thus is "compact." In addition, it is not restricted by the time between step input changes and the process does not have to reach its steady state when the next step input change is made. The performance of the algorithm was evaluated on the simulated seven-input, five-output CSTR with comparison with the classical and restricted algorithms. Also the unrestricted algorithm was evaluated under added noise on the true output at each sampling time. Its accuracy is similar to the classic algorithm, and better than the restricted algorithm. Since it only requires a few previous input changes, it is much attractive than the classical algorithm. The challenge in using the unrestricted algorithm lies in the computation of the derivatives.

All these algorithms focus on the step input changes. Other types of input changes, such as sinusoidal, or ramp change, are usually approximated as piece-wise step input changes. However, this approximation is not adequate especially when the process requires high accuracy. Thus, to set up algorithms for other types input changes besides step input change

are also necessary and crucial.

1.4.4 Statistical design of experiments (SDOE) in parameter estimation

Though the Hammerstein and Wiener models have been widely discussed as reviewed, statistical design of experiments (SDOE) is not always considered and implemented in parameter identification of nonlinear systems.

One of the differences between linear models and nonlinear models is that the nonlinear model is amplitude-dependent, which means that, if the output is $y(t)$ with respect to input $u(t)$, the output corresponding to input $\lambda u(t)$ will not be $\lambda y(t)$ for any constant $\lambda \neq 1$ for a nonlinear model, and the response could be quite different from $\lambda y(t)$. Usually, a pseudo-random sequence (PRS) or a pseudo-random binary sequence (PRBS) is used to excite the system to obtain the dynamic and steady state data for the process identification. PRBS works well for the linear system without interactions, but is not able to provide enough information in estimating parameters for a nonlinear system since there are only two levels (Pearson and Ogunnaike, 1997). When a PRBS is used in SISO Hammerstein model identification, the intermediate output $v(t)$ generated by the static nonlinear mapping is either binary or constant, which is not a good choice for getting information about nonlinearity. Although PRS works in estimation of nonlinear effects as it has multiple levels, it is not able to address the interactions and is likely to partially confound significant effects. Thus, it is clear that the shape of the input sequence is very important for identifying the nonlinear model. Specifying the input sequences over the range of interest is crucial so that extrapolation from the model can be avoided. So are the sequence length and distribution of the input sequence. As pointed out by Pearson and Ogunnaike (1997), advantage should be taken to choose the input sequence whenever it is possible, because "the difference in models obtained with 'good' input sequence and 'poor' input sequence may be great."

Some ideas of experimental design have been applied to linear system identification (Ljung, 1987). However, it is difficult to use the criteria, such as AIC, for nonlinear modeling because the likelihood usually cannot be computed explicitly or is very difficult to calculate for discrete models. Pajunen (1984) proposed a two-pass algorithm for a Wiener model based on this idea, in which a low-amplitude input sequence was used to excite the system to identify the linear dynamics and then a high-amplitude input sequence was used to get information about the nonlinear static part. Pearson and Ogunnaike (1997) proposed some general guidelines for input sequence design. They suggested that a "multiple step model identification algorithm" with several different amplitudes be used at each step.

Rollins et al. (2002) compared two design methods, SDOE and PRS, in identifying a theoretical SISO Hammerstein system by using a quantitative measure — efficiency based on D-optimality. For each design, there are three input levels. For the PRS, they considered the sequences of different orders generated by difference equations. They found that the efficiencies for the PRS designs were between 6%-15% when estimating all parameters and 5%-10% when estimating the steady-state parameters. They ascribed this low efficiency to the rapid changes in the PRS, which would not allow the system to reach steady state so that sufficient information for steady state responses could not be obtained. On the other hand, enough time was given for runs in SDOE to go to steady state. In order to make sure this is the reason, they compared experiments with different time intervals between step changes. The fact that D-optimal efficiency decreased to around 60% when the response reached 86% of its steady state or ultimate gain did support their conclusion.

Furthermore, Pacheco et al. (2002) extended this work to cases with multiple inputs using the quantitative efficiency still based on D-optimality. They compared full factorial design and PRS for a Hammerstein system with first order dynamics and two inputs, each with three levels. The efficiency of PRS was around 10% compared to a full factorial design when

estimating all the parameters. Then they compared Box-Behnken design and PRS for a five-input Hammerstein system. The efficiency of PRS designs was between 8.6%-8.8% as compared to Box-Behnken design when estimating all the parameters. They concluded that the duration of each run in the experiments could be reduced to 3τ, where τ is the time constant of the process with first-order dynamics, and enough information needed to estimate the model parameters could still be obtained.

Hulting et al. (2002b) considered different experimental designs in identifying the H-BEST parameters for a simulated human thermoregulatory system. They tried to find a practical and optimal experimental design for modeling the skin temperature and sweat rate for changes in the environment. D-optimal design and Box-Behnken design with three input variables: ambient temperature, relative humidity, and wind speed were considered. H-BEST predicted the responses closely. The D-optimal design was found to be the design with a small number of experimental trials and also with the experiment length as short as possible. It can also maintain the experiments as informative as possible for estimating the parameters based on the D-optimal criterion, which minimizes the volume of the confidence region of the parameter estimates. The D-optimal design had only half as many experimental trials as the Box-Behnken design.

Rollins et al. (2003) used a central composite design when they investigated a household dryer, a practical MIMO system. They considered four factors, each with five levels. This design allowed them to include interactions and nonlinear effects in the model. Even though only a few of the interactions were significant, it serves as an example that H-BEST has the ability to take advantage of SDOE and address interactions and nonlinearity.

In short, the H-BEST and W-BEST techniques have the ability to make full use of SDOE, especially for a MIMO system. SDOE is able to give high quality information to ensure accurate parameter estimation in the process identification.

References

Al-Duwaish, H. and Karim, M.N., A new method for the identification of Hammerstein model, *Automatica*, **33**: 1871-1875 (1997).

Bai, E.-W., An optimal two-stage identification algorithm for Hammerstein –Wiener nonlinear systems, *Automatica*, **34**: 333-338 (1998).

Bhandari, N. and Rollins, D. K., A continuous-time MIMO Wiener modeling method, *Industrial and Engineering Chemistry Research*, **42**: 5583-5595 (2003).

Bhandari, N. and Rollins, D. K., Application of a continuous-time Hammerstein non-linear modeling technique to distillation, *AIChE Journal*, **50**: 530-533 (2004).

Billings, S.A., Identification of nonlinear systems — a survey, *IEE Proc., Pt. D*, **127**: 272-285 (1980).

Bloemenn, H.H.J., Chou, C.T., van der Boom, T.J.J., Verdult, V., Verhaegen, M., Backx, T.C., Wiener model identification and predictive control for dual composition control of a distillation column, *Journal of Process Control,* **11**: 601-620 (2001).

Chen, H.W., Modeling and identification of parallel nonlinear systems: structural classification and parameter estimation methods, *Proc. IEEE*, **83**: 39-66 (1995).

Chen, V.C.P., and Rollins, D.K., Issues regarding artificial neural network modeling for reactors and fermentation, *Bioprocess and Biosystems Engineering*, **22**: 85-93 (2000).

Chin, S.-T., Bhandari, N., and Rollins, D.K., An unrestricted algorithm for accurate prediction of multiple-input multiple-output (MIMO) Wiener processes, *Industrial and Engineering Chemistry Research*, **43**: 7065-7074 (2004).

Doyle, F.J. III, Pearson, R.K., and Ogunnaike, B.A., *Identification and control using Volterra models*, Springer-Verlag London Limited, Great Britain, 2002.

Emerson, R.C., Korenberg, M.J., and Citron, M.C., Identification of complex-cell intensive nonlinearities in a cascade model of cat visual cortex, *Biological Cybernetics,* **66**:

291-300 (1992).

Eskinat, E., Johnson, S.H. and Luyben, W.L., Use of Hammerstein models in identification of nonlinear systems, *AIChE Journal*, **37**: 255-268 (1991).

Fan, Jianqing, and Gijbels, Irene, *Local polynomial modelling and its applications*, Chapman & Hall, New York, 1996.

French, A.S., Korenberg, M.J., Jarvilehto, M., Kouvalainen, E., Juusola, M., Weckstorm, M., The dynamic nonlinear behavior of fly photoreceptors evoked by a wide range of light intensities, *Biophysical Journal*, **65**: 832-839 (1993).

Fruzzetti, K.P., Palazoglu, A., and McDonald, K.A., Nonlinear model predictive control using Hammerstein models, *Journal of Process Control,* **7**: 31-41 (1997).

Greblicki, W., Nonparametric identification of Wiener systems, *IEEE Transactions on Information Theory*, **38**: 1487-1493 (1992).

Greblicki, W., Nonparametric approach to Wiener system identification, *IEEE Transactions on Circuits Systems I*, **44**: 538-545 (1997).

Greblicki, W., Recursive identification of continuous-time Wiener Systems, *International Journal of Control*, **72**: 981-989 (1999).

Greblicki, W., Continuous-time Hammerstein system identification, *IEEE Transactions on Automatic Control*, **45**: 1232-1236 (2000).

Haber, R., and Unbehauen, H., Structure identification of nonlinear dynamic systems — a survey on Input/output Approaches, *Automatica*, **26**: 651-677 (1990).

Holcomb, T.R., Rhodes, and C.A., Morari, M., Input/output modeling for process control, *Methods of Model Based Process Control*, Kluwer Academic Publishers, Netherlands, 1995.

Huang, H.-P., Lee, M.-W., and Tang, Y.-T., Identification of Wiener model using relay feedback test, *Journal of Chemical Engineering of Japan*, **31**: 604-612 (1998).

Hulting, S., Rollins, D.K., Bhandari, N., Effective MIMO modeling of the human

thermoregulatory system, to be submitted to *IEEE Transactions* (2002a).

Hulting, S., Rollins, D.K., Bhandari, N., Accurate predictive modeling with optimal experimental design of the human thermoregulatory system, to be submitted to *Annals of Biomedical Engineering Journal* (2002b).

Hunter, I.W. and Korenberg, M.J., The identification of nonlinear biological systems: Wiener and Hammerstein cascade model, *Biological Cybernetics*, **55**: 135-144 (1985).

Ikonen, E., and Najim, K., Non-linear process modeling based on a Wiener approach, *Journal of Systems and Control Engineering*, **215**: 15-27 (2001).

Jeong, B.-G., Yoo, K.-Y., and Rhee, H.-Y., Nonlinear model predictive control using a Wiener model of a continuous methyl methacrylate polymerization reactor, *Ind. Eng. Chem. Res.*, **40**: 5968-5977 (2001).

Jyothi, S.N. and Chidambaram M., Identification of Hammerstein model for bioreactors with input multiplicities, *Bioprocess Engineering*, **23**: 323-326 (2000).

Jyothi, S.N. and Chidambaram M., Nonlinear feedforward control of bioreactors with input multiplicities, *Bioprocess and Biosystems Engineering*, **24**: 123-129 (2001).

Kalafatis, A., Arifin, N., Wang, L. and Cluett, W.R., A new approach to the identification of pH process based on the Wiener model, *Chemical Engineering Science*, **50**: 3693-3701 (1995).

Lee, J.H., Modeling and identification for nonlinear model predictive control: requirements, current status and future research needs, *Progress in Systems and Control Theory* (Vol. 26), Birkhauser Verlag, Basel, Switzerland in *Nonlinear Model Predictive Control*, edited by Allgower, F. and Zheng, A. (2000).

Ljung, L., *System Identification: Theory for the User*, Prentice-Hall, New York, 1987.

Loveland, Stephanie D., Advances in nonlinear process modeling using block-oriented exact solution techniques, M.S. thesis, Iowa State University, Ames, IA, 2002.

Narendra, K.S., and Gallman. P.G., An iterative method for the identification of the nonlinear system using the Hammerstein model, *IEEE Trans. Automatic Control*, **12**: 546-550 (1966).

Normandin, A., Thibault, J., and Grandjean, B.P.A., Optimizing control of a continuous stirred tank fermenter using a neutral network, *Bioprocess Engineering*, **10**: 109-113 (1994).

Norquay, S.J., Palazoglu, A., and Romagnoli, A.J., Model predictive control based on Wiener models, *Chemical Engineering Science*, **53**: 75-84 (1998).

Norquay, S.J., Palazoglu, A., and Romagnoli, A.J., Application of Wiener model predictive control to a pH neutralization experiment, *IEEE Transactions on Control Systems Technology*, **7**: 437-445 (1999a).

Norquay, S.J., Palazoglu, A., and Romagnoli, A.J., Application of Wiener model predictive control (WMPC) to an industrial C2-splitter, *Journal of Process Control,* **9**: 461-473 (1999b).

Ogunnaike, B.A., and Ray, W.H., *Process Dynamics, Modeling, and Control*, Oxford University Press, Inc., New York, 1994.

Pacheco, L., Bhandari, N., and Rollins, D.K., A quantitative measure to evaluate competing designs for nonlinear dynamic process identification, *AIChE Annual Meeting,* Indianapolis, IN (2002).

Pajunen, G.A., "Application of a model reference adaptive technique to the identification and control of Wiener type nonlinear processes," PhD thesis, Acta Polytechnica Scandinavica, No.52, Helsinki University of Technology, Department of Electrical Engineering, Finland, 1984.

Patwardhan, R.S., Lakshminarayanan, S., and Shah, S.L., Constrained nonlinear MPC using Hammerstein and Wiener models: PLS Framework, *AIChE Journal*, **44**:1611-1622 (1998).

Pearson, R.K. and Ogunnaike, B.A., Nonlinear process identification, *Nonlinear Process Control*, Edited by Henson, M.A., and Seborg, D.E., Prentice-Hall, Upper Saddle River, New Jersey, p. 11-110, 1997.

Pearson, R.K., Ogunnaike, B.A., and Doyle, F.J., Identification of structurally constrained second-order Volterra models, *IEEE Transactions on Signal Processing*, **44**: 2837-2846 (1996).

Pearson, R.K. and Pottmann, M., Gray-box identification of block-oriented nonlinear models, *Journal of Process Control*, **10**: 301-315 (2000a).

Pearson, R.K. and Pottmann, M., Combining linear dynamics and static nonlinearities, *IFAC Advanced Control of Chemical Processes,* Pisa, Italy, 479-484 (2000b).

Rietz, C.A. and Rollins, D.K., Implementation of a predictive modeling technique on a DCS, *Proceedings of the American Control Conference*, Philadelphia, 2951-55 (1998).

Rollins, D.K. and Bhandari, N., Accurate predictive modeling of response variables under dynamic condition without the use of past response data, *ISA Transactions*, **39**: 29-34 (2000).

Rollins, D.K., Bhandari, N., Bassily, A.M., Colver, G.M., and Chin, S., A continuous-time nonlinear dynamic predictive modeling method for Hammerstein processes, *Industrial and Engineering Chemistry Research,* **42**(4): 861-872 (2003).

Rollins, D.K., Bhandari, N., and Pacheco, L., Experimental designs that maximize information for nonlinear dynamic process, *Foundations of Computer Aided Process Operations Conference (FOCAPO),* Florida (2002).

Rollins, D.K., Liang, J.M., and Smith, P., Accurate simplicity predictive modeling of nonlinear dynamic processes, *ISA Transactions*, **36**: 293-303 (1998).

Rollins, D.K., McNaughton, M. and Schulze-Hewett, C.M., Accurate semi-empirical predictive modeling of an underdamped process, *ISA Transactions*, **38**: 279-290, (1999).

Segal, B.N., and Outerbridge, J.S., A nonlinear model of semicircular canal primary afferents in Bullfrog, *Journal of Neurophysiology*, **47**: 563-578 (1982).

Su, H.-T., and McAvoy, T.J., Integration of multilayer perceptron networks and linear dynamic models: A Hammerstein model approach, *Industrial & Engineering Chemistry Research*, **32**: 1927-1936 (1993).

Walker, J.J., Developmen of an empirical model of human sweating and a semi-empirical predictive modeling of human thermoregulation, Ph.D. Dissertation, Iowa State University, Ames, IA, 1999.

Wigren, T., Recursive prediction error identification using the nonlinear Wiener model, *Automatica*, **29**: 1011-1025 (1993).

Zhu, Xuefeng, and Seborg, Dale E., Nonlinear predictive control based on Hammerstein models, control theory and applications, **11**: 564-575 (1994).

Zhu, Yucai, Distillation column identification for control using Wiener model, *Proceedings of American Control Conference*, San Diego, CA, June 1999.

Chapter 2. Block-Oriented Continuous-Time Modeling for Nonlinear Systems Under Sinusoidal Inputs

2.1 Introduction

Many physical processes are nonlinear and dynamic in nature. Few of those nonlinear dynamic problems can be solved analytically because usually there is no closed-form algorithm for the nonlinear descriptive equations and the rigorous analytical techniques to analyze nonlinear processes are usually thought to have limited practical applications. Instead, numerical analysis and discrete modeling are widely used because data are sampled at discrete times and stored in computer databases. The variables are assumed to remain fixed at their sampled values between one sample instant and the next, though variables in most physical processes are continuously changing. Thus, information between the sampling time points is missing in discrete sampling. Furthermore, in DTM, the sampling conditions, such as sampling time and sampling frequency, play an important role in prediction. In systems engineering, CTM has seen limited applications even though it has the advantage of prediction at any time, and not just at discrete times. Other advantages of CTM over DTM include fewer model coefficients and parameters with physical meaning. With DTM, the continuous process input has to be approximated as piece-wise step changes. For a continuous model, it is possible to have a compact closed-form algorithm (Rollins et al., 2003), which does not require iterative calculation. Another advantage of CTM is the ability to apply analytical treatment when require such as in D-optimal experimental design (Rollins et al., 2004). Also, CTM identification can be easier than DTM identification due to fewer parameters and a clearer analytical algorithm form. In addition, when the error term of a model is considered to be stochastically continuous and must be treated as such, DTM is not appropriate to use and CTM has to be employed.

Hammerstein and Wiener models are two simple and popular block-oriented model structures with relatively few dynamic model parameters. Due to their simple structures and efficient parameterization, the Hammerstein and Wiener models have many applications in practice and are becoming more popular. For example, the Hammerstein and Wiener models have been shown to represent many nonlinear chemical processes very well, such as pH neutralizations, distillation columns, and continuous-stirred tank reactors (CSTR). Much work has been done to investigate the extent of the applications of this model. Almost all of the work involves use of discrete-time models (Eskinat et al., 1991; Su and McAvoy, 1993; Wigren, 1993; Zhu and Seborg, 1994; Kalafatis et al, 1995; Huang et al., 1998; Ikonen and Najim, 2001; Doyle et al, 2002). Noted exceptions include Greblicki (Greblicki, 1992; 1997; 2000), Rollins et al. (2003), and Bhandari and Rollins (2003a and 2003b). Greblicki introduced a nonparametric continuous-time approach with the dynamic block identified by impulse response methods, and our research group has proposed parametric continuous-time Hammerstein and Wiener modeling methods.

The closed-form algorithms for step input changes for Hammerstein and Wiener systems with various dynamics have been determined by Rollins et al. (2003) and Bhandari and Rollins (2003b) in a compact form, referred to as H-BEST and W-BEST, respectively, and demonstrate exact agreement with true Hammerstein or Wiener systems. H-BEST was applied to a household dryer (Rollins et al., 2003) and a distillation column (Bhandari and Rollins, 2003a). Application of W-BEST includes a CSTR (Bhandari and Rollins, 2003b).

In all the studies involving H-BEST and W-BEST techniques, only step input changes were considered. Under real conditions, input changes are often gradual or periodical (Seborg et al., 1989), which can be described as a ramp or a sinusoidal function, respectively, in some cases. For example, any device operating by AC current can potentially induce periodic variability into the process. Also, cooling water temperatures can fluctuate with ambient

conditions and exhibit day-to-night-to-day fluctuations. These cyclic process changes can often be approximated as sinusoidal functions. For these kinds of periodical changes, it is important to have a high sampling frequency to obtain adequate information for the system and to avoid aliasing. However, sufficiently frequent sampling is not always possible or not always available, especially for some variables such as concentration measurements of distillation columns. Of course, the periodical input changes can be approximated as piece-wise step changes. Either DTM or the current H-BEST methodology could then be employed. However, these approaches may perform unacceptably with inadequate sampling. Note that noisy measurements can often be described as summations of sinusoidal waves with an additive noise term (Hajjari, and Eloutassi, 1999). Once the spectral decomposition is done and the amplitudes and frequencies of the sinusoidal waves are identified, the proposed algorithm can be employed to obtain the process outputs efficiently for even noisy input signals.

However, to our knowledge, no closed-form algorithm has been presented for Hammerstein and Wiener systems under the sinusoidal input sequences. Kalafatis *et al.* (1995) made use of sinusoidal inputs to excite a pH process, which was modeled as a Wiener system; however, they used a frequency sampling filter (FSF) method for the linear dynamics of a Wiener model with periodical excitation of the system, which is quite different from the approach proposed here.

Rollins et al. (2003) presented a non-compact algorithm without restriction and a compact algorithm for piece-wise step input sequences. This paper extends their work to a compact CTM algorithm for sinusoidal input changes in Hammerstein and Wiener modeling. The compact, closed-form algorithms given by process analysis, along with some simulation results are presented for Hammerstein and Wiener systems with first- and second-order process dynamics when they are excited by different sinusoidal input changes. Our proposed

algorithms can be exploited for creating a methodology for block-oriented predictive modeling.

After briefly describing the Hammerstein and Wiener systems in Section 2.2, Section 2.3 presents general algorithms to the Hammerstein and Wiener systems when the inputs follow sinusoidal functions. The algorithms are presented for single-input, single-output (SISO) systems, which hold analogously for multiple-input, multiple-output (MIMO) systems. This section also includes an extension to systems with time delay. Two sinusoidal input sequence cases are considered for each model. Applications to theoretical Hammerstein or Wiener systems are also presented to verify the closed-form compact algorithms. In Section 2.4, the algorithms are applied to a MIMO system. Section 2.5 gives the concluding remarks of the proposed method.

2.2 The Hammerstein and Wiener systems

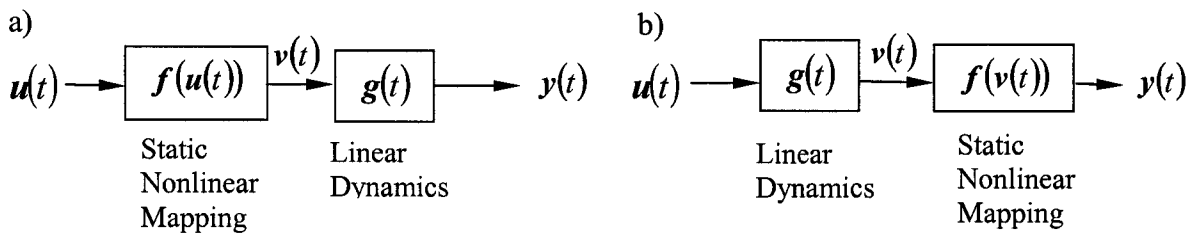

Figure 2.1. a) General Hammerstein model structure and b) General Wiener model structure.

A Hammerstein system (Narendra, and Gallman, 1966) consists of a static nonlinear mapping or gain followed by a linear dynamic block, as shown in Figure 2.1a, where $u(t)$ is the input vector, $v(t)$ is the intermediate vector, which is not measurable, and $y(t)$ is the output vector; $f(u(t))$ represents the nonlinear static gain functions, and $g(t)$ describes the linear dynamic block. Note that $v(t) = f(u(t))$ and each element of $y(t)$ can be obtained by convolution of $v(t)$ and $g(t)$. For simplicity, it is assumed that all these variables are

deviations variables. $\boldsymbol{u(t)}$, $\boldsymbol{v(t)}$, and $\boldsymbol{y(t)}$ are all vectors, and $\boldsymbol{f(u(t))}$ and $\boldsymbol{g(t)}$ could be several different nonlinear mappings and linear dynamic relations, respectively.

A Wiener system consists of the same two blocks but in a reverse order, which is a dynamic block followed by a static nonlinear mapping or gain, as shown in Figure 2.1b. Each element of $\boldsymbol{v(t)}$ can be obtained by convolution of $\boldsymbol{u(t)}$ and $\boldsymbol{g(t)}$ and $\boldsymbol{y(t)} = \boldsymbol{f(v(t))}$.

2.3 Hammerstein and Wiener algorithms

In this section, we present closed-form, compact algorithms for the Hammerstein and Wiener systems with first- and second-order dynamics for specific forms, without loss of generality, of sinusoidal input sequences. The algorithms are in closed-form and only depend on the most recent input changes (i.e. are compact). Once the changing point is identified, and the information on amplitude, frequency, phase angle, and the step change is obtained, the outputs can be predicted by employing the results in this section. In this section, all processes are initially at steady state and only deviation variables from this steady state are used.

2.3.1 The Hammerstein system with first-order dynamics

The following algorithms are based on a SISO Hammerstein system with first-order dynamics, as described by (2.1) and (2.2) below:

$$\tau \frac{dy(t)}{dt} + y(t) = v(t) = f(u(t)) \tag{2.1}$$

giving the transfer function in the Laplace domain as:

$$G(s) = \frac{Y(s)}{V(s)} = \frac{1}{\tau s + 1} \tag{2.2}$$

where $g(t)$ is its corresponding function in the time domain with a unit step forcing function. Here, τ is the time constant.

Case I. The sinusoidal input change introduced to the Hammerstein system is imposed on the step input changes and can be described mathematically as:

$$u(t) = b_n + A_n \sin(\omega_n (t - t_{n-1})) \qquad \text{for } t_{n-1} < t \le t_n \tag{2.3}$$

For the nonlinear polynomial static mapping relationship shown in (2.4), the algorithm for the Hammerstein system, for the interval $t_{n-1} < t < t_n$, is given by (2.5) to (2.8).

$$f(u(t)) = a_1 u(t) + a_2 u^2(t), \tag{2.4}$$

$$\begin{aligned} y(t) = &\left(a_1 b_n + a_2 b_n^{\,2} + \frac{1}{2} a_2 A_n^{\,2} \right) \cdot g_0(t - t_{n-1}; \tau) + (a_1 A_n + 2 a_2 b_n A_n) \cdot g_s(t - t_{n-1}; \omega_n, \tau) \\ &- \frac{1}{2} a_2 A_n^{\,2} \cdot g_c(t - t_{n-1}; 2\omega_n, \tau) + y(t_{n-1}) \cdot e^{-(t - t_{n-1})/\tau} \end{aligned} \tag{2.5}$$

where $g_0(t;\tau)$, $g_s(t;\omega,\tau)$, and $g_c(t;\omega,\tau)$ are defined as:

$$g_0(t;\tau) = 1 - e^{-t/\tau} \tag{2.6}$$

$$g_s(t;\omega,\tau) = \frac{1}{1 + (\omega t)^2} \left[\omega\tau \cdot e^{-t/\tau} - \omega\tau \cdot \cos(\omega t) + \sin(\omega t) \right] \tag{2.7}$$

$$g_c(t;\omega,\tau) = \frac{1}{1 + (\omega t)^2} \left[-e^{-t/\tau} + \omega\tau \cdot \sin(\omega t) + \cos(\omega t) \right] \tag{2.8}$$

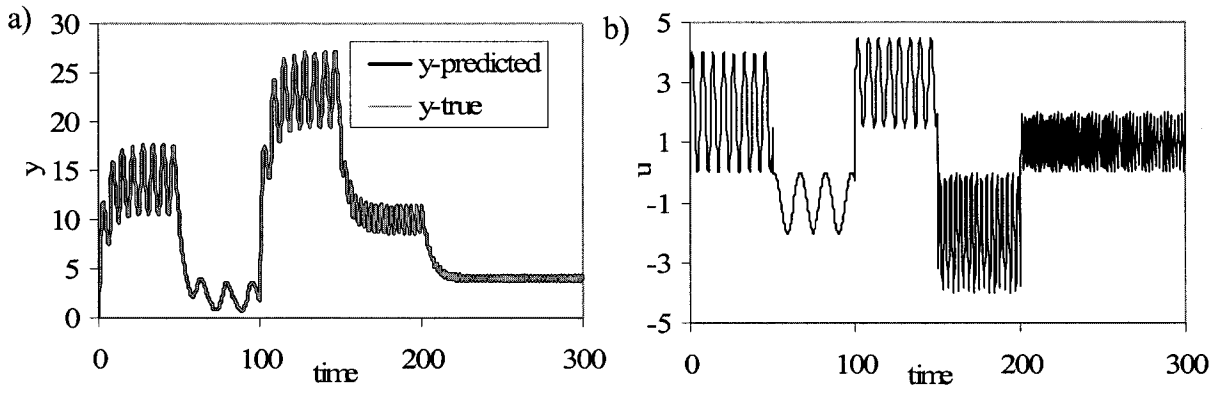

Figure 2.2. a) Simulated outputs (y-true) and predicted outputs (y-predicted) on a theoretical Hammerstein process for Case I when forced by b) sinusoidal input change sequence (u) with different ω_i, b_i, and A_i values.

The simulation is done for quadratic nonlinear static mapping on a theoretical Hammerstein process. The dataset of y-true is simulated from a Hammerstein process that can be described as follows:

$$v(t)=1.0\cdot u(t)+2.0\cdot u^2(t) \text{ and } 5.0\frac{dy(t)}{dt}+y(t)=v(t) \text{ with } y(0)=0$$

As shown in Figure 2.2, the predicted outputs based on the provided formula and the true process values show perfect agreement for the arbitrary input sequence given in Figure 2.2b.

Case II. The sinusoidal input change with changing phase described by (2.9) is introduced to the Hammerstein system:

$$u(t)=\sin(\omega_n(t-t_{n-1})+\phi_n) \quad \text{for } t_{n-1}<t\le t_n \tag{2.9}$$

For different polynomial static mapping relationships, the algorithms in the interval $t_{n-1}<t\le t_n$ for the Hammerstein system are given below. In (A), the summation is up to an even order, while it is up to an odd order in (B). The same Hammerstein process is employed here but with a different input sequence. The simulation results are shown in Figure 2.3 for quadratic nonlinear static mapping on a true Hammerstein model. As shown, the predicted outputs and the true process values overlap exactly.

(A) $$f(u(t))=\sum_{i=1}^{2m}a_i u^i(t), \tag{2.10}$$

$$\begin{aligned}y(t)=&\sum_{j=1}^{m}a_{2j}\binom{2j}{j}\frac{1}{2^{2j}}g_0(t-t_{n-1};\tau)\\&+\sum_{j=1}^{m}\frac{a_{2j-1}}{2^{2j-2}}\left[\sum_{k=1}^{m}(-1)^{k-1}\cdot\binom{2j-1}{j-k}\cdot(\cos((2k-1)\phi_n)\cdot g_s(t-t_{n-1};(2k-1)\omega_n,\tau)\right.\\&\left.+\sin((2k-1)\phi_n)\cdot g_c(t-t_{n-1};(2k-1)\omega_n,\tau))\right]\\&+\sum_{j=1}^{m}\frac{a_{2j}}{2^{2j-1}}\left[\sum_{k=1}^{m}(-1)^k\binom{2j}{j-k}(\cos(2k\phi_n)\cdot g_c(t-t_{n-1};2k\omega_n,\tau)-\sin(2k\phi_n)\cdot g_s(t-t_{n-1};2k\omega_n,\tau))\right]\\&+y(t_{n-1})\cdot e^{-(t-t_{n-1})/\tau}\end{aligned} \tag{2.11}$$

$$\textbf{(B)}\quad f(u(t)) = \sum_{i=1}^{2m-1} a_i \cdot u^i(t), \tag{2.12}$$

$$\begin{aligned} y(t) = & \sum_{j=1}^{m} a_{2j} \binom{2j}{j} \frac{1}{2^{2j}} g_0(t - t_{n-1}; \tau) \\ & + \sum_{j=1}^{m} \frac{a_{2j-1}}{2^{2j-2}} \left[\sum_{k=1}^{m} (-1)^{k-1} \cdot \binom{2j-1}{j-k} \cdot (\cos((2k-1)\phi_n) \cdot g_s(t - t_{n-1}; (2k-1)\omega_n, \tau) \right. \\ & \left. + \sin((2k-1)\phi_n) \cdot g_c(t - t_{n-1}; (2k-1)\omega_n, \tau)) \right] \\ & + \sum_{j=1}^{m-1} \frac{a_{2j}}{2^{2j-1}} \left[\sum_{k=1}^{m-1} (-1)^k \binom{2j}{j-k} (\cos(2k\phi_n) \cdot g_c(t - t_{n-1}; 2k\omega_n, \tau) - \sin(2k\phi_n) \cdot g_s(t - t_{n-1}; 2k\omega_n, \tau)) \right] \\ & + y(t_{n-1}) \cdot e^{-(t-t_{n-1})/\tau} \end{aligned} \tag{2.13}$$

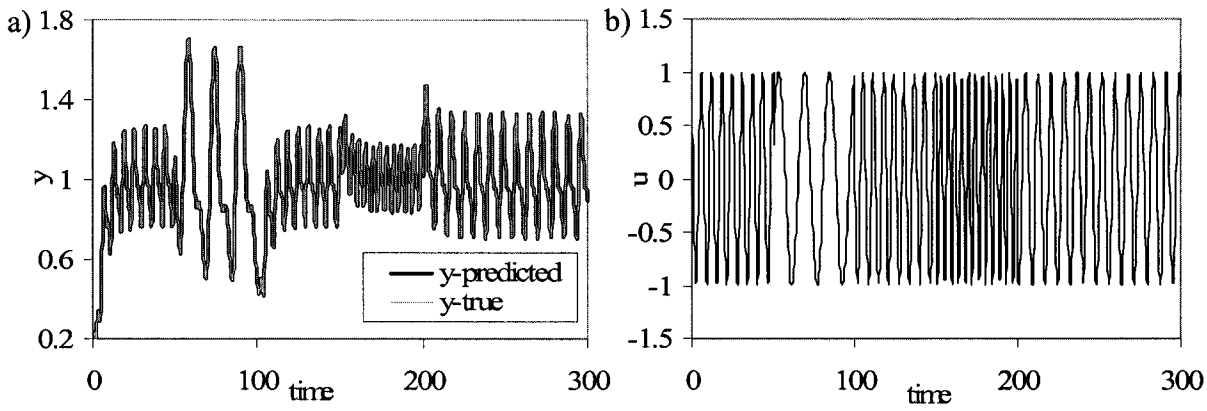

Figure 2.3. a) Simulated outputs (y-true) and predicted outputs (y-predicted) by (2.11) on a theoretical Hammerstein model described above for Case II (A) with b) the input sequence (u); the ω_i varies from 0.4 to 1.5, and ϕ_i varies arbitrarily.

2.3.2 The Hammerstein system with 2nd-order dynamics

The following results are for a SISO Hammerstein system with second-order dynamics as described in (2.14) and (2.15):

$$\tau_1\tau_2 \frac{d^2y(t)}{dt^2} + (\tau_1 + \tau_2) \cdot \frac{dy(t)}{dt} + y(t) = v(t) = f(u(t)) \tag{2.14}$$

with the transfer function in the Laplace domain as:

$$G(s)=\frac{Y(s)}{V(s)}=\frac{1}{(\tau_1 s+1)(\tau_2 s+1)} \tag{2.15}$$

Case I. The sequence with sinusoidal input changes imposed on the step input changes described in (2.3) is introduced to the above Hammerstein system. For the quadratic nonlinear static mapping relationship given in (2.4), the algorithm for the Hammerstein system are written in (2.16) to (2.21) for the time interval $t_{n-1} < t \le t_n$:

$$\begin{aligned} y(t)=&\left(a_1 b_n + a_2 b_n{}^2 + \frac{1}{2}a_2 A_n{}^2\right)\cdot g_{20}(t-t_{n-1};\tau_1,\tau_2)+(a_1 A_n + 2a_2 b_n A_n)\cdot g_{2s}(t-t_{n-1};\omega_n,\tau_1,\tau_2) \\ &-\frac{1}{2}a_2 A_n{}^2\cdot g_{2c}(t-t_{n-1};2\omega_n,\tau_1,\tau_2)+y(t_{n-1})\cdot g_{02}(t-t_{n-1};\tau_1,\tau_2)+y'(t_{n-1})\cdot g_{12}(t-t_{n-1};\tau_1,\tau_2) \end{aligned} \tag{2.16}$$

where:

$$\begin{aligned} g_{2s}(t;\omega,\tau_1,\tau_2)=&\frac{\omega\tau_1^2\cdot e^{-t/\tau_1}}{(\tau_1-\tau_2)(1+\omega^2\tau_1^2)}+\frac{\omega\tau_2^2\cdot e^{-t/\tau_2}}{(\tau_2-\tau_1)(1+\omega^2\tau_2^2)} \\ &+\frac{(1-\omega^2\tau_1\tau_2)\sin(\omega t)-\omega(\tau_1+\tau_2)\cdot\cos(\omega t)}{(1+\omega^2\tau_1^2)(1+\omega^2\tau_2^2)} \end{aligned} \tag{2.17}$$

$$\begin{aligned} g_{2c}(t;\omega,\tau_1,\tau_2)=&\frac{-\tau_1\cdot e^{-t/\tau_1}}{(\tau_1-\tau_2)(1+\omega^2\tau_1^2)}+\frac{-\tau_2\cdot e^{-t/\tau_2}}{(\tau_2-\tau_1)(1+\omega^2\tau_2^2)} \\ &+\frac{(1-\omega^2\tau_1\tau_2)\cos(\omega t)-\omega(\tau_1+\tau_2)\cdot\sin(\omega t)}{(1+\omega^2\tau_1^2)(1+\omega^2\tau_2^2)} \end{aligned} \tag{2.18}$$

$$g_{20}(t;\tau_1,\tau_2)=1+\frac{\tau_1}{\tau_2-\tau_1}e^{-t/\tau_1}-\frac{\tau_2}{\tau_2-\tau_1}e^{-t/\tau_2} \tag{2.19}$$

$$g_{02}(t;\tau_1,\tau_2)=\frac{\tau_1 e^{-t/\tau_1}-\tau_2 e^{-t/\tau_2}}{\tau_1-\tau_2} \tag{2.20}$$

$$g_{12}(t;\tau_1,\tau_2)=\frac{\tau_1\tau_2\cdot e^{-t/\tau_1}-\tau_1\tau_2 e^{-t/\tau_2}}{\tau_1-\tau_2} \tag{2.21}$$

The simulation results are shown in Figure 2.4 for quadratic static mappings on a theoretical Hammerstein model. The dataset of y-true is simulated from a nonlinear process

that can be described as follows:

$$v(t) = 1.0 \cdot u(t) + 2.0 \cdot u^2(t) \text{ and } 15.0\frac{d^2y(t)}{dt^2} + 8.0\frac{dy(t)}{dt} + y(t) = v(t) \text{ with } y(0) = 0,\ y'(0) = 0$$

As shown by Figure 2.4, the predicted process outputs and the simulated process values have exact agreement for nonlinear static mappings. In this example, the nonlinear Hammerstein system enlarges the oscillation considerably and shows larger deviations from the steady state than the input variable. Even though the behavior of the nonlinear system is highly complex, exact prediction is obtained from the proposed algorithm.

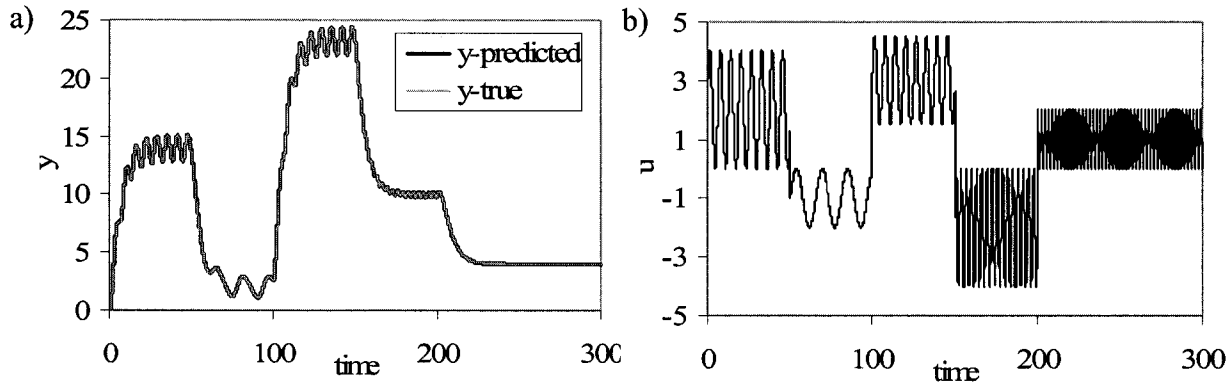

Figure 2.4. a) Simulated outputs (y-true) and predicted outputs (y-predicted) by (2.16) on a theoretical Hammerstein process described above with $\tau_1 = 5.0$, $\tau_2 = 3.0$, $a_1 = 1.0$, $a_2 = 2.0$ for b) a sinusoidal input sequence with ω_i varying from 0.4 to 3.0.

Case II. The sinusoidal input change with changing phase as described by (2.9) is introduced to the Hammerstein system. The algorithm for the Hammerstein system can be written as (2.22) for the static mapping given in (2.4) in the time interval $t_{n-1} < t \leq t_n$.

The same Hammerstein process described for Case I is used in this case but with a sinusoidal input sequence with phase changes. The simulation results are shown in Figure 2.5 for nonlinear (quadratic) static mappings on a true Hammerstein model. As before, the predicted response and the true response agree exactly.

$$
\begin{aligned}
y(t) = {} & \frac{1}{2} a_2 A_n{}^2 \cdot g_{20}(t - t_{n-1}; \tau_1, \tau_2) + a_1 A_n \cos\phi_n \cdot g_{2s}(t - t_{n-1}; \omega_n, \tau_1, \tau_2) \\
& + \frac{a_2 A_n{}^2}{2} \sin 2\phi_n \cdot g_{2s}(t - t_{n-1}; 2\omega_n, \tau_1, \tau_2) \\
& + a_1 A_n \sin\phi_n \cdot g_{2c}(t - t_{n-1}; \omega_n, \tau_1, \tau_2) - \frac{1}{2} a_2 A_n{}^2 \cos 2\phi_n \cdot g_{2c}(t - t_{n-1}; 2\omega_n, \tau_1, \tau_2) \\
& + y(t_{n-1}) \cdot g_{02}(t - t_{n-1}; \tau_1, \tau_2) + y'(t_{n-1}) \cdot g_{12}(t - t_{n-1}; \tau_1, \tau_2)
\end{aligned}
\tag{2.22}
$$

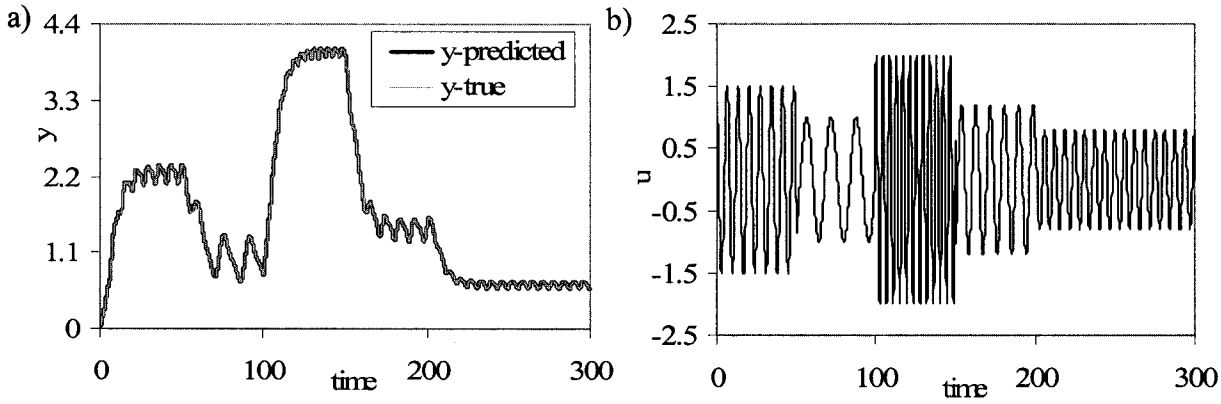

Figure 2.5. a) Simulated outputs (y-true) and predicted outputs (y-predicted) by (2.22) on a theoretical Hammerstein process described above for Case II with τ_1=5.0, τ_2=3.0, a_1=1.0, a_2=2.0 and b) input sequence u with ω_i, A_i, and ϕ_i varying arbitrarily.

2.3.3 The Wiener system with first-order dynamics

The following algorithms are for a SISO Wiener system with first-order dynamics, as described by (2.23) and (2.24) below:

$$
\tau \frac{dv(t)}{dt} + v(t) = u(t) \tag{2.23}
$$

which gives the transfer function in the Laplace domain as:

$$
G(s) = \frac{V(s)}{U(s)} = \frac{1}{\tau s + 1} \tag{2.24}
$$

g(t) is its corresponding function in the time domain. And $y(t) = f(v(t))$ gives the nonlinear static mapping, which can be any nonlinear relation.

Case I. When the sinusoidal input change described by (2.3) is introduced into the Wiener system, the algorithm for the interval $t_{n-1} < t < t_n$ is given by (2.25):

$$v(t) = b_n \cdot g_0(t - t_{n-1}; \tau) + A_n \cdot g_s(t - t_{n-1}; \omega_n, \tau) + v(t_{n-1}) \cdot e^{-(t-t_{n-1})/\tau} \qquad (2.25)$$

where $g_0(t;\tau)$, and $g_s(t;\omega,\tau)$ are defined as before.

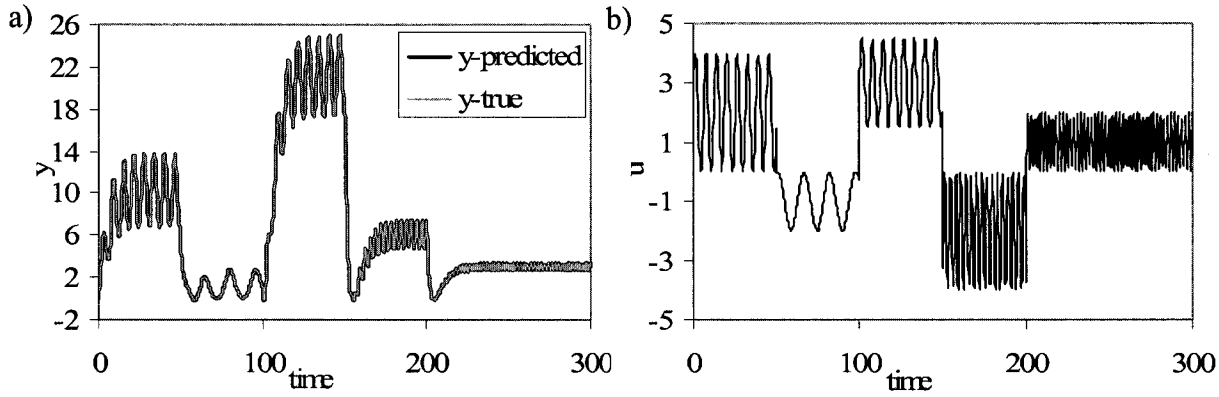

Figure 2.6. a) Simulated outputs (y-true) and predicted outputs (y-predicted) on a theoretical Wiener process for Case I when forced by b) a sinusoidal input change sequence (u) with different ω_i, b_i, and A_i values.

The simulation is done for quadratic nonlinear static mapping on a theoretical Wiener process as shown in Figure 2.6. The dataset of y-true is simulated from a Wiener process that can be described as follows:

$$5.0\frac{dv(t)}{dt} + v(t) = u(t) \text{ with } v(0) = 0 \text{ and } y(t) = 1.0 \cdot v(t) + 2.0 \cdot v^2(t)$$

As shown by Figure 2.6a, the predicted outputs and the true process show perfect agreement for the arbitrary input sequence given in Figure 2.6b.

Case II. The same Wiener process as given in the previous subsection is employed here but with a different input sequence. More specifically, the sinusoidal input change with changing phase described by (2.7) is considered here. The algorithms in the interval

$t_{n-1} < t \le t_n$ for the Wiener system are given below:

$$v(t) = A_n \sin(\phi_n) \cdot g_c(t - t_{n-1}; \omega_n, \tau) + A_n \cos(\phi_n) \cdot g_s(t - t_{n-1}; \omega_n, \tau) + v(t_{n-1}) \cdot e^{-(t-t_{n-1})/\tau} \quad (2.26)$$

The simulation results are shown in Figure 2.7 for quadratic static mapping on a true Wiener system. The predicted outputs and the process values overlap exactly.

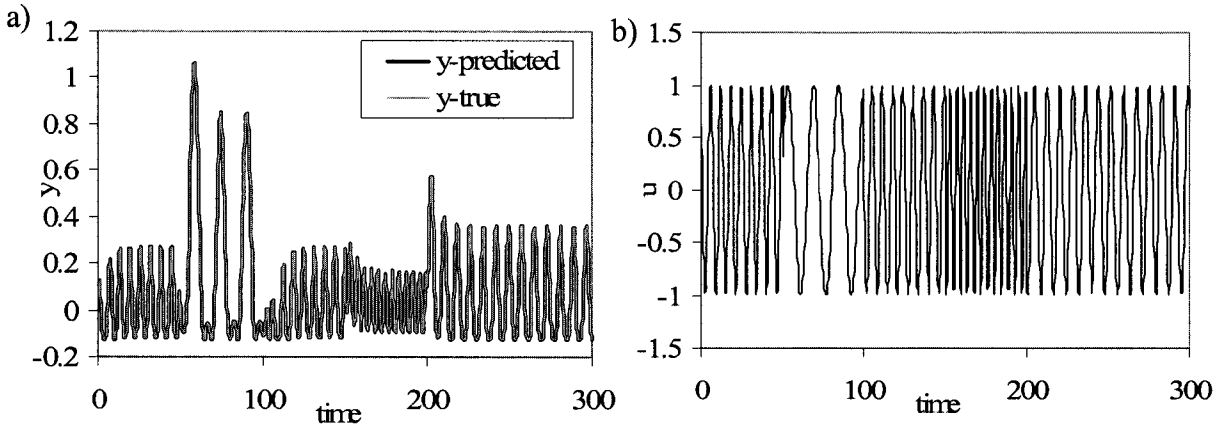

Figure 2.7. a) Simulated outputs (y-true) and predicted outputs (y-predicted) by (2.26) on a true Wiener model described above for Case II; b) the input sequence (u) has ω_i varying from 0.4 to 1.5, and ϕ_i varying arbitrarily.

2.3.4 The Wiener system with 2nd-order dynamics

The results in this section are based on a SISO Wiener system with second-order dynamics as described by (2.27) and (2.28):

$$\tau_1 \tau_2 \frac{d^2 v(t)}{dt^2} + (\tau_1 + \tau_2) \cdot \frac{dv(t)}{dt} + v(t) = u(t) \quad (2.27)$$

with the transfer function in the Laplace domain as:

$$G(s) = \frac{V(s)}{U(s)} = \frac{1}{(\tau_1 s + 1)(\tau_2 s + 1)} \quad (2.28)$$

Case I. The sinusoidal input change sequences described in (2.3) is introduced to the Wiener system with second-order dynamics. The algorithm for the Wiener system is written in

(2.29) below for the time interval $t_{n-1} < t \le t_n$:

$$v(t) = b_n \cdot g_{20}(t - t_{n-1}; \tau_1, \tau_2) + A_n \cdot g_{2s}(t - t_{n-1}; \omega_n, \tau_1, \tau_2) + v(t_{n-1}) \cdot g_{02}(t - t_{n-1}; \tau_1, \tau_2) + v'(t_{n-1}) \cdot g_{12}(t - t_{n-1}; \tau_1, \tau_2) \quad (2.29)$$

The simulation results are shown in Figure 2.8 for quadratic static mappings on a true Wiener model. The dataset of y-true is simulated from a nonlinear process that can be described as follows:

$$15.0\frac{d^2v(t)}{dt^2} + 8.0\frac{dv(t)}{dt} + v(t) = u(t) \text{ with } v(0) = 0, v'(0) = 0 \text{ and } y(t) = 1.0 \cdot v(t) + 2.0 \cdot v^2(t)$$

As seen from this figure, the predicted process outputs and the simulated process values have exact agreement for the nonlinear static mappings. In this example, the output sometimes shows much larger deviations from the initial steady state than the input.

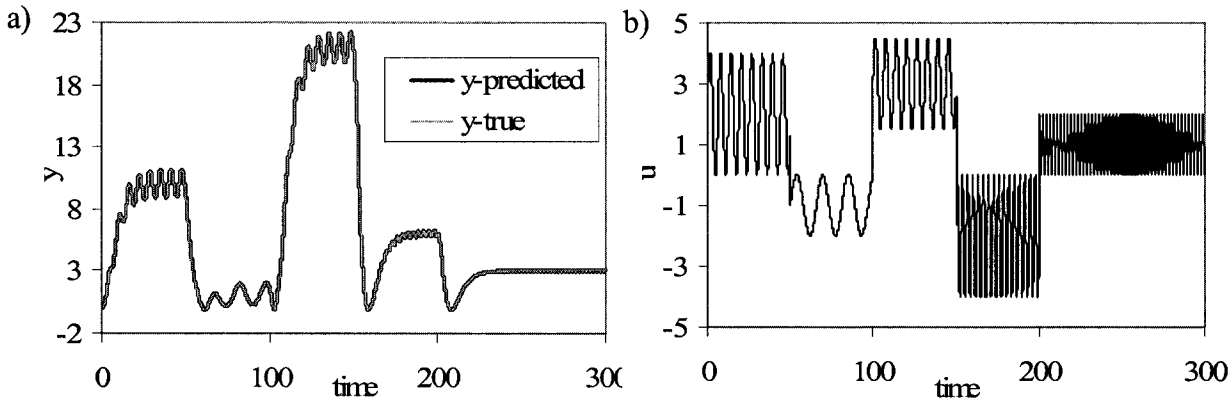

Figure 2.8. a) Simulated outputs (y-true) and predicted outputs (y-predicted) by (2.29) on a true Wiener process described above for Case I with $\tau_1 = 5.0$, $\tau_2 = 3.0$, $a_1 = 1.0$, $a_2 = 2.0$, and b) the input sequence (u) has ω_i varying from 0.4 to 3.0, A_i, and b_i varying arbitrarily.

Case II. The sinusoidal input change with changing phase as described by (2.7) is introduced to the Wiener system. The algorithm for the Wiener system can be written as (2.17) in the time interval $t_{n-1} < t \le t_n$.

$$v(t) = A_n \cos\phi_n \cdot g_{2s}(t - t_{n-1}; \omega_n, \tau_1, \tau_2) + A_n \sin\phi_n \cdot g_{2c}(t - t_{n-1}; \omega_n, \tau_1, \tau_2) + v(t_{n-1}) \cdot g_{02}(t - t_{n-1}; \tau_1, \tau_2) + v'(t_{n-1}) \cdot g_{12}(t - t_{n-1}; \tau_1, \tau_2) \quad (2.30)$$

The same Wiener process described for Case I is used in this case but with a sinusoidal input sequence with phase changes. The simulation results are shown in Figure 2.9 for nonlinear (quadratic) static mappings on a true Wiener model. As previously, the predicted response and the true response agree exactly.

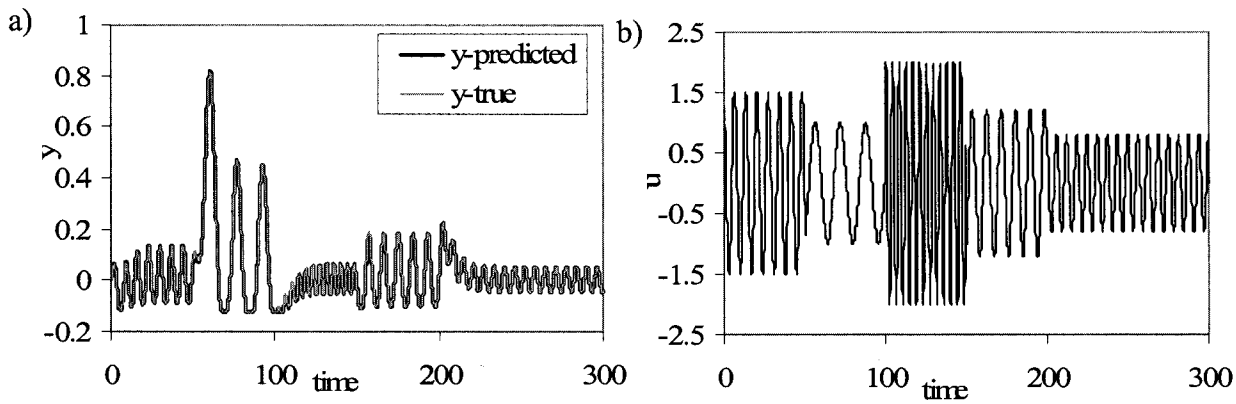

Figure 2.9. a) Simulated outputs (y-true) and predicted outputs (y-predicted) by (2.30) on a theoretical Wiener process described above for Case II with τ_1=5.0, τ_2=3.0, a_1=1.0, a_2=2.0 for b) a sinusoidal input sequence with ω_i, A_i, and ϕ_i varying arbitrarily.

2.3.5 Systems with time delay

Often a high order system can be approximated by lower order dynamics (either first-order or second-order) with dead time (Seborg et al, 1989). Thus, algorithms for a system with time delay can be useful and are therefore, needed in practice.

Once the dead time θ for a process is identified, it can be used with our proposed algorithms with the following modification: for each time interval, replacing t in the formulas for the system without time delay (as given in the previous sections) with $(t-\theta)$ gives the formulas for the system with time delay.

2.4 Applications

Though the algorithms provided in the previous section are all for SISO Hammerstein and Wiener systems, it is not difficult to apply them to the MIMO systems as shown below.

2.4.1 Application to MIMO Hammerstein system

To illustrate this application, suppose that a process is modeled by a two-input, two-output (TITO) Hammerstein system (see Figure 2.10) and the simulation results and predicted outputs are presented in this section.

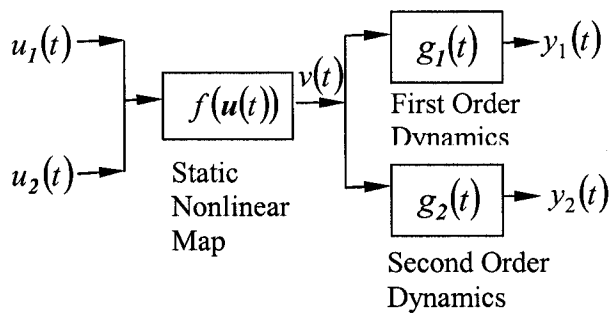

Figure 2.10. A TITO Hammerstein system.

The nonlinear static mapping function with the interaction term can be written as:

$$v(t) = f(u_1(t), u_2(t)) = a_1 \cdot u_1(t) + a_2 \cdot u_1^2(t) + a_3 \cdot u_2(t) + a_4 \cdot u_2^2(t) + a_5 \cdot u_1(t) \cdot u_2(t) \quad (2.31)$$

where $v(t)$ goes through first-order dynamics to give $y_1(t)$ and through second-order dynamics to give $y_2(t)$. The coefficient matrix is arbitrarily chosen as $[1 \quad 1 \quad -1 \quad -1 \quad 1]$.

Arbitrary sinusoidal sequences are introduced into this TITO Hammerstein system. The corresponding outputs for first- and second-order dynamics are plotted in Figure 2.11. The predicted responses and the true process responses overlap exactly, as shown. The system with second-order dynamics has a less oscillatory response than that with first-order dynamics, which confirms the frequency analysis results.

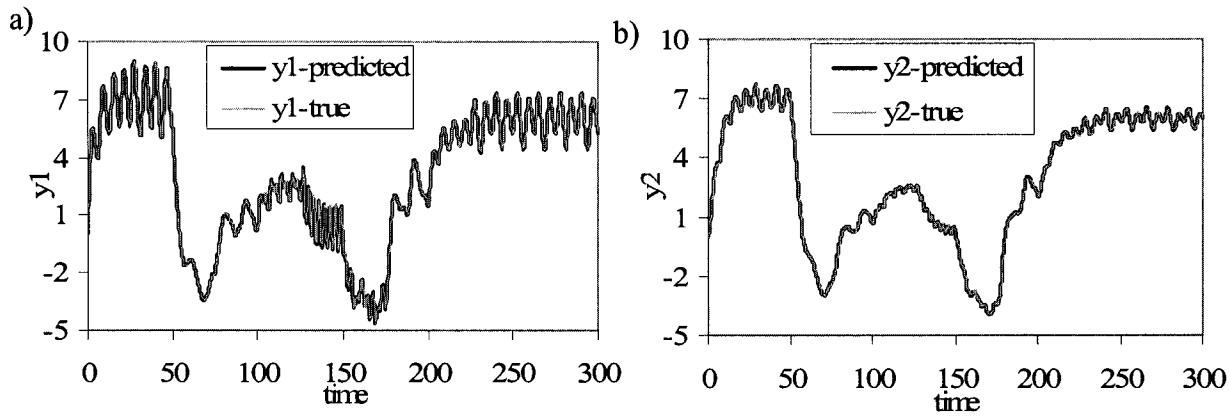

Figure 2.11. The predicted TITO Hammerstein process outputs (y1-predicted and y2-predicted) and the corresponding theoretical outputs (y1-true and y2-true) for first- and second-order dynamics, respectively, agree exactly.

2.4.2 Application to MIMO Wiener system

Assume that a process can be modeled by a TITO Wiener system (see Figure 2.12) and sinusoidal input changes are introduced into it. Furthermore, assume that this process can be represented by the following TITO Wiener system theoretically as shown in Figure 2.12. One input $u_1(t)$ follows the first order dynamics to give $v_1(t)$ and the other input $u_2(t)$ follows the second order dynamics to give $v_2(t)$. Thus, the final responses are obtained by the following nonlinear static function (2.32) and (2.33) with the interaction term.

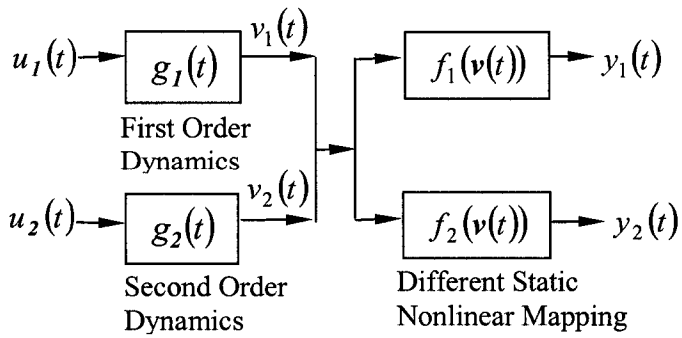

Figure 2.12. A TITO Wiener system.

$$y_1(t) = f_1(v_1(t), v_2(t)) = a_{11} \cdot v_1(t) + a_{12} \cdot v_1^{\,2}(t) + a_{13} \cdot v_2(t) + a_{14} \cdot v_2^{\,2}(t) + a_{15} \cdot v_1(t) \cdot v_2(t) \quad (2.32)$$

$$y_2(t) = f_2(v_1(t), v_2(t)) = a_{21} \cdot v_1(t) + a_{22} \cdot v_1^{\,2}(t) + a_{23} \cdot v_2(t) + a_{24} \cdot v_2^{\,2}(t) + a_{25} \cdot v_1(t) \cdot v_2(t) \quad (2.33)$$

where $a_{11} = 1$, $a_{12} = 1$, $a_{13} = -1$, $a_{14} = -1$, and $a_{15} = 1$; $a_{21} = -1$, $a_{22} = 1$, $a_{23} = 1$, $a_{24} = 0$, and $a_{25} = -1$ are chosen arbitrarily.

The process outputs with different static mappings after the sinusoidal input change sequences with arbitrary amplitudes and frequencies are introduced into the TITO Wiener system are shown in Figure 2.13. As shown, the predicted outputs by the closed-form compact algorithm agree with the true Wiener system outputs exactly. Since each input has its own dynamic block, to include more inputs is straightforward once the dynamic relations, static nonlinear mapping, and the corresponding parameters are identified.

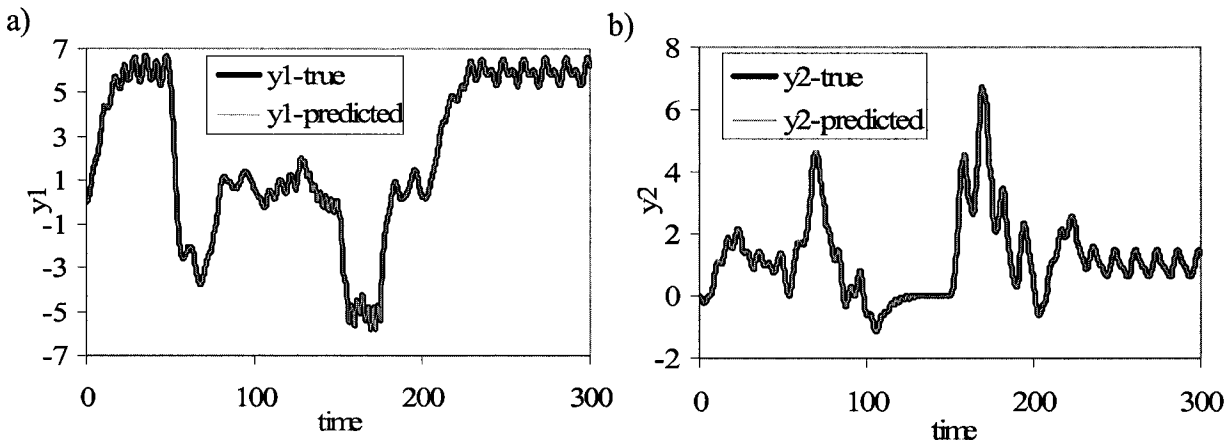

Figure 2.13. The predicted TITO Wiener process outputs (y1-predicted and y2-predicted) and the corresponding theoretical outputs (y1-true and y2-true) for different static mappings agree exactly.

2.5 Concluding remarks

The process dynamics analysis of the nonlinear systems under sinusoidal input changes is performed for first-order and second-order overdamped dynamics of block-oriented

Hammerstein and Wiener systems. The closed-form compact algorithms for sinusoidal input changes considering the amplitude, frequency and phase changes are provided. By simulation on theoretical Hammerstein and Wiener systems, the predicted responses by these algorithms demonstrate exact agreement with the true process responses. Only the previous input information, the output response, and its derivative (for the second-order dynamics) at the time of change are needed for the algorithm. The single-input, single-output (SISO) algorithms can be applied to multiple -input, multiple-output (MIMO) systems as demonstrated in the two-input, two-output (TITO) example. The predictions and the simulated theoretical system responses agree exactly in all cases.

The proposed first-order and second-order overdamped algorithms, and their extensions to the dynamics with dead time, can cover a wide range of dynamic processes that can be modeled as Hammerstein and Wiener systems. As pointed out by Hajjari and Eloutassi (1999), noisy measurements can be described as summations of sinusoidal waves with an additive noise term. Once the sine wave parameters for the input sequence and the model parameters are estimated, the closed-form compact algorithms provided in this work can be applied to obtain the system outputs. See Hajjari and Eloutassi (1999) for a method to obtain periodic functions from noisy signal in practice.

References

Bhandari, N. and Rollins, D.K., Continuous-time Hammerstein nonlinear modeling applied to distillation, *AIChE Journal,* **50**(2): 530-533 (2003a).

Bhandari, N. and Rollins, D.K., Continuous-time multi-input, multi-output Wiener modeling method, *Industrial & Engineering Chemistry Research,* **42**(22): 5583-5595 (2003b).

Doyle, F.J. III, Pearson, R.K., and Ogunnaike, B.A., *Identification and Control Using*

Volterra Models, Springer-Verlag London Limited, Great Britain, 2002.

Eskinat, E., Johnson, S.H. and Luyben, W.L., Use of Hammerstein models in identification of nonlinear systems, *AIChE Journal*, **37**: 255-268 (1991)

Greblicki, W., Nonparametric identification of Wiener systems, *IEEE Transactions on Information Theory*, **38**: 1487-1493 (1992).

Greblicki, W., Nonparametric approach to Wiener system identification, *IEEE Transactions on Circuits Systems I*, **44**: 538-545 (1997).

Greblicki, W., Continuous-time Hammerstein system identification, *IEEE Transactions on Automatic Control*, **45**: 1232-1236 (2000).

Hajjari, A. and Eloutassi, O., Extracting sine waves from noisy measurements and estimating their parameters, *Proceeding of the IASTED International Conference, Intelligent Systems and Control*, Santa Barbara, CA, 341-345, 1999.

M.A. Henson and D.E. Seborg, *Nonlinear process control*, Upper Saddle River, NJ; Prentice Hall PTR, 1997.

Huang, H.-P., Lee, M.-W. and Tang, Y.-T., Identification of Wiener model using relay feedback test, *Journal of Chemical Engineering of Japan*, **31**: 604-612 (1998).

Ikonen, E. and Najim, K., Non-linear process modeling based on a Wiener approach, *Journal of Systems and Control Engineering*, **215**: 15-27 (2001).

Kalafatis, A., Arifin, N., Wang, L. and Cluett, W.R., A new approach to the identification of pH process based on the Wiener model, *Chemical Engineering Science*, **50**: 3693-3701 (1995).

Narendra, K.S. and Gallman, P.G., An iterative method for the identification of the nonlinear system using the Hammerstein model, *IEEE Trans. Automatic Control*, **12**: 546-550 (1966).

Rollins, D.K., Bhandari, N., Bassily, A.M., Colver, G.M. and Chin, S.-T., A continuous-time nonlinear dynamic predictive modeling method for Hammerstein processes, *Industrial & Engineering Chemistry Research,* **42**(4): 861-872 (2003).

Rollins, D.K., Pacheco, L. and Bhandari, N., A quantitative measure to evaluate competing designs for nonlinear dynamic process identification, submitted to *The Canadian Journal of Chemical Engineering*, 2004.

Seborg, D.E., Edgar, T.F. and Mellichamp, D.A., *Process dynamics and control*, New York, NY: John Wiley & Sons, 1989.

Su, H.-T. and McAvoy, T.J., Integration of multilayer perceptron networks and linear dynamic models: A Hammerstein model approach, *Industrial & Engineering Chemistry Research*, **32**: 1927-1936 (1993).

Wigren, T., Recursive prediction error identification using the nonlinear Wiener model, *Automatica*, **29**: 1011-1025 (1993).

Zhu, X. and Seborg, D.E., Nonlinear predictive control based on Hammerstein models, *Control Theory and Applications*, **11**: 564-575 (1994).

Chapter 3. Compact Continuous-Time Modeling for Nonlinear Systems With More Complicated Dynamics Under Sinusoidal Forcing Inputs

3.1 Introduction

Most real physical processes behave nonlinearly to some extent. Examples of such chemical processes include: higher-order reaction, distillation, pH neutralization, heat exchange, and incomplete mixing that follows a power law. Since many processes exhibit only mildly nonlinear dynamic behavior over limited ranges, linear models, which are simple and convenient, can usually approximate them reasonably. Thus, with effective regulatory control where deviations from steady state are small, it is often reasonable to treat such systems as approximately linear. However, this is not adequate for systems that have strong nonlinear behavior and deviate significantly from normal operating conditions. For these systems, nonlinear models, which are more realistic and accurate, though less simple, should be adopted. During the past decade, more and more researchers have been working on developing nonlinear models instead of approximate linear models. This is motivated by the need for improving the product quality and reducing energy and material consumption. The model should match the requirements of control — harmonious in structure and complexity, and approximate the true process closely as pointed out by Pearson and Ogunnaike (1997).

Empirical model building from the input and output data gathered from experiments on the process, is one approach to model the process. The principles or internal mechanism of the process can be unknown and the process is treated as a "black box." After selecting a model structure, for example, Artificial Neural Network (ANN) (Normandin et al., 1994), or multiple linear regression. Model parameters are estimated based on the experimental input and output data. Hence, for empirical model building, extensive measurements of process behavior are required although detailed process knowledge is not required.

Hammerstein and Wiener models belong to the class of block-oriented models, which are series or parallel combinations of linear dynamics blocks and static nonlinear mappings. A Hammerstein model consists of a static nonlinear mapping or gain followed by a linear dynamic block. The input vector **u**(t) goes through the nonlinear static mapping block and gives an unobservable intermediate vector **v**(t). Then **v**(t) goes through the linear dynamic block to give the output vector, **y**(t) with **f**(**u**(t)) and **g**(t) denoting the nonlinear static gain vector and the linear dynamic vector respectively, **v**(t) = **f**(**u**(t)) and each element of **y**(t) is $y_i(t) = \int_0^t v_i(\xi) \cdot g_i(t-\xi) \cdot d\xi$. The Wiener model has the same two type of blocks as the Hammerstein model, but in the reverse order. In the Wiener model structure, the input vector **u**(t) is transformed by the linear dynamic block to get **v**(t), and then **v**(t) goes through the static nonlinear block to produce **y**(t). Mathematically, each element of **v**(t) is $v_i(t) = \int_0^t u_i(\xi) \cdot g_i(t-\xi) \cdot d\xi$ and **y**(t) = **f**(**v**(t)).

The Hammerstein and Wiener models have simple structures are among most popular block-oriented nonlinear model structures. They can represent many processes with nonlinear characteristics adequately. They have been employed to model nonlinear chemical processes, including pH neutralization (Zhu and Seborg, 1994; Kalafatis et al., 1995; Norquay et al. 1999a,b;), high purity distillation (Eskinat et al., 1991) and polymerization process (Su and McAvoy, 1993). Due to their simple structures and efficient parameterization, the Hammerstein and Wiener models have many applications in practice and are increasing in popularity. Most modeling problem have involved the use of discrete-time methods (Doyle et al., 2002; etc., Greblicki, 1992, 1997; Wigren, 1993; etc.); exception include Greblicki (1999, 2000), Rollins at al. (2003), and Bhandari and Rollins (2003a), who employed continuous-time approaches. The method proposed by Greblicki (2000) was nonparametric and the dynamic block was identified using impulse response methods.

However, this article concentrated on the parametric continuous-time approaches proposed by Rollins and coworkers, called the block-oriented exact solution technique (H-BEST and W-BEST) for the Hammerstein and Wiener models respectively.

Discrete-time data are often obtained by observing a continuous-time process at a discrete sequence of times. Thus, discrete modeling with numerical analysis is widely used. The variables are assumed to remain fixed between one sample instant and the next, though variables in most physical processes are continuously changing, which means the information in between is missing. Furthermore, in discrete-time method (DTM), the sampling conditions, such as sampling time and frequency, play an important role in prediction. It is then nature to model the underlying process as a continuous-time process even though the observations are made at discrete times. The advantage of the continuous-time model (CTM) is obvious when the sampling times are irregular. However, in system engineering, CTM has seen limited applications even though it has the advantage of prediction at any time. Other advantages of CTM over DTM include fewer coefficients and parameters with physical meaning. For a continuous model, it is possible to have a compact closed-form algorithm (Rollins et al. 2003), which does not require iterative calculations. As shown by Rollins et al. (Rollins et al. 2002b), statistical experimental design, such as a D-optimal design, can be carried out with an analytical algorithm. Also, CTM identification is often more convenient than DTM identification due to fewer parameters and a clear analytical algorithm form.

The H-BEST (Rollins et al., 2003) and W-BEST techniques (Bhandari and Rollins, 2003a) give the compact closed-form algorithms to the non-linear Hammerstein and Wiener block-oriented systems when they are excited by a sequence of step input changes. These techniques have been successfully applied to a household dryer (Rollins et al., 2003), a simulated continuous stirred tank reactor (CSTR) (Bhandari and Rollins, 2003a) and a distillation column (Bhandari and Rollins, 2003b). All these processes are multiple-input,

multiple-output (MIMO) nonlinear systems. The household dryer and distillation column processes were identified as Hammerstein systems, while the CSTR was identified as a Wiener system. It has been demonstrated that the block-oriented exact algorithm technique (BEST) can predict the process responses closely to the true process outputs based on the experimental and simulated processes. Comparisons with the corresponding discrete time models were carried out for both the CSTR and distillation column processes to demonstrate the advantage of the BEST techniques (Bhandari and Rollins, 2003a,b).

The algorithms provided by BEST technique are compact since they do not depend on all past input changes, but only a few recent input changes. With the compact algorithm, the response can be predicted without much previous output and input information except a few recent ones under the dynamics conditions. Based on the closed-form compact algorithm, it is possible to get the D-optimal design for identifying the parameters.

The BEST methods, including H-BEST and W-BEST, were extended to the sinusoidal input changes for the first-order and second-order dynamics and the algorithms for various input sequences and nonlinear static mapping have been shown to be the exact closed-form compact algorithms to the true Hammerstein and Wiener processes, and they were applied to two-input, two-output Hammerstein and Wiener systems, as an example of MIMO system and predict the outputs successfully (Zhai et al., 2004). This work extends the BEST techniques further to Hammerstein or Wiener systems with more complicated dynamics, second order plus lead (two poles, one zero) when the systems are subjected to the sinusoidal input changes. The closed-form compact algorithms are provided in Section 3.3. A MIMO CSTR is simulated by programming in C and this process was identified to be a MIMO Wiener system with second order plus lead dynamics by Bhandari and Rollins (2003a). It is assumed that the periodical input sequences or noisy step input changes are introduced into the CSTR. By adopting the dynamic parameters and the static mapping coefficients

identified by the BEST technique for this seven-input, five-output system, the prediction based on the proposed algorithms for the sinusoidal input change in this work is done and the methodology is then evaluated in Section 3.4. Conclusions are drawn in Section 3.5.

3.2 Problem statement

Periodic phenomena, either forced or natural, exist in many engineering applications. For example, the natural cycle of the upstream processes or environmental influences cause the periodical fluctuations. Sometimes, forced periodic operations are introduced to a system to improve selectivity and yield. But the drawback is also obvious. These periodically time-varying (PTV) systems are nonstationary and are thus hard to control, and the operation is more complicated (Pan and Lee, 2003). Analysis, control, and the system identification of a PTV system are interesting topics in the control area. Systems with sinusoidal changes are one special type of the PTV system. Periodic ARMA models and some other discrete time methods were used in modeling the PTV systems (Pan and Lee, 2003).

For such periodical changes, it is important to have a high sampling frequency to get the adequate information of the system to avoid aliasing. However, sufficiently frequent sampling is not always possible or available, especially for some variables, such as concentration of the distillation column. Of course, the periodical input changes can be approximated as piece-wise step changes. Either the discrete time method or the H-BEST methodology could be employed then. But these are not always accurate enough, and the predictions are available only at a discrete time points if the discrete time method is used. This problem can be partially solved by the continuous-time dynamic modeling method based on understanding of dynamic behavior and the nonlinearity of the system. Thus, there is a need for finding compact closed-form algorithm to sinusoidal input changes for a system that can be presented by a block-oriented model.

Meanwhile, a stationary time series can be decomposed into a sum of sinusoidal components with uncorrelated random coefficients with frequencies $\omega \in [0, \pi]$.

$$X(t) = \sum_{j=1}^{k} \left(A_j \cos(\omega_j t) + B_j \sin(\omega_j t) \right), \quad 0 < \omega_1 < \ldots < \omega_k < \pi \tag{3.1}$$

where, A_1, B_1, ..., A_k, B_k are uncorrelated random variables with $E(A_j) = 0$, and $Var(A_j) = Var(B_j) = \sigma^2$, $j = 1,\ldots,k$. In general, infinitely many sinusoids rather than a finite number should be included in the above equation. However, once the sinusoids with large amplitudes and major frequencies are included, this approximation works reasonable well for a stationary time series (Brockwell and Davis, 2002). Therefore, the sum of sinusoidal components can be employed to approximate a noisy step input changes after the spectral decomposition. Actually, Hajjari and Eloutassi (1999) proposed a method to obtain periodic components from noisy signal in practice.

The results from the process analysis will help us understand the process thoroughly. They can be employed to improve nonlinear modeling and predictive control, and to optimize the experimental design. Model predictive control (MPC) can be a promising way to control the PTV system efficiently and a good prediction model is the basis or core of MPC. The proposed algorithms can also be utilized for quantitatively comparing the information content of competing experimental designs using an optimality criterion. With the analytical closed-form algorithm to the process output, it is possible to calculate the derivation matrix, which determines the information content.

3.3 The algorithms to the Hammerstein and Wiener systems

In this section, the closed-form compact algorithms obtained based on the process analysis and the simulation results are presented for the Hammerstein and Wiener systems with second-order plus lead (SOPL) dynamics when they are excited by sinusoidal input

changes with phase changes, imposed on the step functions. Note that u, v and y are all deviation variables. Algorithms for systems with time delay are given in Section 3.3.3. Though only algorithms to a single-input, single-output (SISO) case are presented, it is straightforward to extend them to MIMO Hammerstein or Wiener systems. Applications to the true Hammerstein and Wiener systems are presented to show how the closed-form compact algorithms perform in predicting the process responses to the true Hammerstein and Wiener systems. Later on, the algorithms are applied to a MIMO simulated CSTR to demonstrate its ability to predict the outputs. The systems are subjected to the following input changes sequence.

$$u(t)=\begin{cases}0 & t\le 0\\ b_1+A_1\sin(\omega_1 t+\phi_1) & 0<t\le t_1\\ b_2+A_2\sin(\omega_2(t-t_1)+\phi_2) & t_1<t\le t_2\\ \vdots & \vdots\\ b_n+A_n\sin(\omega_n(t-t_{n-1})+\phi_n) & t_{n-1}<t\le t_n\end{cases} \tag{3.2}$$

For each time interval, the deviation of the input from the steady state is composed of a different step component and a sinusoidal component with different amplitude, frequency, and phase.

3.3.1 The Hammerstein system with SOPL dynamics

A SISO Hammerstein system with the SOPL dynamics can be described by (3.3) or (3.4):

$$\tau_1\tau_2\frac{d^2y(t)}{dt^2}+(\tau_1+\tau_2)\cdot\frac{dy(t)}{dt}+y(t)=\tau_a\frac{dv(t)}{dt}+v(t) \tag{3.3}$$

with initial condition $y(0)=0$ and $y'(0)=0$, which means the output is at its steady state. Here, $v(t)=f(u(t))$ is the static nonlinear mapping, τ_1 and τ_2 are the time constants, and τ_a is the time constant for the lead term. The corresponding transfer function in Laplace domain for (3.3) is

$$G(s)=\frac{Y(s)}{V(s)}=\frac{\tau_a s+1}{(\tau_1 s+1)(\tau_2 s+1)}. \tag{3.4}$$

It is assumed that the system is at the steady state at $t=0$ with $u(0)=0$. Note that (3.3) includes the effect of input dynamics. The sinusoidal input change given by (3.2) is introduced to the above Hammerstein system.

For the nonlinear static mapping relations $f(u(t))$ given by (3.5), the algorithms can be written as (3.6) shown below. The functions used in expressing the algorithm are given in (3.7) to (3.11).

For $f(u(t))=a_1u(t)+a_2u^2(t)$, (3.5)

$$\begin{aligned} y(t)=&\left(a_1b_i+a_2b_i^{\,2}+a_2A_i^{\,2}/2\right)\cdot g_{20}(t-t_{i-1};\tau_1,\tau_2)\\ &+(a_1A_i+2a_2b_iA_i)\cdot(\cos\phi_i-\omega_i\tau_a\sin\phi_i)\cdot g_{2s}(t-t_{i-1};\omega_i,\tau_1,\tau_2)\\ &+(a_1A_i+2a_2b_iA_i)\cdot(\sin\phi_i+\omega_i\tau_a\cos\phi_i)\cdot g_{2c}(t-t_{i-1};\omega_i,\tau_1,\tau_2)\\ &+a_2A_i^{\,2}/2\cdot(\sin 2\phi_i+2\omega_i\tau_a\cos 2\phi_i)\cdot g_{2s}(t-t_{i-1};2\omega_i,\tau_1,\tau_2)\\ &+a_2A_i^{\,2}/2\cdot(2\omega_i\tau_a\sin 2\phi_i-\cos 2\phi_i)\cdot g_{2c}(t-t_{i-1};2\omega_i,\tau_1,\tau_2)\\ &+y(t_{i-1})\cdot g_{02}(t-t_{i-1};\tau_1,\tau_2)+y'(t_{i-1})\cdot g_{12}(t-t_{i-1};\tau_1,\tau_2) \qquad \text{for } t_{i-1}<t\le t_i \end{aligned} \tag{3.6}$$

where $i=1,...,n$, the functions $g_{20}(t;\tau_1,\tau_2)$, $g_{02}(t;\tau_1,\tau_2)$, $g_{12}(t;\tau_1,\tau_2)$ $g_{2s}(t;\omega,\tau_1,\tau_2)$, and $g_{2c}(t;\omega,\tau_1,\tau_2)$, are defined as follows.

$$g_{20}(t;\tau_1,\tau_2)=1+\frac{\tau_1}{\tau_2-\tau_1}e^{-t/\tau_1}-\frac{\tau_2}{\tau_2-\tau_1}e^{-t/\tau_2} \tag{3.7}$$

$$\begin{aligned} g_{2s}(t;\omega,\tau_1,\tau_2)=&\frac{\omega\tau_1^2e^{-t/\tau_1}}{(\tau_1-\tau_2)(1+\omega^2\tau_1^2)}+\frac{\omega\tau_2^2e^{-t/\tau_2}}{(\tau_2-\tau_1)(1+\omega^2\tau_2^2)}\\ &+\frac{(1-\omega^2\tau_1\tau_2)\sin(\omega t)-\omega(\tau_1+\tau_2)\cos(\omega t)}{(1+\omega^2\tau_1^2)(1+\omega^2\tau_2^2)} \end{aligned} \tag{3.8}$$

$$\begin{aligned} g_{2c}(t;\omega,\tau_1,\tau_2)=&\frac{-\tau_1e^{-t/\tau_1}}{(\tau_1-\tau_2)(1+\omega^2\tau_1^2)}+\frac{-\tau_2e^{-t/\tau_2}}{(\tau_2-\tau_1)(1+\omega^2\tau_2^2)}\\ &+\frac{(1-\omega^2\tau_1\tau_2)\cos(\omega t)+\omega(\tau_1+\tau_2)\sin(\omega t)}{(1+\omega^2\tau_1^2)(1+\omega^2\tau_2^2)} \end{aligned} \tag{3.9}$$

$$g_{02}(t;\tau_1,\tau_2)=\frac{\tau_1 e^{-t/\tau_1}-\tau_2 e^{-t/\tau_2}}{\tau_1-\tau_2} \tag{3.10}$$

$$g_{12}(t;\tau_1,\tau_2)=\frac{\tau_1\tau_2 e^{-t/\tau_1}-\tau_1\tau_2 e^{-t/\tau_2}}{\tau_1-\tau_2} \tag{3.11}$$

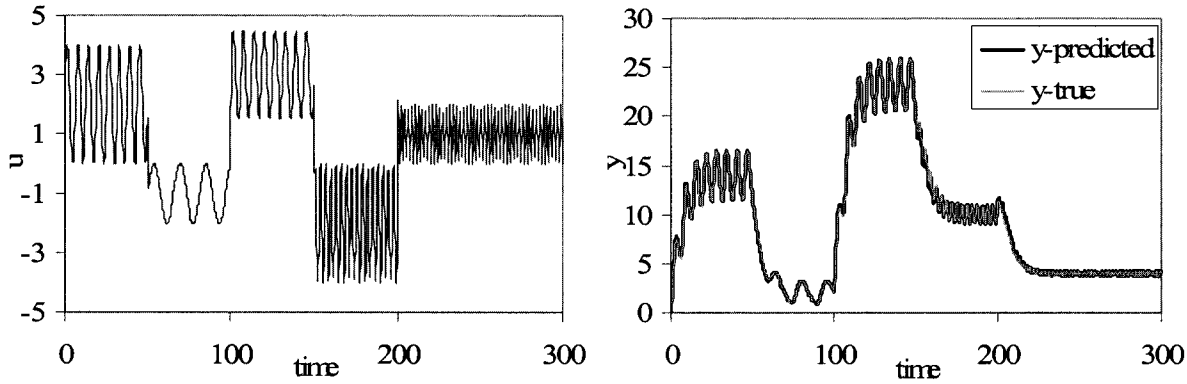

Figure 3.1. Simulated sinusoidal input (u), output (y) and predicted output by (3.6) on a true Hammerstein system described above with $\phi_i = 0$, $a_1 = 1.0$, $a_2 = 2.0$, $\tau_1 = 5.0$, $\tau_2 = 3.0$, $\tau_a = 2.0$, ω_i varying from 0.4 to 3.0, and b_i and A_i values varying arbitrarily.

The simulation results are shown in Figure 3.1 for nonlinear static mapping on a true Hammerstein process with SOPL dynamics. It is clear that the predicted outputs by (3.6) and the process outputs have almost exact agreement for quadratic static mapping when there was no phase change considered. The behavior of the nonlinear Hammerstein system shows large deviations from the steady state comparing with the input change. The nonlinear Hammerstein system enlarges the deviation considerably in this example.

Figure 3.2 is for a true Hammerstein model with quadratic nonlinear static mapping considering only the phase change but not any step input changes. Again, the predicted response and the true response overlap. The agreement is nearly perfect.

These two figures confirm that the algorithm are valid for true Hammerstein systems with SOPL dynamics.

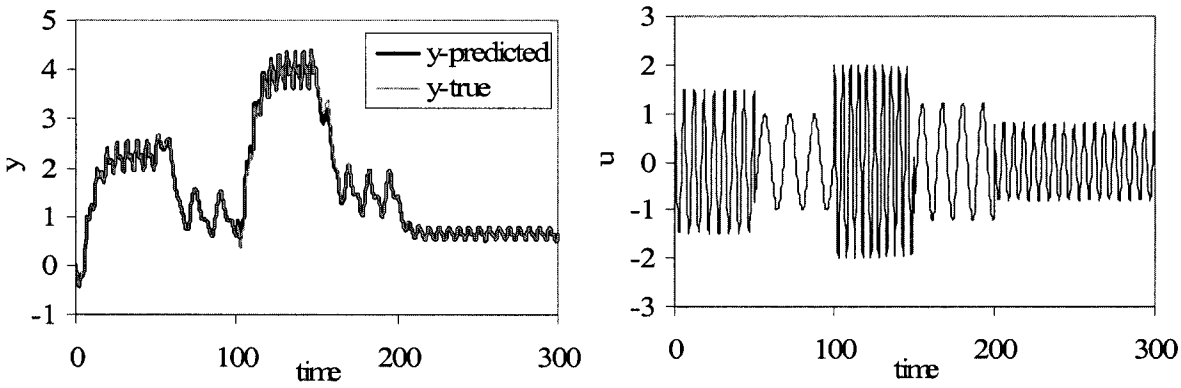

Figure 3.2. Simulated sinusoidal input (u), output (y) and predicted output by (3.6) on a true Hammerstein system described above with $b_i = 0$, $a_1 = 1.0$, $a_2 = 2.0$, $\tau_1 = 5.0$, $\tau_2 = 3.0$, $\tau_a = 2.0$, ω_i varying from 0.4 to 1.5, and ϕ_i and A_i values varying arbitrarily.

3.3.2 The Wiener system with SOPL dynamics

A SISO Wiener system with the SOPL dynamics can be described by

$$\tau_1\tau_2 \frac{d^2v(t)}{dt^2} + (\tau_1 + \tau_2)\cdot\frac{dv(t)}{dt} + v(t) = \tau_a \frac{du(t)}{dt} + u(t) \tag{3.12}$$

with $y(t) = f(v(t))$. τ_1 and τ_2 are the time constants; τ_a is the time constant for the lead term. Or, in Laplace domain, the dynamic block can be written as

$$G(s) = \frac{V(s)}{U(s)} = \frac{\tau_a s + 1}{(\tau_1 s + 1)(\tau_2 s + 1)}. \tag{3.13}$$

The sinusoidal input change given in (3.2) is introduced to the above Wiener system. The algorithm to *v(t)* is

$$\begin{aligned} v(t) &= b_i \cdot g_{20}(t - t_{i-1}; \tau_1, \tau_2) + A_i(\cos\phi_i - \omega_i\tau_a \sin\phi_i)\cdot g_{2s}(t - t_{i-1}; \omega_i, \tau_1, \tau_2) \\ &+ A_i(\sin\phi_i + \omega_i\tau_a \cos\phi_i)\cdot g_{2c}(t - t_{i-1}; \omega_i, \tau_1, \tau_2) \\ &+ v(t_{i-1})\cdot g_{02}(t - t_{i-1}; \tau_1, \tau_2) + v'(t_{i-1})\cdot g_{12}(t - t_{i-1}; \tau_1, \tau_2) \quad \text{for } t_{i-1} < t \le t_i \end{aligned} \tag{3.14}$$

where $i = 1,...,n$, and the definitions of those g functions are the same as (3.7) to (3.11). Therefore, the final process output y(t) can be obtained by plug v(t) into the $f(v(t))$ function, which can be any nonlinear function.

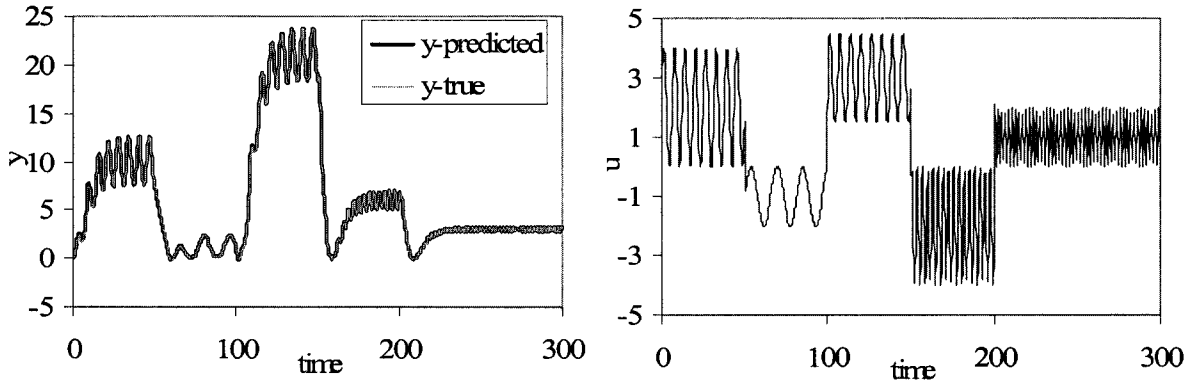

Figure 3.3. Simulated sinusoidal input (u), true output (y) and predicted output based on the algorithm for a true Wiener system described above when $\phi_i = 0$, and f is a quadratic polynomial function in (3.5) with $a_1 = 1.0$, $a_2 = 2.0$, $\tau_1 = 5.0$, $\tau_2 = 3.0$, $\tau_a = 2.0$, ω_i varying from 0.4 to 3.0, and b_i and A_i values varying arbitrarily.

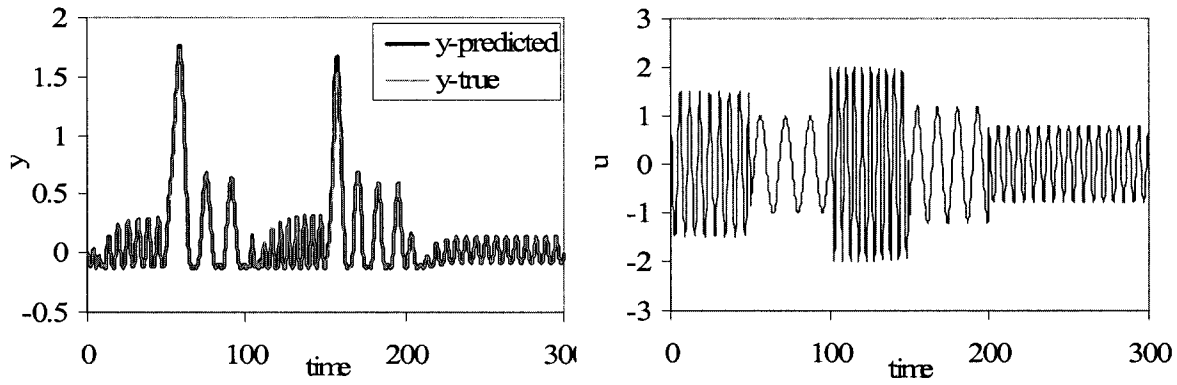

Figure 3.4. Simulated sinusoidal input (u), true output (y) and predicted output based on the algorithm for a true Wiener system described above with $b_i = 0$, where f is a quadratic polynomial function with $a_1 = 1.0$, $a_2 = 2.0$, $\tau_1 = 5.0$, $\tau_2 = 3.0$, $\tau_a = 2.0$, ω_i varying from 0.4 to 1.5, and ϕ_i and A_i values varying arbitrarily.

The simulation results are shown in Figure 3.3 for quadratic nonlinear static mapping on a true Wiener system without considering the phase changes. The predicted output and the process true output overlap for this Wiener system. The Hammerstein and the Wiener system behave quite differently sometimes though the parameters are all set to be exactly the same as seen in Figures 3.1 and 3.3. The inverse response can be seen for the Wiener system. Again, the case where the phase changes are considered only is shown in Figure 3.4. The agreement between the predicted output based on the algorithm and the true outputs confirms that the algorithm is exact to the nonlinear Wiener system.

3.3.3 System with time delay

Usually the higher order dynamic system can be approximated as lower order dynamics (either first order or second order) with dead time (Ogunnaike and Ray, 1994). Therefore, the algorithm to the system with time delay is valuable in practice, especially in the chemical engineering industry. After modeling the process as Hammerstein or Wiener system having lower order dynamics with time delay, and identifying the process parameters, including the dead time θ of the process, the algorithm to the system with time delay can be applied. For time interval (0, θ] or $0 < t \le \theta$, there is no deviation in the output or response yet; thus, the algorithm gives the output which is zero. For each of the rest of time intervals, the algorithm can be obtained by replacing *t* by *(t-θ)* in the formulas for the system without time delay given in the previous sections. For example, the algorithm to the Wiener system with the second order plus lead dynamics becomes

$$v(t)=\begin{cases} 0 & \text{for } 0 < t \le \theta \\ b_i \cdot g_{20}(t-\theta-t_{i-1};\tau_1,\tau_2)+A_i(\cos\phi_i-\omega_i\tau_a\sin\phi_i)\cdot g_{2s}(t-\theta-t_{i-1};\omega_i,\tau_1,\tau_2) & \\ \quad +A_i(\sin\phi_i+\omega_i\tau_a\cos\phi_i)\cdot g_{2c}(t-\theta-t_{i-1};\omega_i,\tau_1,\tau_2) & \\ \quad +v(t_{i-1})\cdot g_{02}(t-\theta-t_{i-1};\tau_1,\tau_2)+v'(t_{i-1})\cdot g_{12}(t-\theta-t_{i-1};\tau_1,\tau_2) & \\ & \text{for } t_{i-1}+\theta < t \le t_i+\theta \end{cases} \tag{3.15}$$

where $i = 1,...,n$. and final output *y(t)* can be obtained based on the nonlinear static mapping relationship $f(v(t))$.

3.4 Case study: The simulated CSTR

This section presents the simulation and prediction results when applying the closed-form compact algorithms obtained in Section 3 to a simulated CSTR introduced by Bhandari and Rollins (2003a). This CSTR will be used to demonstrate and evaluate the ability of the algorithm to handle nonlinear behavior of a physical system.

The mathematical model of the simulated CSTR is first presented. The jacketed CSTR schematic is shown in Figure 3.5. The valve on the outlet stream makes the system self-regulating. This is a multiple input system. The concentrations, temperature, flow rates of the reactants are all subjected to changes due to the operation of the environments since the system is never completely isolated.

The seven inputs and five outputs considered in this CSTR process are given below.
Input variables: feed flow rate of A and B, q_{Af} and q_{Bf}, inlet concentration of A and B, C_{Af} and C_{Bf}, inlet temperature of A and B, T_{Af} and T_{Bf}, flow rate of coolant, q_c.
Output variables: concentrations of A, B and C in the product flow, denoted as C_A, C_B, and C_C, tank temperature T_t and coolant temperature T_c.

Table 3.1 gives notation and values for the steady state conditions, initial conditions and parameters values for the non-isothermal jacketed CSTR.

The second-order reaction taking place in the jacketed CSTR is an irreversible exothermic reaction and can be described by

$$A + B \xrightarrow{k} C$$

The reactants A and B enter the jacketed CSTR and form C. The reaction rate is given by (3.16) below. Note that the rate constant, *k*, has Arrhenius temperature dependence.

$$-r_A = -r_B = k \cdot C_A \cdot C_B = k_0 \cdot e^{-\frac{E}{RT}} \cdot C_A \cdot C_B \tag{3.16}$$

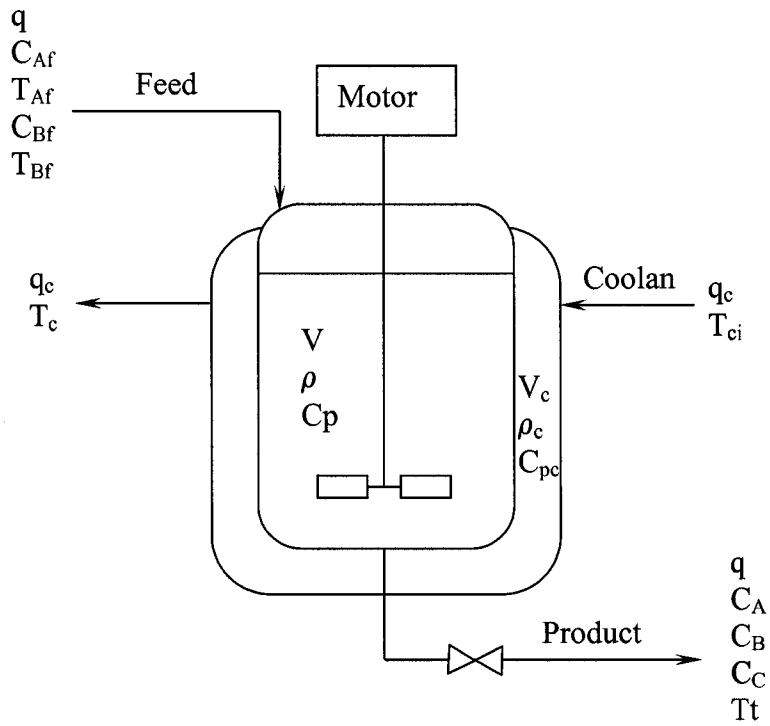

Figure 3.5. Schematic of the jacketed continuous stirred tank reactor (CSTR).

The process model consists of the overall mass balance, the component mole balance, the energy balance on the tank contents, and the jacketed contents. It is assumed that the contents of the reactor and the jacket are perfectly mixed and there are no heat losses. The feed and product streams, as well as the tank contents, have the same density and heat capacity, which do not change with the stream compositions. The tank volume is changing since the level of the tank h is changing.

The physical models for the CSTR system are

$$\frac{dh}{dt} = \frac{q_{Af} + q_{Bf} - q}{A} = \frac{q_{Af}}{A} + \frac{q_{Bf}}{A} - \frac{C_V \cdot f(l)}{A}\sqrt{\frac{\rho g h}{g_s}} \tag{3.17}$$

$$\frac{dC_A}{dt} = \frac{1}{V}\left(q_{Af} \cdot C_{Af} - \left(q_{Af} + q_{Bf}\right) \cdot C_A\right) - k_0 \cdot e^{-\frac{E}{RT}} \cdot C_A \cdot C_B \tag{3.18}$$

Table 3.1. Nomenclature and the parameter values for the CSTR.

Variable	Symbol	Value (unit)
Steady State values:		
Concentration of A	C_A	0.4670 (mol l^{-1})
Concentration of B	C_B	0.1593 (mol l^{-1})
Concentration of C	C_C	0.5587 (mol l^{-1})
Tank Temperature	T_t	3944 (K)
Coolant temperature	T_c	372.11 (K)
Liquid level	h	0.5704 (m)
Initial conditions:		
Coolant inlet temperature	T_{cf}	350.0 (K)
Reactant A inlet temperature	T_{Af}	350.0 (K)
Reactant B inlet temperature	T_{Bf}	350.0 (K)
Reactant A inlet concentration	C_{Af}	1.6 (mol l^{-1})
Reactant B inlet concentration	C_{Bf}	2.0 (mol l^{-1})
Coolant flowrate	q_c	150.0 (l min^{-1})
Reactant A Feed flowrate	q_{Af}	125.0 (l min^{-1})
Reactant B Feed flowrate	q_{Bf}	70.0 (l min^{-1})
Parameter values:		
Heat of reaction	$-\Delta H$	1.1×10^5 (cal mol^{-1})
Heat transfer characteristics	h'A'	7.0×10^5 (cal min^{-1} K^{-1})
Exponential factor	E/R	9.98×10^3 (K)
Pre-exponential factor	k_0	7.5×10^{11} (min^{-1})
Specific heats of tank content and coolant	C_p and C_{pc}	1.0 (cal g^{-1} K^{-1})
Density of tank content and coolant	ρ and ρ_c	1.0×10^3 (g l^{-1})
Tank area	A	0.33 (m^2)
Tank volume	V	200.0 (l)
Coolant volume	V_c	50.0 (l)

$$\frac{dC_B}{dt} = \frac{1}{V}\left(q_{Bf} \cdot C_{Bf} - \left(q_{Af} + q_{Bf}\right) \cdot C_B\right) - k_0 \cdot e^{-\frac{E}{RT}} \cdot C_A \cdot C_B \tag{3.19}$$

$$\frac{dC_C}{dt} = \frac{-\left(q_{Af} + q_{Bf}\right) \cdot C_C}{V} + k_0 \cdot e^{-\frac{E}{RT}} \cdot C_A \cdot C_B \tag{3.20}$$

$$\frac{dT_c}{dt} = \frac{q_c}{V_c}\left(T_{cf} - T_c\right) + \frac{q_c}{V_c}\left(1 - e^{\frac{-h'A'}{q_C \rho_C C_{pc}}}\right)\left(T_t - T_c\right) \tag{3.21}$$

$$\begin{aligned}\frac{dT_t}{dt} = {} & \frac{q_{Af} \cdot T_{Af} + q_{Bf} \cdot T_{Bf} - \left(q_{Af} + q_{Bf}\right) \cdot T_t}{V} + \frac{\left(-\Delta H\right) \cdot k_0 \cdot e^{-\frac{E}{RT}} \cdot C_A \cdot C_B}{\rho \cdot C_p} \\ & + \frac{q_c \cdot \rho_c \cdot C_{pc}}{V \cdot \rho \cdot C_p}\left(1 - e^{\frac{-h'A'}{q_C \rho_C C_{pc}}}\right)\left(T_c - T_t\right)\end{aligned} \tag{3.22}$$

It was assumed that either a Hammerstein or a Wiener model could approximate this reactor system. The system parameters were identified by using the H-BEST and W-BEST techniques based on the training sequence designed by statistical design of experiments (SDOE) and were tested for some testing sequence. The nonlinear static gain and dynamic model parameters in the Hammerstein or Wiener model were identified as described in Bhandari and Rollins (2003a) by exciting the CSTR with sequence step changes of the seven inputs. The training phase showed that the prediction based on the Wiener model is more reasonable when comparing with the true process responses. Then, the Wiener model and its parameters identified by W-BEST were employed to model the CSTR process.

Totally there are 35 different dynamic blocks, and for each output variable, there are 36 coefficients to describe the quadratic nonlinear static gain, including the two factor interactions. The Wiener block diagram of this MIMO reactor system is shown in Figure 3.6. In this figure, $g_{i,j}$ and $v_{i,j}$ stand for the dynamic block transfer function and the intermediate output for ith output variable and jth input variable, $i = 1,2,...,5$, and $j = 1,2,...,7$.

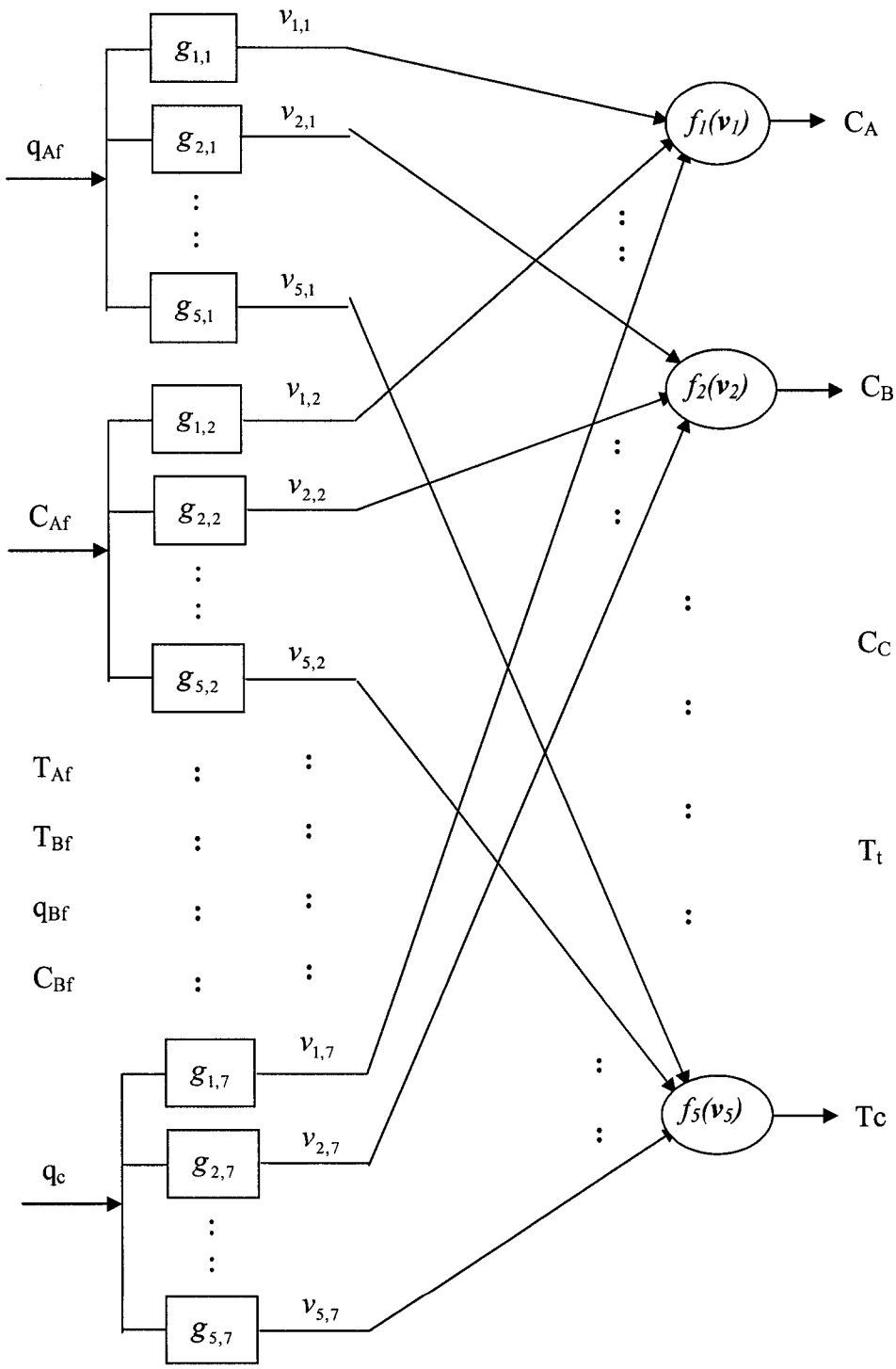

Figure 3.6. The Wiener block diagram of the MIMO CSTR system.

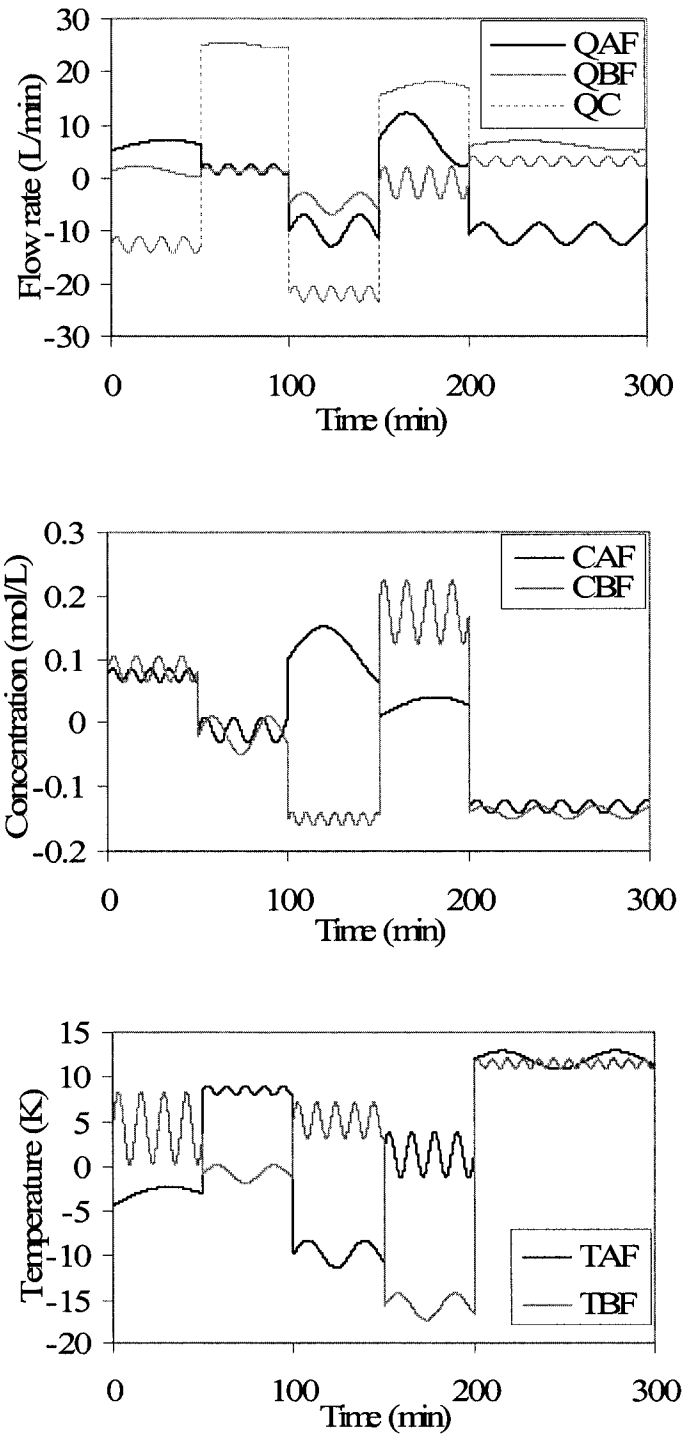

Figure 3.7. The input change sequences for seven input variables.

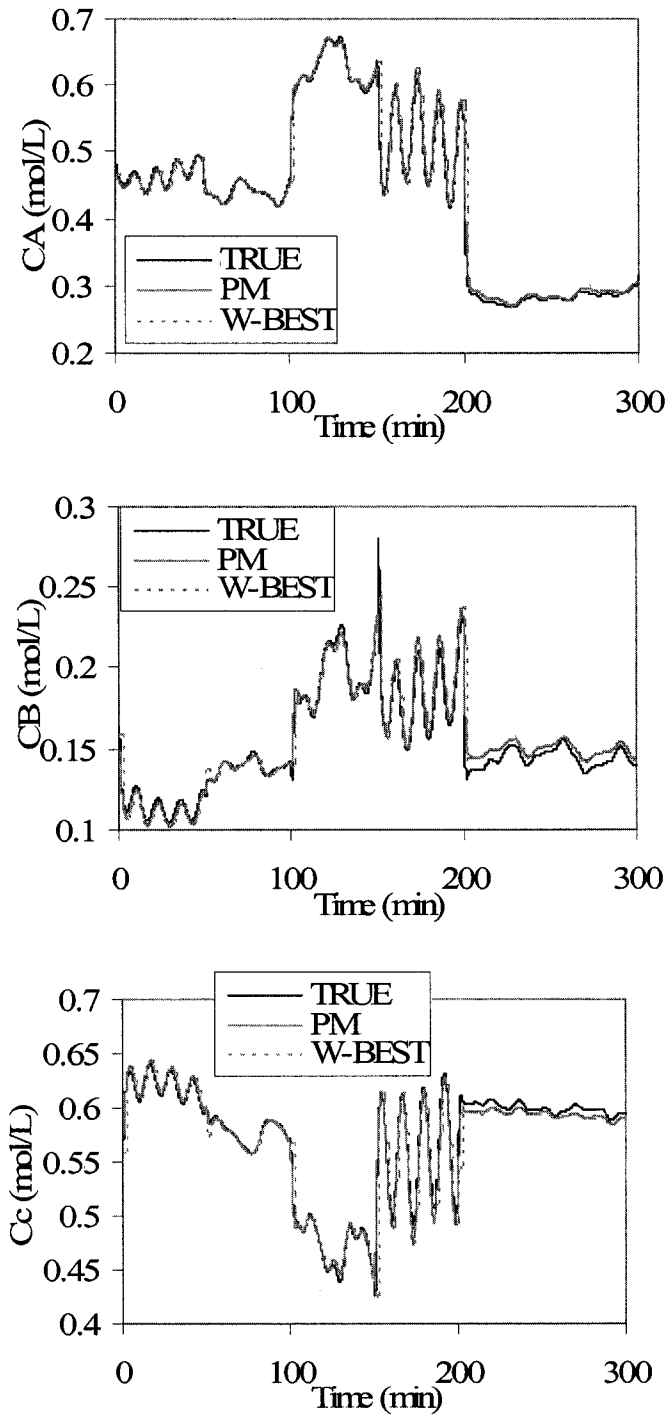

Figure 3.8. The concentrations of the reactants A and B, and the product C in the outflow. "TRUE" denotes the simulated true process responses, while "PM" denotes the responses predicted by the closed-form compact algorithms proposed in this work, and "W-BEST" denotes the piece-wise step input approximation based on W-BEST algorithm.

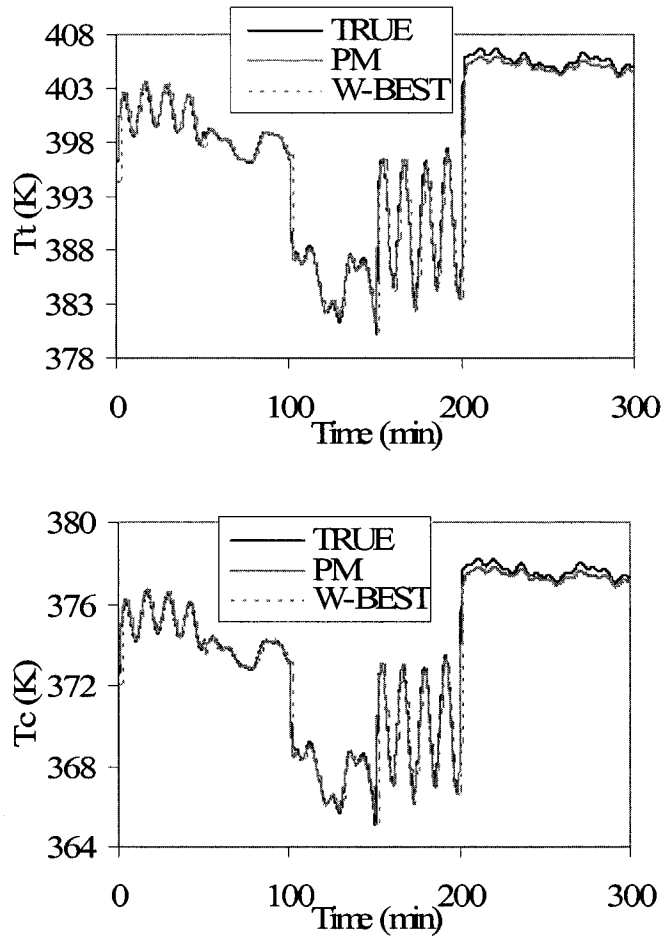

Figure 3.9. The tank temperature and coolant outflow temperature of the CSTR. Notations are the same as those used in Figure 3.8.

3.4.1 Comparison study

The sinusoidal input changes shown in Figure 3.7 are introduced into the CSTR system. These changes are all sinusoidal changes imposed on the step changes, following the form of $b_i + A_i \sin(\omega_i(t - t_{i-1}))$. The b_i, ω_i, and A_i for each input variable are chosen arbitrarily. For each time interval, these values keep the same for each input variable.

The process true responses and the predicted ones by employing the algorithms proposed in this work are shown in Figures 3.8 and 3.9 for each of the five outputs. At the same time, the input sequences were approximateded by piece-wise step input changes, which was how

the discrete-time method would treat the inputs, and then the W-BEST algorithm was applied for each step change. The sampling interval was set to be 2.0 time unit (minitue here), which was very fast sampling especially for the concentration. The outputs based on these two prediction methods were denoted as "PM" and "W-BEST" respectively. As can be seen clearly in Figures 3.8 and 3.9, the closed-form compact algorithms for the Wiener system with the SOPL dynamics when it was excited by the sinusoidal input changes can predict the process responses closely to the simulated true process responses. However, the predictions based on piece-wise step approximation also followed the simulated true process responses closely. It is hard to compare by just looking at the figures.

In order to evaluate the agreement between the simulated true responses and the predicted ones, and compare the proposed method with the piece-wise step approximation quantitively, the following two creteria are used.

A. Sum of squared prediction errors (SSPE)

$$SSPE = \sum_{i=1}^{N} \left(y_i - \hat{y}_i\right)^2 \tag{3.23}$$

where, N is the total number of equally spaced sampling points used over the testing interval, y_i is the true response and $\hat{y}_i$ is the predicted response.

B. Average relative error (ARE)

$$\text{ARE} = \frac{1}{N} \sum_{i=1}^{N} \left| \frac{y_i - \hat{y}_i}{y_i} \right| \tag{3.24}$$

Table 3.2 listed the calculated SSPE and ARE values for the five outputs of the CSTR system based on the algorithm proposed in this work (PM), which belongs to the continuous time method, and those based on the approximation of the sinusoidal as the piece-wise step changing and the W-BEST algorithm, which can be looked as the pseudo discrete time

method (W-BEST). The relative SSPE and ARE values are also provided based on those with PM.

Table 3.2. The comparison of prediction based on the proposed algorithm with the simulated CSTR and the other prediction method described above.

A) SSPE comparison

Output	Absolute SSPE values		Relative SSPE values	
	PM	W-BEST	PM	W-BEST
C_A	0.1051	0.8373	1.000	7.964
C_B	0.1107	0.1957	1.000	1.767
C_C	0.09910	0.3310	1.000	3.340
T_t	903.460	6368.665	1.000	7.049
T_c	209.294	1335.62	1.000	6.382

B) ARE comparison

Output	Absolute ARE values		Relative ARE values	
	PM	W-BEST	PM	W-BEST
C_A	0.00988	0.01597	1.000	1.168
C_B	0.0267	0.03119	1.000	1.167
C_C	0.00763	0.01073	1.000	1.407
T_t	0.000871	0.001558	1.000	1.788
T_c	0.000478	0.000803	1.000	1.680

The SSPE values are not large considering the magnitude of the variables and the ARE values are all less than 3% for the five output variables for the proposed method. These results indeicate that the predictions agree well with the simulated true process responses and the proposed algorithm can predict the process outputs efficiently. To approximate the sinusoidal input as a sequence of piece-wise step input changes often gives larger SSPE and ARE values than the proposed method. As have been pointed out, the sampling frequency

2.0 time unit is actually small for many physical processes. In spite of that, it still cannot beat the proposed method in prediction.

The deviation of the prediction was partially due to the fact that the CSTR is just approximated by a Wiener model reasonably. It is not a true Wiener system. The prediction error is actuallypartially due to the model error.

3.4.2 The noisy process input case

When a step input change is introduced into a system, it is physically difficult to keep the level of each step change at constant. It is often not a perfect step change due to disturbances and some other reasons. Therefore, the input signal is actually noisy around the nominal step input change value. It is not possible to predict the system outputs stisfactorily if the sampling frequence is not very high. Even with a high sampling frequence, the system ouputs are hard to predict because the process input is randomly changing as shown in the Figures 3.10 and 3.11. One way to deal with such kind of signal is to filter it first. After filtering, the true input lever can be identified and the prediction with the step input change can be carried out. The control action can be taken based on the predictions. However, a filter is an additional dynamic block basically and causees a phase lag. Also, it is not necessarily true that good predictions can be provided after filtering the input signals.

As we mentioned before, a stationary time series can be decomposed into a sum of sinusoidal components with uncorrelated random coefficients with frequencies. Once the sine wave parameters for the input sequences are estimated by the spectral decomposition, the closed-form compact algorithms provided in this work can be applied to predict the system outputs after the dynamic and static nonlinear parameters are identified. This might provide a good way to treat the noisy signals.

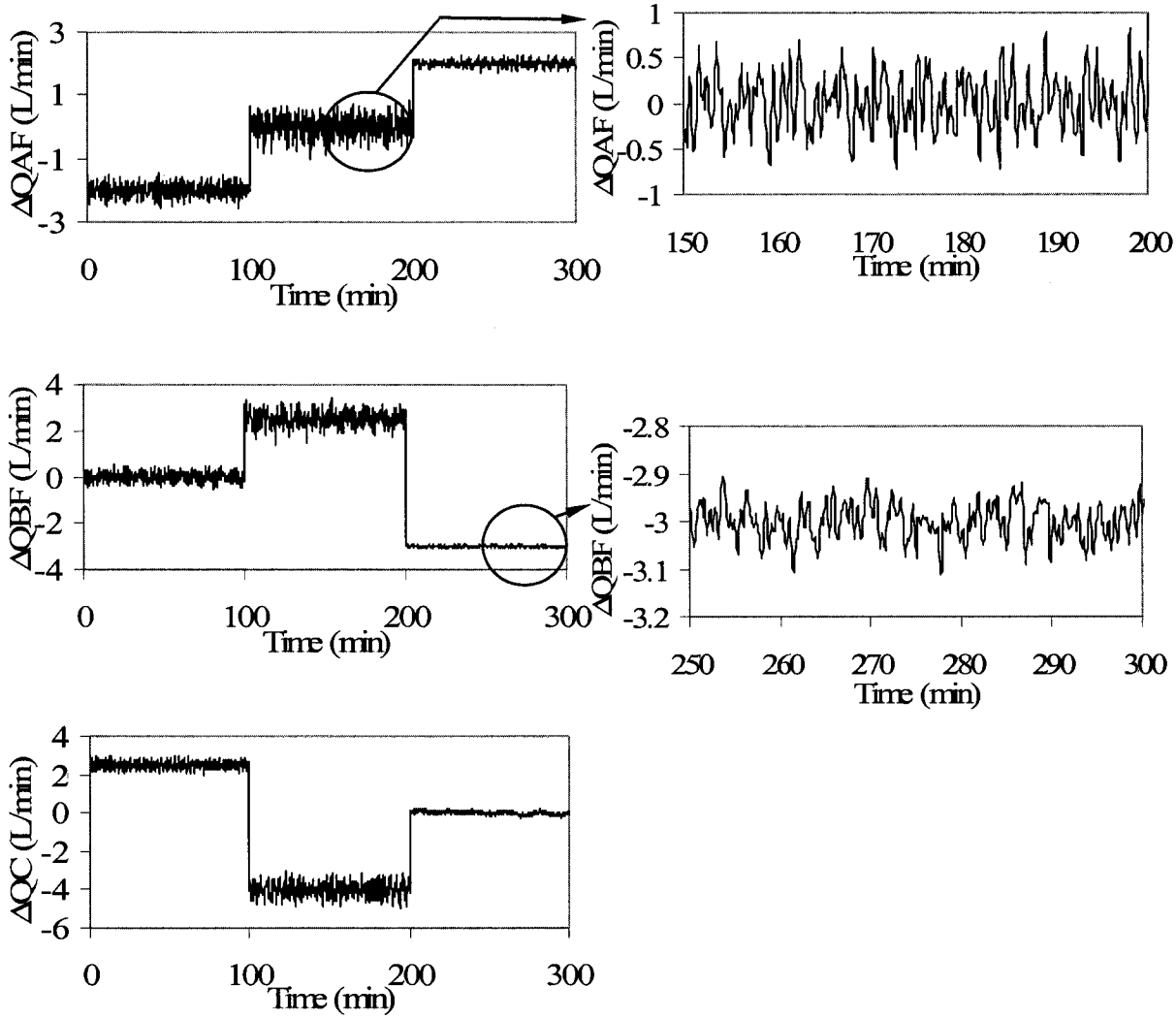

Figure 3.10. The noisy deviations of the inflow flow rates of reactants A and B, and the flow rate of coolant to the CSTR.

Each of the noisy input variables, shown in Figures 3.10 and 3.11, was actually composed of eight sinusoidal signals with different uncorrelated frequencies, and amplitudes. These signals looked stable and it was reasonable to employ the sum of sine waves to approximate the step input change sequencies with noises.

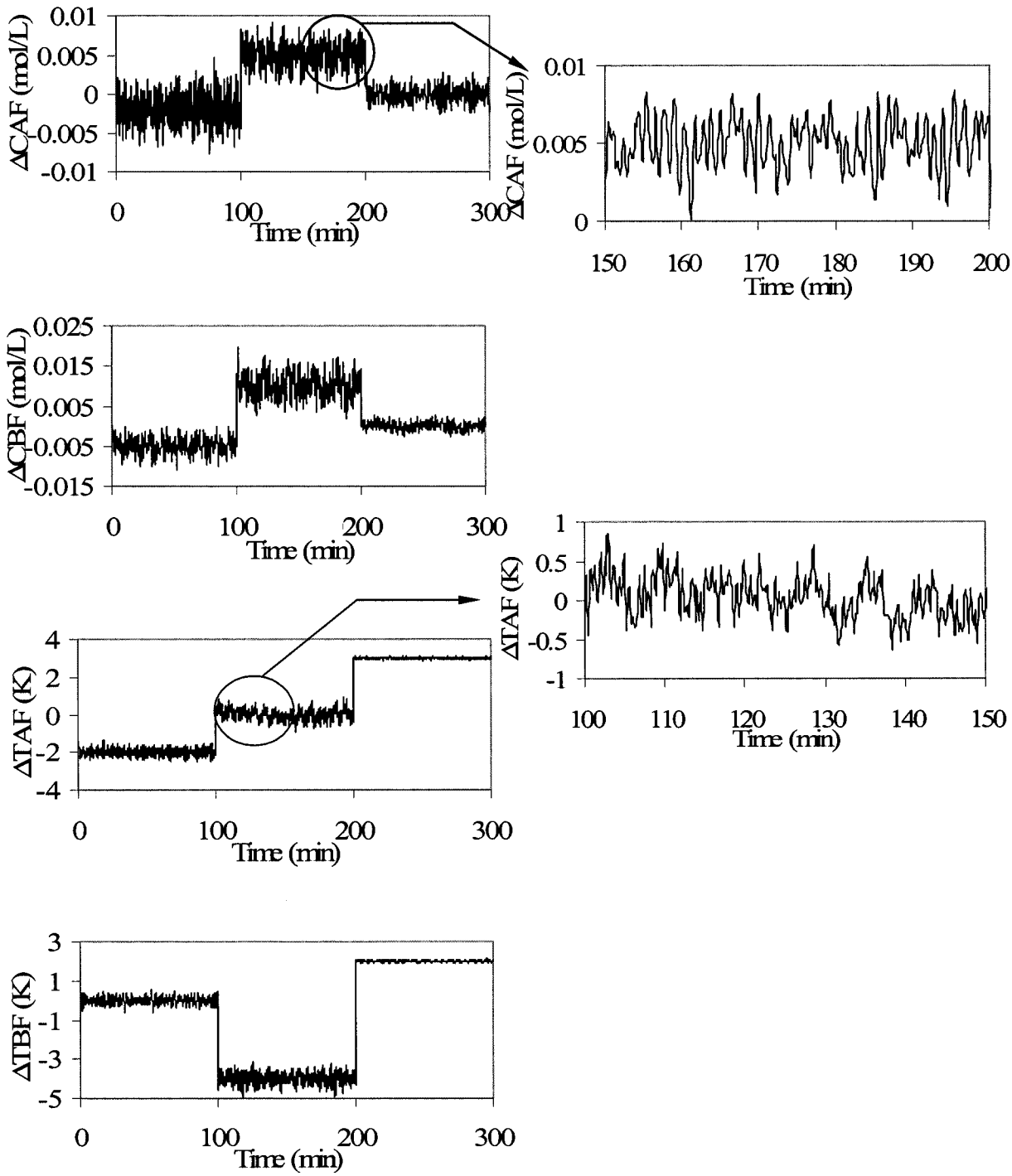

Figure 3.11. The noisy deviations of the reactants A and B inflow concentrations and inflow temperatures to the CSTR.

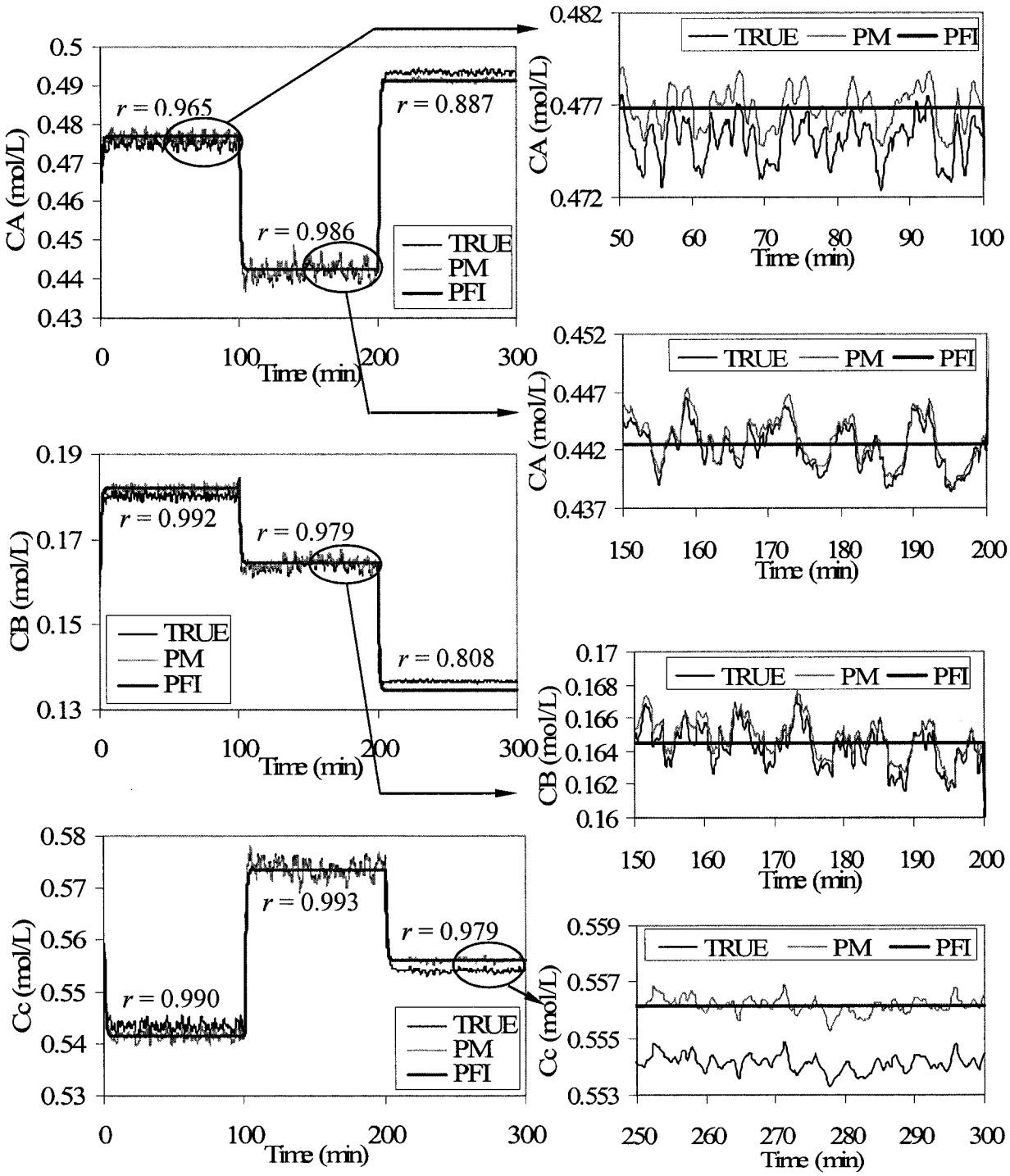

Figure 3.12. The simulated concentrations of reactants and product in the outflow of the CSTR, denoted as 'TRUE', their corresponding predicted values based on the proposed method after the noisy input modeled, denoted as 'PM', and the predicted outputs with perfect filtered inputs, denoted as 'PFI'.

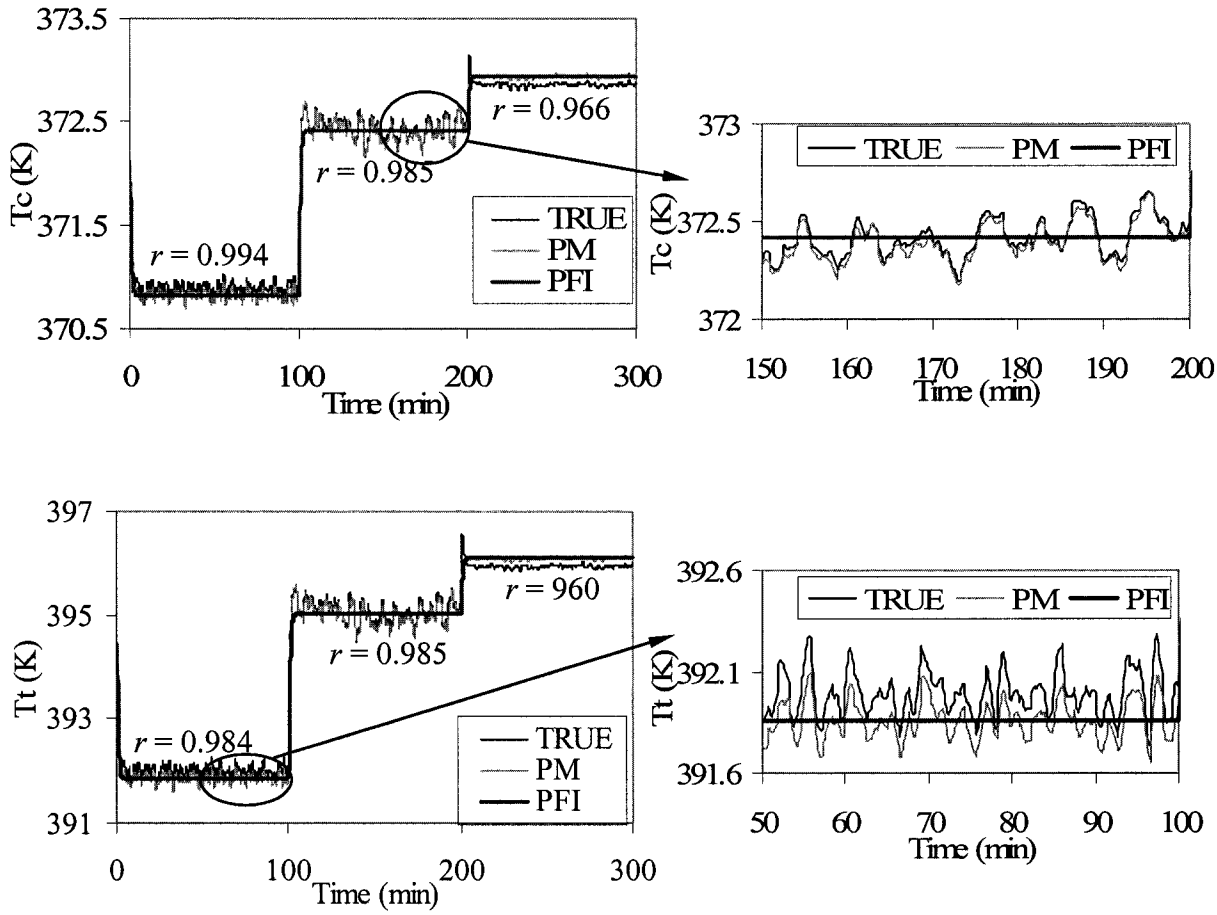

Figure 3.13. The simulated temperatures of the jacket (Tc) and the outflow (Tt) of the CSTR, denoted as 'TRUE', their corresponding predicted values based on the proposed method after the noisy input modeled, denoted as 'PM', and the predicted outputs with perfect filtered inputs, denoted as 'PFI'.

In practice, it is hard to predict the system outputs with such kind of noisy input signals. By noting the facts that the noisy signal can be decomposed into a sum of sinusoidal components with uncorrelated random coefficients and frequencies, and the linear dynamics is linear, the proposed algorithms for the Wiener systems with the sinusoidal input sequencies can be employed. As shown in Figures 3.12 and 3.13, the predicted outputs were

all close to the simulated true outputs. As mentioned before, this CSTR is not truly a Wiener system, but can be approximated by a Wiener model reasonably. Therefore, the algorithms for the Wiener system can not predict the outputs exactly, and the deviations from the true outputs are due to the lack of fit of the Wiener model.

The perfect filtered inputs are assumed available and the outputs based on perfect filtered inputs are also predicted by W-BEST, which were denoted as 'PFI'. Those outputs go to steady states soon after changing points and keep at those states then.

Table 3.3. The evaluation of the proposed algorithm prediction for the noisy deviations of the inputs to the simulated CSTR.

A) SSPE comparison

Output	Absolute SSPE values		Relative SSPE values	
	Proposed Method	Perfect Filtered Inputs	Proposed Method	Perfect Filtered Inputs
C_A	0.003945	0.006559	1.000	1.663
C_B	0.004005	0.005121	1.000	1.279
C_C	0.004062	0.005895	1.000	1.451
T_t	28.7271	57.5142	1.000	2.002
T_c	6.6268	13.2972	1.000	2.007

B) ARE comparison

Output	Absolute ARE values		Relative ARE values	
	Proposed Method	Perfect Filtered Inputs	Proposed Method	Perfect Filtered Inputs
C_A	0.003038	0.003913	1.000	1.288
C_B	0.00942	0.01064	1.000	1.130
C_C	0.002598	0.003202	1.000	1.232
T_t	0.000304	0.000416	1.000	1.367
T_c	0.000158	0.000216	1.000	1.366

The SSPE and ARE values of these predictions are shown in Table 3.3. It is clear that the SSPE and the average relative errors values for PM are smaller than those of PFI, therefore a better prediction is provided by PM. The average relative errors are all less than 1.5%, which is acceptable in industry. These tell us that the predictions were close to the true values satisfactorily. The prediction with PFI cannot catch the noisy character of the process, while the prediction with PM does. The deviations of the predictions with PM are mostly caused by the lack of fit when employing the Wiener model to approximate the CSTR.

The piece-wise step approximation will give larger deviations from the true process outputs for noisy input signals shown in Figure 3.11 and 12 because the signals have lots of spikes and things will get worse if the spikes happen to be sample to represent the input changes.

3.5 Conclusions

The closed-form compact algorithms to the Hammerstein and Wiener systems with second order plus lead dynamics developed in this work are the exact algorithms to the systems when they are excited by the sinusoidal input changes. These algorithms are in the compact form. Therefore, the prediction of the system response does not depend on all past input changes, but only a few recent input changes are needed. The algorithms are given for the SISO Hammerstein and Wiener systems, but it is straightforward to extend and apply them to the MIMO systems. The proposed algorithms predict the outputs almost exactly for the true Hammerstein and Wiener systems. It is demonstrated on a seven-input, five-output simulated CSTR, which can be approximated by a Wiener model reasonably, that the developed algorithms had the ability to predict the multiple outputs closely and they performed better than the piece-wise approximation. These algorithms can also be employed to predict the process outputs when the input deviations are noisy step changes after the

spectral decomposition of the noisy input signals. The predictions with noisy input modeled are better than those with the inputs filtered first. Even with the perfect filtering of the input signals, the predictions have higher SSPE and ARE values. Therefore, it would be better to decompose the noisy input signals and employ the proposed algorithm for sinusoidal inputs than to filter the noisy inputs.

References

Bhandari, N. and Rollins, D. K., Continuous-time multi-input, multi-output Wiener modeling method, *Industrial & Engineering Chemistry Research,* **42**: 22, 5583-5595. (2003a).

Bhandari, N. and Rollins, D. K., Continuous-time Hammerstein nonlinear modeling applied to distillation, *AIChE Journal,* **50**: 2, 530-533 (2003b).

Brockwell, P.J. and Davis, R.A., *Introduction to Time Series and Forecasting*, Springer, New York, 2002.

Doyle, F.J. III, Pearson, R.K., and Ogunnaike, B.A., *Identification and Control Using Volterra Models*, Springer-Verlag London Limited, Great Britain, 2002.

Eskinat, E., Johnson, S.H. and Luyben, W.L., Use of Hammerstein models in identification of nonlinear systems, *AIChE Journal*, **37**: 255-268 (1991).

Greblicki, W., Nonparametric identification of Wiener systems, *IEEE Transactions on Information Theory*, **38**: 1487-1493 (1992).

Greblicki, W., Nonparametric approach to Wiener system identification, *IEEE Transactions on Circuits Systems I*, **44**: 538-545 (1997).

Greblicki, W., Recursive identification of continuous-time Wiener systems, *International Journal of Control*, **72**: 981-989 (1999).

Greblicki, W., Continuous-time Hammerstein system identification, *IEEE Transactions*

on Automatic Control, **45**: 1232-1236 (2000).

Hajjari, A. and Eloutassi, O., Extracting sine waves from noisy measurements and estimating their parameters, *Proceeding of the IASTED International Conference, Intelligent Systems and Control*, Santa Barbara, CA, 1999, 341-345.

Kalafatis, A., Arifin, N., Wang, L. and Cluett, W.R., A new approach to the identification of pH process based on the Wiener model, *Chemical Engineering Science*, **50**: 3693-3701 (1995).

Normandin, A., Thibault, J., and Grandjean, B.P.A., Optimizing control of a continuous stirred tank fermenter using a neutral network, *Bioprocess Engineering*, **10**: 109-113 (1994).

Norquay, S.J., Palazoglu, A., and Romagnoli, A.J., Application of Wiener model predictive control to a pH neutralization experiment, *IEEE Transactions on Control Systems Technology*, **7**: 437-445 (1999a).

Norquay, S.J., Palazoglu, A., and Romagnoli, A.J., Application of Wiener model predictive control (WMPC) to an industrial C2-splitter, *Journal of Process Control,* **9**: 461-473 (1999b).

Ogunnaike, B.A., and Ray, W.H., *Process Dynamics, Modeling, and Control*, Oxford University Press, Inc., New York, 1994.

Pan, Yangdong, and Lee, Jay H., Identification and control of processes with periodic operation or disturbances, *Ind. Eng. Chem. Res.*, **42**:1938-1947 (2003).

Pearson, R.K. and Ogunnaike, B.A., Nonlinear process identification, *Nonlinear Process Control*, Edited by Henson, M.A., and Seborg, D.E., Prentice-Hall, Upper Saddle River, New Jersey, p. 11-110, 1997.

Pearson, R.K. and Pottmann, M., Gray-box identification of block-oriented nonlinear models, *Journal of Process Control*, **10**: 301-315 (2000).

Rollins, D.K., Bhandari, N., and Pacheco, L., Experimental designs that maximize

information for nonlinear dynamic process, Submitted to *Foundations of Computer Aided Process Operations Conference (FOCAPO),* Florida (2002b).

Rollins, D.K., Bhandari, N., Bassily, A.M., Colver, G.M., and Chin, S., A continuous-time nonlinear dynamic predictive modeling method for Hammerstein processes, *Industrial and Engineering Chemistry Research,* **42**(4): 861-872 (2003).

Su, H.-T., and McAvoy, T.J., Integration of multilayer perceptron networks and linear dynamic models: A Hammerstein model approach, *Industrial & Engineering Chemistry Research*, **32**: 1927-1936 (1993).

Wigren, T., Recursive prediction error identification using the nonlinear Wiener model, *Automatica*, **29**: 1011-1025 (1993).

Zhai, D., Rollins, D.K., and Bhandari, N., Compact block-oriented continuous-time dynamic modeling for nonlinear systems under sinusoidal input sequences, *Proceeding of the IASTED International Conference, Intelligent Systems and Control*, Honolulu, Hawaii (2004).

Zhu, X., and Seborg, D. E., Nonlinear predictive control based on Hammerstein models, *Control Theory and Applications*, **11**: 564-575 (1994).

Chapter 4. Parameter Estimation of the Continuous-Time Block-Oriented Wiener Dynamic System With Stochastic Input Noises

4.1 Introduction

Many physical dynamic systems can be approximated by mathematical models. Most of these systems, in nature, are nonlinear, dynamic, stochastic, and time-varying. The block-oriented model, such as the Wiener dynamic process model, is one type of the mathematical model that is widely used in chemical engineering to model physical processes. The Wiener dynamic model basically consists of two blocks, the linear dynamic block and the non-linear static mapping block in sequence. With a simple structure, the Wiener dynamic model can approximate the real processes well (Kalafatis et al., 1995; Huang et al., 1998; Bhandari & Rollins, 2003; etc.). It can also be used to model multiple-inputs, multiple-outputs processes. More explanation about the Wiener dynamic model will be provided in Section 4.2.

When dealing with the block-oriented dynamic models, either the continuous-time method or the discrete-time method can be employed. Most processes encountered in the physical world are continuous in time. It is intuitive to treat the models continuously. Nevertheless, with the development of the computer technology, the discrete-time method started to dominate the modeling and the control areas in recent decades. However, discretization can only approximate a continuous-time model and the sampling rate directly affects the model identification and parameter estimation for the discrete-time method. This work considers the continuous-time Wiener dynamic model. When the continuous-time method is used, the error term for a model has to be assumed to be stochastically continuous in time, but not discrete time series.

Once the model structure is chosen, not much can be done with the model error. The model usually involves several parameters, which govern the behavior of the model and are

to be estimated based on some experimental data or so called training data. Estimating these parameters accurately and precisely is critical in the whole model building procedure. Otherwise, the prediction and model predictive control of the system could fail. First of all, it is important to obtain reliable input and output data, where there often exist noises and errors, such as random process disturbances caused by the previous procedure or environment as well as the measurement errors. Such noises and errors, if not appropriately accounted for, prevent efficient estimation of the parameters. The measurement errors can be reasonably assumed to be white noises, and their effect on the parameter estimation can be recovered when there are reasonably enough data points. However, this is not the case for the random process disturbances, which can be highly correlated. For continuous-time modeling, these noises, which are continuous in time, cannot be described by any discrete-time stochastic processes, such as the ARMA models.

Most existing works in the literature used the discrete-time method and considered only the input and output measurement errors. These errors were assumed to be additive to the deterministic part of the process inputs or outputs when the input-output data pairs were simulated and collected and the estimation was then carried out (Nordsjo, 1997; Nordsjo & Wigren, 2002; Schoukens *et al.*, 2003). For the block-oriented Wiener dynamic system, Hagenblad (1999) and Gomez and Baeyen (2004) added measurement errors to the intermediate output variable, which is unobservable. Vandersteen *et al.* (1997) and Bai (2003) considered both the input and output measurement errors in the Wiener dynamic model. Both errors were treated as white noises independent of the signals and did not go through the dynamic process at all. However, a process is usually related to the environment, and the input variables are often the outputs of the previous processes and are thus are with various correlated random disturbances and noisy signals. Input disturbance can also be introduced by the inaccuracy of valve and electronic noise. So, the input variable along with

correlated disturbance or noise are sent to the next process or block directly, which may eventually lead to large variation of the output variables. Furthermore, correlated input disturbance can be enlarged or diminished during the process and often cause complicated correlated output noises, which make it more difficult to estimate the process parameters. So far, little work has been done in the literature to address the estimation problem for this case, especially in the context of process control. In this work, correlated continuous-time input disturbances are imposed on the nominal input variables and then go through the continuous-time process. The estimation method for such input-output data pairs will be presented.

Accurate predictions are critical in the model predictive control (MPC) where reliable estimation of parameters is a premise. It is critical to identify appropriate parameter estimation methods when the stochastic input noises are considered in the continuous-time Wiener dynamic system. Such estimates of the dynamic and covariance parameters may also provide information on whether the input variable (or sometimes actually the output of previous process) is in control or not. In this chapter, some concepts used in this work are introduced in Sections 4.2 and 4.3, including the continuous-time block-oriented Wiener dynamic model and stochastic processes. Section 4.4 states the estimation problem and Section 4.5 presents the approach to simulate the Wiener dynamic process with stochastic input noise, and demonstrates the sensitivity of the process to the correlated input noise. Section 4.6 proposes a new method to estimate the model parameters when stochastic input noises are considered for the continuous-time block-oriented Wiener dynamic process with first order dynamics. The method is based on estimating equations and is applied to such a simulated process with the stochastic input noises. The estimates based on the proposed method are compared to the true values and the conclusions are drawn in Section 4.7. Some future work is also listed in Section 4.7.

4.2 Continuous-time block-oriented Wiener dynamic models

The continuous-time block-oriented Wiener dynamic model is what this work is based on. Block-oriented models are series or parallel combinations of linear dynamics blocks and static nonlinear mappings. A Wiener dynamic model consists of a linear dynamic block followed by a static nonlinear mapping or gain block, as depicted in Figure 4.1. The intermediate vector $\boldsymbol{v}(t)$, which is not observable, is the convolution of the input vector $\boldsymbol{u}(t)$ and the linear dynamic block transform function $\boldsymbol{g}(t)$. The output variable is $\boldsymbol{y}(t) = \boldsymbol{f}(\boldsymbol{v}(t))$, where $\boldsymbol{f}(\boldsymbol{v}(t))$ represents the nonlinear static gain functions. Notations in bold mean vectors.

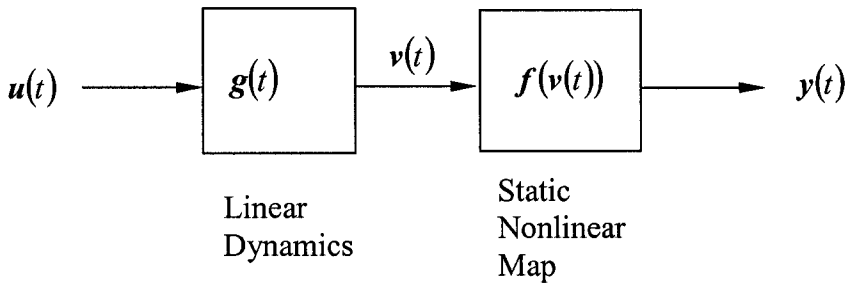

Figure 4.1. A Wiener dynamic model structure.

The Wiener dynamic model has a simple structure with relatively few parameters, making this model one of the simplest and most popular block-oriented, nonlinear models. Due to its simple structure and efficient parameterization, the Wiener dynamic model has many applications in practice and is becoming more popular. It can represent the nonlinear dynamics well. For example, the Wiener dynamic model has been shown to represent many nonlinear, chemical processes effectively, such as pH neutralizations, distillation columns, and continuous-stirred tank reactors (CSTR) (Greblicki, 1992, 1997; Wigren, 1993; Kalafatis et al., 1995; Huang et al., 1998; Bhandari & Rollins, 2003; etc.). Much work has been done to investigate the extent of the applications of this model. Almost all of the work involves the use of the discrete-time method except for Greblicki (1992, 1997) and Bhandari &

Rollins (2003). Greblicki (1992, 1997) introduced a nonparametric continuous-time approach with the dynamic block identified by impulse response methods, and Bhandari & Rollins (2003) proposed the continuous-time Wiener modeling method, which was named Wiener Block-oriented Exact Solution Technique (W-BEST).

The discrete-time modeling (DTM) dominates the system engineering literature in the applications of block-oriented modeling because of the discrete environment of computer-based process control systems and because the sampling is usually discrete (Henson and Seborg, 1997). Furthermore, DTM is easier to obtain because all input changes can be approximated by piecewise step input sequences. Nonetheless, DTM has (potentially) two critical drawbacks relative to continuous-time modeling (CTM). DTM requires constant and frequent sampling, and may not be as accurate as CTM since, at best, DTM can only approximate continuous-time processes. In system engineering, CTM has seen limited applications even though it has the advantage of prediction at any time. Other advantages of CTM over DTM include fewer coefficients and parameters but with physical meaning. For a continuous-time model, it is possible to have a compact closed-form algorithm (Rollins et al., 2003; Bhandari & Rollins, 2003), which does not require iterative calculations. As shown by Rollins and Bhandari (2004), statistical experimental design can be carried out with an analytical algorithm. Also, CTM identification is often easier than DTM identification due to fewer parameters and a clear analytical algorithm form.

After deciding to employ the continuous-time Wiener dynamic model to approximate a real process, the next task is to estimate the nonlinear static mapping relation and the dynamic parameters. This is done in two stages as described by Bhandari & Rollins (2003) as W-BEST. Following a statistical experimental design of the sequence of step input changes, the training data are collected after each step change of the inputs with different amplitudes is introduced to the dynamic system of interest. Note that $u(t) \approx v(t)$ as

$t > 5\tau$ after each step input change. The input-output data pairs after the system reaches its steady state provide the nonlinear static mapping information, while those at the transition state after each step input change contain more dynamic information. Therefore, the nonlinear static parameters can be obtained by using the data after steady states are reached for step input changes. Then, the order of the dynamic relation and its corresponding parameters can be estimated based on the transition data by using some general estimation methods, such as nonlinear regression.

In this work, we concentrate on a theoretical single-input, single-output (SISO) Wiener process with first order dynamics. It is assumed that the nonlinear static mapping relationship has been identified and is invertible, so that the intermediate output *v(t)* can be obtained. This is not a problem with W-BEST technique due to the two-stage model identification procedure, and the invertibility is feasible for a SISO Wiener process especially with the low parameterization. We focus on the dynamic block with stochastic input noises and estimate the dynamic parameter and the covariance structure of the input noises. The estimation method is demonstrated on a SISO Wiener process with first order dynamics. The estimation in the multiple-input, multiple-output case can be accomplished similarly, but the procedure can be much more complicated and will not be discussed here.

4.3 Stochastic processes

Some basic concepts of the stochastic processes are introduced in this section. Random variables are usually used to describe random phenomena. The characteristic of a random phenomenon can be described through the probability distribution of a random variable. However, in engineering and the physical sciences, many random phenomena are related to time; for example, the reaction rate of certain batch reactor is fast at the beginning and gets slower and slower over time. In these cases, it is necessary to consider a family of random

variables that is a function of time. A stochastic process is thus defined (Ochi, 1990). A family of random variables *x(t)*, where *t* is a parameter belonging to an index set *T*, is called a stochastic process or a random process, and is denoted as $\{x(t), t \in T\}$.

Every time a random phenomenon is recorded over time, it is a different path. Consider a set of *n* records of a random phenomenon varying over time, denoted as ${}^1x(t)$, ${}^2x(t)$, ..., ${}^nx(t)$. At a specific time t_1, we have a set of random variables consisting of *n* elements, $\{{}^1x(t_1), {}^2x(t_1), \cdots, {}^nx(t_1)\}$. At time t_i, we have another set of random variables consisting of *n* elements, $\{{}^1x(t_i), {}^2x(t_i), \cdots, {}^nx(t_i)\}$, $i = 1, 2, \cdots$. The collection of *n* records simultaneously observed at a specified time is called an ensemble. The mean value function of a random process *x(t)*, $E[x(t)]$, is the expect value of *x(t)* at time *t*. The covariance function of a random process *x(t)* is defined as

$$Cov_x(t_1, t_2) = Cov[x(t_1), x(t_2)] = E[(x(t_1) - E[x(t_1)])(x(t_2) - E[x(t_2)])] \quad (4.1)$$

Note that both the expectation and covariance of the stochastic process are functions of time. At different time points, the mean value can be quite different, so can the autocovariance function. If the mean value function $E[x(t)]$ is constant independent of *t*, and its covariance function $Cov[x(t), x(t+\tau)]$ depends only on τ, which is the distance between the two time points, for all *t*, a stochastic process is said to be weakly stationary. It is assumed that the input stochastic processes discussed in this work are all weakly stationary. However, this is not necessarily the case for the output stochastic processes.

A stochastic process *x(t)* is said to be a Gaussian process if for any given $k \geq 1$ and $t_1, \ldots, t_k$, the random vector ($x(t_1), \ldots, x(t_k)$) is jointly normally distributed. This is a common and reasonable assumption for many stochastic processes in reality and it is employed in this work for the input noises.

These concepts will be used later when simulating the process of interest and discussing the parameter estimation methods.

4.4 The estimation problem

In practice, step input changes with different amplitudes are designed statistically in order to identify the static and dynamic parameters for the Wiener dynamic system as described in the W-BEST technique. It is physically difficult to keep the level of each step change at constant as designed. A step input change in reality may be described as the nominal input variable with a random disturbance or noise term, as shown in (4.2).

$$u(t) = \eta(t) + \varepsilon(t) \tag{4.2}$$

where $\eta(t)$ is the nominal value of the input variable, which is deterministic, and $\varepsilon(t)$ is a random disturbance or noise, which is assumed to be stochastically correlated.

Thus, the dynamics equation for a single-input, single-output (SISO) Wiener dynamic process with first order dynamics becomes

$$\tau \frac{dv(t)}{dt} + v(t) = u(t) = \eta(t) + \varepsilon(t) \tag{4.3}$$

where, τ is the time constant, which is always positive, and the initial condition is at the steady state, $v(0) = 0$ at $t = 0$. The final Wiener dynamic process output can be obtained by some nonlinear static mapping, for example,

$$y(t) = f(v(t)) = a_1 v(t) + a_2 v^2(t) \tag{4.4}$$

Here input $u(t)$, intermediate output $v(t)$ and output $y(t)$ are all in terms of the deviation variables. The process outputs can have various properties when the random disturbance or noise term $\varepsilon(t)$ has different covariance structures. For some specific cases, analytical solutions can be obtained. Assume that $\varepsilon(t)$ is a weakly stationary Gaussian process with

$$E[\varepsilon(t)] = 0 \text{ and } Cov[\varepsilon(t_1), \varepsilon(t_2)] = \sigma_\varepsilon^2 e^{-\alpha|t_2 - t_1|}, \tag{4.5}$$

where $\alpha > 0$ is a constant and σ_ϵ^2 is the variance of $\varepsilon(t)$. This kind of covariance structure is common, where the covariance between the two points decreases as the interval between those two time points increases. Therefore, this disturbance has the property to be nearly uncorrelated at different time points t_1 and t_2 that have a large distance, and to be more correlated in a small neighborhood. The speed of the correlation change depends on the parameter α. When α is large, the covariance decreases fast as the time interval increases. This assumption as to the structure of $\varepsilon(t)$ is reasonable and acceptable though it is strong.

Equation (4.3) is a stochastic differential equation (SDE) and its analytical solution can be written as (Sobczyk, 1991)

$$v(t) = v_0\, e^{-at} + a\, e^{-at} \int_0^t e^{as}\, \varepsilon(s)\, ds + \eta(t)\left(1 - e^{-at}\right), \text{ where } a = 1/\tau. \tag{4.6}$$

The first two moments of the stochastic process $v(t)$ are

$$E[v(t)] = v_0\, e^{-at} + \eta(t)\left(1 - e^{-at}\right) \tag{4.7}$$

$$Cov_v(t_1, t_2) = \frac{a^2\, \sigma_\varepsilon^{\,2}}{a^2 - \alpha^2}\left[e^{-\alpha|\tau|} - \frac{\alpha}{a} e^{-a|\tau|} + \left(1 + \frac{\alpha}{a}\right) e^{-a(t_1+t_2)} - e^{-at_1 - at_2} - e^{-\alpha t_1 - at_2}\right] \tag{4.8}$$

$$Var_v(t) = \frac{a^2\, \sigma_\varepsilon^{\,2}}{a^2 - \alpha^2}\left[1 - \frac{\alpha}{a} + \left(1 + \frac{\alpha}{a}\right) e^{-2at} - 2e^{-(a+\alpha)t}\right] \tag{4.9}$$

where $\tau = t_1 - t_2$. Note that all of these moments depend on time t. The output of this specific process is not weakly stationary any more. The correlation of outputs between two different time points is remarkable when the distance is not large for some parameter setting.

As $t_1, t_2 \to \infty$, the stationary solution can be reached, and the corresponding first two moments of the process $v(t)$ become

$$\lim_{t\to\infty} E[v(t)] \to \eta \text{ where } \eta = \lim_{t\to\infty} \eta(t) \tag{4.10}$$

$$Cov_v(t_1, t_2) \to \frac{a^2\, \sigma_\varepsilon^{\,2}}{a^2 - \alpha^2}\left[e^{-\alpha|\tau|} - \frac{\alpha}{a} e^{-a|\tau|}\right] = Var_v(t)\, \frac{1}{a - \alpha}\left[a\, e^{-\alpha|\tau|} - \alpha\, e^{-a|\tau|}\right]$$

$$\text{with } t_1, t_2 \to \infty \text{ and } |t_1 - t_2| = \tau \text{ fixed} \tag{4.11}$$

$$Var_v(t) \to \frac{a\,\sigma_\varepsilon^{\,2}}{a+\alpha} \text{ as } t \to \infty \tag{4.12}$$

These moments become less complicated and the process *v(t)* becomes weakly stationary. Basically, the moment structures of the outputs are determined by the input covariance structure and the dynamic process. These moment properties of the outputs will be employed later in the parameter estimation, including that for the dynamic parameter a, and the covariance parameters α and σ_ε.

Here, we concentrated on the block described by (4.3), where the input disturbances or noises have the moment structure described in (4.5). Only the outputs need to be observed, but not the input disturbances or noises. In other words, this is an estimation problem with unobserved disturbances in the control area. The simulation of the Wiener dynamic process will be performed first to generate the output data, and some simulated outputs will be presented, which provide information about the process more directly. Note that the SDE in (4.3) cannot be solved by the general numerical method for the ordinary differential equations (ODE). The numerical method for the SDE is different. The dynamic parameter a, and the covariance parameters α and σ_ε are of interest and the method to estimate these three parameters will be presented in Section 4.6.

4.5 Simulation of Wiener dynamic processes with Gaussian input noises

It is intuitive to simulate an noise process $\epsilon(t)$ with specified covariance structure first and then introduce it into the SDE in (4.3) to obtain the process $v(t)$. In order to simulate a Gaussian process with a specified covariance function directly, the following algorithm from Ripley (1987) is used. The Fourier transform and inverse Fourier transform are employed in the algorithm.

Algorithm: (Ripley, 1987)

With the specified covariance function $c(\tau) = Cov(t, t+\tau)$ for a stationary Gaussian process, the values of function $c(r\delta)$ are calculated first for r = 0, 1, ..., N/2-1 for some even N, where r is an index; N is the total number of data points simulated, and it has to be a power of 2; δ is the lag distance. The complete set of covariance function values $c_0, c_1, \cdots c_{N-1}$ are given by

$$c_r = \begin{cases} c(r\delta) & \text{if } 0 \le r \le N/2 \\ c_{N-r} & \text{if } N/2+1 \le r < N \end{cases} . \tag{4.13}$$

Denote the Fourier transform of c_r as $\tilde{c}_s$ and form $\tilde{c}_s$ based on the formulas $\tilde{c}_s = \sum_{r=0}^{N-1} e^{2\cdot\pi\cdot i\cdot r\cdot s/N} c_r$, where i is the imaginary unit and $s = 0, 1, \ldots, N-1$, and then get $\phi_s = \sqrt{\tilde{c}_s}$. For each simulation of Gaussian process $X(0), \ldots, X((N-1)\delta)$, it is also needed to generate the following random samples $U_0 \sim Norm(0, N)$, $U_1, \ldots, U_{N/2} \sim Norm(0, N/2)$, $V_1, \ldots, V_{N/2-1} \sim Norm(0, N/2)$, and let $U_{N-r} = U_r$ for r = 1, ..., N/2 − 1 , $V_0 = V_{N/2} = 0$, $V_{N-r} = -V_r$ for r = 1, ..., N/2 − 1 , where *Norm* denotes the normal distribution. Then, for $j = 1, 2, \ldots, N-1$, the Gaussian process $X(0), \ldots, X((N-1)\delta)$ can be obtained by doing the following inverse Fourier transform:

$$X(j\delta) = \frac{1}{N} \sum_{r=0}^{N-1} \left\{ e^{-2\cdot\pi\cdot i\cdot j\cdot r/N} \cdot (U_r + iV_r) \cdot \phi_r \right\} \tag{4.14}$$

This algorithm generates a stationary Gaussian process in $\{0, 1, \ldots, N-1\}$ with specified covariance structure, and can be used to generate the input noises in this work. Different seeds will give different stochastic processes with approximately the same moment structure. Once this is done, which gives a continuous path of the input noises with the

specified moment structure; the solution in (4.6) can be used. After calculating the integration, the intermediate process $v(t)$ can be obtained, so can the final output $y(t)$.

The first two moments of the numerically simulated stochastic processes are calculated and compared to the theoretical moments to make sure nothing goes wrong with the simulation. Note that the moments have to be calculated with at least several ensembles of records. The more the simulated ensembles are included in the calculation, the closer the calculated moments are to the theoretical values.

As an example, consider a SISO Wiener dynamic system with first order dynamics, where time constant is $\tau = 5.0$, and linear static mapping block, where the final output *y(t)* is proportional to the intermediate output *v(t)* with $a_1 = 1.0$ and $a_2 = 0.0$ in (4.4).

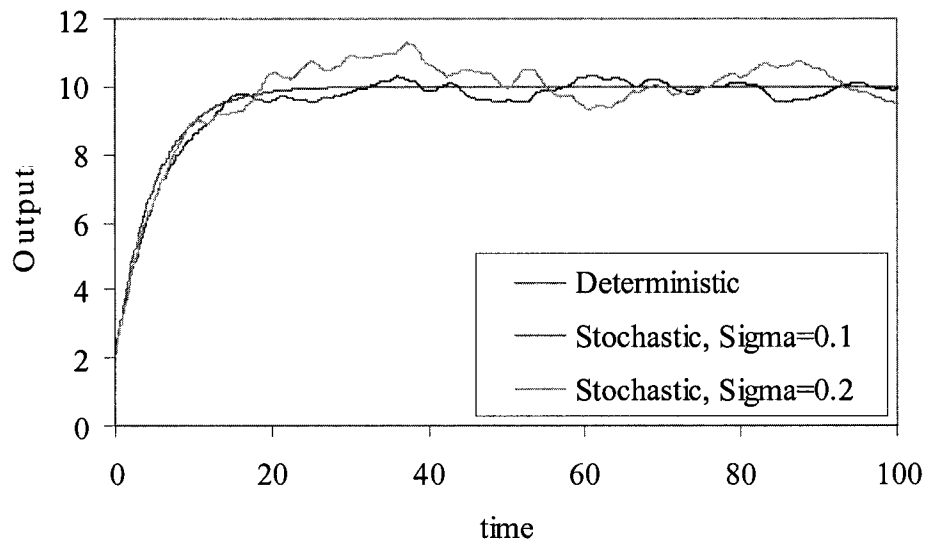

Figure 4.2. The simulated output of the Wiener dynamic system with first order dynamics when the stochastic noises are imposed on the step input change with sampling frequency as 0.1 time unit.

One record of the outputs *y(t)* of this Wiener dynamic system is shown in Figure 4.2 based on simulation for one step input change. The output deviates considerably from the theoretical deterministic output when the noises follow the specification in (4.5) with $\sigma_\epsilon = 0.1$

and 0.2, which is 1% and 2% of the step input change $\eta(t) = 10$, for $\alpha = 0.5$. Though 1-2% deviation is not large in many cases in the chemical industry, the simulated responses of the Wiener dynamic systems can vary from the deterministic one considerably. The outputs sometimes drift away, and come back to the deterministic values slowly. It is noticeable that this output stochastic process is not weakly stationary. The mean value function and autocovariance functions both depend on time t. More critically, the outputs in a near neighborhood are highly correlated. Therefore, the usual approach for the parameter estimation, such as nonlinear regression methods, is not applicable to this kind of data because of the existence of high correlation. The first stage of the parameter identification in W-BEST is still applicable in this case since what needed in this stage is the average values of the several output data points after the process goes to the steady state for each step input change. These average values can be looked as independent of each other if there is long enough time for the process to go to the steady state and the correlation between points that are far away from each other can be neglected. However, this is not the case for the dynamic parameter identification. In W-BEST, the dynamic parameter is estimated by employing the nonlinear regression or linear regression after the data transformation. These methods assume that the response variables are independent of each other and the errors are independent and identically distributed. This is not true for the process outputs when considering the input stochastic noises. It is necessary to propose a parameter estimation method that is applicable to the highly correlated stochastic process data, such as the input-output data collected from a process with input stochastic noises. An estimation method, which does not depend on the independence and constant variances assumptions, will be proposed in Section 4.6. The dynamic parameter is critical in model prediction, while the information of the input noise, including the variance and correlation parameters, can help the engineer to determine if the system input is still in control and if any action should be

taken on the input to keep the system under control. Again, the focus is put on the linear dynamic block and it is assumed that the static mapping relationship is invertible so that the intermediate output $v(t)$ can be obtained given that the final output $y(t)$ is observed and the static mapping relationship has been identified.

4.6 The proposed parameter estimation method

So far, little work has been done on this estimation problem under the Wiener dynamic process with the Gaussian input noise in the literature found, though an approximate model was discussed in some papers that will be discussed in next chapter. The parameters, including one dynamic parameter and two covariance structure parameters, need to be estimated efficiently. From now on, we use σ^2 to stand for σ_ϵ^2.

The method proposed in this work is very intuitive. The original SDE was treated as it is. The idea of the proposed method is to make use of the estimating functions based on the first two moments of the output process as described below.

Analytically, the solution to the SDE, $\frac{dv(t)}{dt} + av(t) = a\varepsilon(t) + a\eta(t)$ with $v(0) = v_0$ is $v(t) = v_0 e^{-at} + a\, e^{-at} \int_0^t e^{as}\, \varepsilon(s)\, ds + \eta(t)\left(1 - e^{-at}\right)$ as given in (4.6). In practice, $v(t)$ is available once the output data are collected and the nonlinear static mapping relationship is determined, which is assumed to be invertible. The mean of $v(t)$ at each time point is changing with time as mentioned before and it is not weakly stationary. Based on the discretely-available $v(t_i)$ values over the time scale, the following estimating equation was established

$$\sum_{i=1}^{N}{}^{k} v(t_i) = \sum_{i=1}^{N} \left(v_0\, e^{-a t_i} + \eta(t)\left(1 - e^{-a t_i}\right)\right). \tag{4.15}$$

where i denotes the number of observations in one path, $i = 1,2,\ldots, N$, and N is the total number of sampled observations for each path; k denotes the number of paths, and

$k = 1,2,...,Nsiml$, $Nsiml$ is the total number of the sampled paths. For each path, one estimating equation can be set up.

This means that the sample average of the discretely observed outputs of one path is supposed to approximate its expected theoretical one as the sample size increases, though these values are changing over time. Since $a\,e^{-at}\int_0^t e^{as}\,\varepsilon(s)\,ds$ is a random term and has an expectation zero, it does not show up in the right hand side of (4.15). This equation does not contain the covariance parameters so that it can be used for estimating the dynamic parameter a even when the covariance parameters α and σ are unknown.

The covariance of the output variable at two different time points is changing with time as well as the distance between the two time points. Thus, it does not make sense to calculate the covariance for a particular lag distance since the covariance value also depends on the specific time point. Nevertheless, this idea can still be employed to set up the other two estimating equations as follows to estimate the covariance parameters α and σ.

$$\sum_{d=1}^{m}\sum_{k=1}^{Nsiml}\sum_{i=1}^{N-d}\left({}^{k}v(t_{i+d})-v_0\,e^{-\hat{a}\,t_{i+d}}-\eta(t)\left(1-e^{-\hat{a}\,t_{i+d}}\right)\right)\left({}^{k}v(t_i)-v_0\,e^{-\hat{a}\,t_i}-\eta(t)\left(1-e^{-\hat{a}\,t_i}\right)\right)$$
$$=\sum_{d=1}^{m}\sum_{k=1}^{Nsiml}\sum_{i=1}^{N-d}\left(\frac{\hat{a}^2\,\sigma^2}{\hat{a}^2-\alpha^2}\left[e^{-\alpha|\tau|}-\frac{\alpha}{\hat{a}}e^{-\hat{a}|\tau|}+\left(1+\frac{\alpha}{\hat{a}}\right)e^{-\hat{a}\,(t_{i+d}+t_i)}-e^{-\hat{a}\,t_{i+d}-\alpha\,t_i}-e^{-\alpha\,t_{i+d}-\hat{a}\,t_i}\right]\right) \tag{4.16}$$

$$\sum_{d=m+1}^{p}\sum_{k=1}^{Nsiml}\sum_{i=1}^{N-d}\left({}^{k}v(t_{i+d})-v_0\,e^{-\hat{a}\,t_{i+d}}-\eta(t)\left(1-e^{-\hat{a}\,t_{i+d}}\right)\right)\left({}^{k}v(t_i)-v_0\,e^{-\hat{a}\,t_i}-\eta(t)\left(1-e^{-\hat{a}\,t_i}\right)\right)$$
$$=\sum_{d=m+1}^{p}\sum_{k=1}^{Nsiml}\sum_{i=1}^{N-d}\left(\frac{\hat{a}^2\,\sigma^2}{\hat{a}^2-\alpha^2}\left[e^{-\alpha|\tau|}-\frac{\alpha}{\hat{a}}e^{-\hat{a}|\tau|}+\left(1+\frac{\alpha}{\hat{a}}\right)e^{-\hat{a}\,(t_{i+d}+t_i)}-e^{-\hat{a}\,t_{i+d}-\alpha\,t_i}-e^{-\alpha\,t_{i+d}-\hat{a}\,t_i}\right]\right) \tag{4.17}$$

where d is the distance between two time points and other notations are the same as before. These two equations make use of the idea that the covariance structure of the available stochastic process is supposed to approximate the theoretical one and the summation of the covariance based on the observed process should approximate the summation of the theoretical ones. Note that p is not supposed to be very large since the covariance for large

distance away time points gets very small and the estimation using such small covariance is not reliable.

The above set of nonlinear equations looks hard to solve. Noting that σ^2 appears once only in the left hand side of both (4.16) and (4.17), after dividing (4.16) by (4.17), σ^2 is canceled out. Thus, what left is an equation with only one parameter α and this makes the root finding procedure more stable. After estimating parameter α, the parameter σ^2 can be obtained by employing the estimating equations based on the variance also.

$$\begin{aligned}&\sum_{i=1}^{N}\left({}^{k}v(t_i)-v_0\,e^{-\hat{a}\,t_i}-\eta(t)\left(1-e^{-\hat{a}\,t_i}\right)\right)^2\\&=\sum_{i=1}^{N}\frac{\hat{a}^2\,\sigma^2}{\hat{a}^2-\hat{\alpha}^2}\left[1-\frac{\hat{\alpha}}{\hat{a}}+\left(1+\frac{\hat{\alpha}}{\hat{a}}\right)e^{-2\,\hat{a}\,t_i}-2\,e^{-(\hat{a}+\hat{\alpha})t_i}\right]\end{aligned}\qquad(4.18)$$

The proposed method only rely on the stochastic process *v(t)* and it is not necessary to estimate the derivatives of *v(t)*. The results will be presented in the next section.

4.7 Results and conclusions

4.7.1 Simulation results

A single-input, single-output Wiener dynamic process with first order dynamics and with stochastic input noise with specified covariance structure is simulated by the approach discussed in Section 4.5. The mean and variance at each time point, as well as the covariance values of the simulated process are calculated and compared with the theoretical ones. In these simulations, the sampling instance is 0.1 time unit, and the sampling frequency is fixed. The good agreement between the simulated output moments and the theoretical ones ensures that there is no obvious deviation of the simulation except those caused by the numerical rounding.

The proposed estimating equations are applied to the stochastic processes in three stages. The parameter a is estimated first, then α, and finally σ. All the parameters are estimated

successfully by the proposed method and the estimates are listed below in Table 4.1. The estimation of the parameters α and σ as proposed in this work has to be done with several sample paths since the covariance of the stochastic process has to be calculated based on several sample paths. Thus, ten or more sample paths, as a group, are sampled in order to get one set of the estimated covariance parameters. More than one group of such simulated paths are sampled to get the variances of the estimated parameters and their confidence intervals (C.I.) as the variance and C.I. are good indicators of the reliability of the estimator. Since the estimator based on the estimating equation is approximately normally distributed, the 95% C.I. of θ can be approximated by $\hat{\theta} \pm 1.96 \times s.e.\left(\hat{\theta}\right)$ (*s.e.* stands for standard error.) Here, the dynamic parameter is estimated for each sampled path; the covariance parameters are estimated based on groups of 10 sampled paths. Each of the simulated paths has 1000 sampled observations. Totally 500 estimates are obtained for each parameter.

The proposed estimating equation method works well for estimating all three parameters. The estimated parameters are all close to the true values as shown in Table 4.1. The proposed method never failed to converge for all these simulations. Thus we can say it is robust and stable. The proposed method does not require the observations of input noises or the derivatives of the outputs. It only requires the output process itself.

Table 4.1. The parameter estimates based on the proposed method.

	Dynamic parameter a	Covariance parameter α	Covariance parameter σ
True value	0.20	0.60	0.50
Mean of the estimates	0.214	0.635	0.495
Standard error of the estimates	0.0616	0.141	0.0293
Approximate 95% confidence interval	(0.0932, 0.335)	(0.358, 0.912)	(0.438, 0.552)

For the proposed method, it was also checked how many data points are necessary for the

dynamic parameter estimation and the results are shown in Table 4.2. All the estimated values are close to the true value $a = 0.2$. It is more proper to check how long the data should be collected over time while keeping the time constant value in mind. It turned out that the dynamic parameter could be estimated pretty close to the true value with limited sampled points as small as 100 (sampling instant 0.1 time unit). Since the estimators are asymptotically normally distributed and the estimates are independent of each other, t-test is approximately all right to use here. None of these estimates are significantly different from the true value 0.2 based on the *t*-test. However, too much steady state information is probably contained in the collected data if the sampling interval is too long comparing to the time constant as we can see that the variance of the estimate increased when the number of observations increased. The underlying reason is that the data points are all from a process with stochastic noises. We would suggest collecting data for around two to four times of the time constants. We probably will have an idea on how large the time constant is after estimating the dynamic parameter based on the first sampled process.

Table 4.2. The estimates for dynamic parameter a based on different number of observations (all are from the beginning, based on 1000 simulated sample paths; true value is $a = 0.2$).

Number of observations	100	200	400	600	800
Sampling interval time units	10	20	40	60	80
Mean of $\hat{a}$	0.1999	0.2001	0.2024	0.2056	0.2086
Standard error of $\hat{a}$	0.01390	0.01716	0.02718	0.03621	0.04591
Approximate 95% C. I.	(0.1726, 0.2272)	(0.1664, 0.2337)	(0.1491, 0.2556)	(0.1346, 0.2766)	(0.1186, 0.2986)

It is obvious that the more the sampled paths are included in the estimation procedure, the closer the estimates are to the true values ($\alpha = 0.6$, $\sigma = 0.5$); the smaller the variances of the estimates, the shorter the approximate 95% confidence intervals as shown in Table 4.3. None of the above estimates are significantly different from their corresponding true values.

Note that the variances of the estimates were calculated from 500 estimates each, which means that there are different numbers of total paths. It is not surprising that the more paths (data) are collected, the more precise the estimates are, because more information has been captured.

Table 4.3. The estimates for the covariance parameter based on the proposed method (True values are $\alpha = 0.6$ and $\sigma = 0.5$).

Number of sample paths for estimating each α and σ	*10*	*15*	*20*
Mean of $\hat{\alpha}$	0.635	0.610	0.617
Standard error of $\hat{\alpha}$	0.141	0.102	0.0909
Approximate 95% C. I.	(0.358, 0.912)	(0.409, 0.811)	(0.439, 0.795)
Mean of $\hat{\sigma}$	0.496	0.491	0.493
Standard error of $\hat{\sigma}$	0.0293	0.0220	0.0188
Approximate 95% C. I.	(0.439, 0.553)	(0.448, 0.534)	(0.456, 0.530)

With the same number of available paths, the estimates, their corresponding variances and 95% confidence intervals are listed in Table 4.4 a, b and c for three different total numbers of simulated paths, 60, 600 and 6000, considering different number of paths as a group to estimate the covariance parameters. In Tables a, b and c, it is clear that the approximate 95% confidence intervals become shorter and more centered at the true values as the number of sample paths for estimating each α and σ increased from 5 to 10 and 15. However, to increase the group size from 15 to 20 does not make much improvement. Thus, we would suggest employing 10 to 15 sampled paths when estimating the covariance parameters.

It is a little bit tricky when dealing with the estimating equations for α and σ. The starting point is important when solving those equations since they are nonlinear. The choice of p and m values is also critical. Several different p and m values were tried in estimating

Table 4.4. The Investigation of group size for estimating the covariance parameters (True values are $\alpha = 0.6$ and $\sigma = 0.5$).

a. Total number of simulated paths is 60.

Number of sample paths for estimating each α and σ	*5*	*10*	*15*	*20*
Mean of $\hat{\alpha}$	0.650	0.577	0.667	0.575
Standard error of $\hat{\alpha}$	0.242	0.167	0.112	0.0782
Approximate 95% C. I.	(0.176, 1.124)	(0.250, 0.904)	(0.448, 0.886)	(0.422, 0.728)
Mean of $\hat{\sigma}$	0.499	0.504	0.500	0.491
Standard error of $\hat{\sigma}$	0.0455	0.0459	0.00752	0.0138
Approximate 95% C. I.	(0.410, 0.588)	(0.413, 0.594)	(0.485, 0.514)	(0.464, 0.518)

b. Total number of simulated paths is 600.

Number of sample paths for estimating each α and σ	*5*	*10*	*15*	*20*
Mean of $\hat{\alpha}$	0.701	0.604	0.590	0.616
Standard error of $\hat{\alpha}$	0.281	0.155	0.101	0.110
Approximate 95% C. I.	(0.150, 1.252)	(0.301, 0.907)	(0.391, 0.789)	(0.401, 0.831)
Mean of $\hat{\sigma}$	0.511	0.491	0.490	0.497
Standard error of $\hat{\sigma}$	0.0640	0.0346	0.0212	0.0206
Approximate 95% C. I.	(0.385, 0.636)	(0.423, 0.559)	(0.448, 0.531)	(0.457, 0.538)

c. Total number of simulated paths is 6000.

Number of sample paths for estimating each α and σ	*5*	*10*	*15*	*20*
Mean of $\hat{\alpha}$	0.673	0.624	0.605	0.617
Standard error of $\hat{\alpha}$	0.241	0.135	0.0315	0.0891
Approximate 95% C. I.	(0.201, 1.145)	(0.360, 0.888)	(0.543, 0.667)	(0.442, 0.792)
Mean of $\hat{\sigma}$	0.501	0.496	0.491	0.493
Standard error of $\hat{\sigma}$	0.0544	0.0308	0.0215	0.0194
Approximate 95% C. I.	(0.394, 0.608)	(0.436, 0.556)	(0.449, 0.533)	(0.455, 0.531)

Equations (4.16) and (4.17) for the estimating of α. They gave slightly different estimates if p and m values are reasonably chosen. The values of m cannot be too large since the estimated covariance is not reliable when the distance between the two points gets large. Very large m values were tried, say $m = N = 1000$, but the estimators turned out to be much worse than those with reasonable m values, say $m = 50$.

The estimator for σ is robust to the change of estimating equations (choice of p and m) and the estimated α. This was always seen in the simulation and estimation.

4.7.2 Conclusions

This work focused on the single-input, single-output (SISO) Wiener dynamic process with first order dynamics. As shown in the work, for such a process, the correlated input noises can cause significant drifts in the output variables, and more critically, those outputs over time are highly correlated. The linear or nonlinear regression methods, which are applicable only to the independent observations, are not valid here any more. It is worthwhile to propose a new methodology for the model parameter estimation in such cases and investigate its efficiency.

To my best knowledge, no one has considered the continuous-time modeling of the process with stochastic input noise under the framework of control, and no one has ever proposed the estimating equation method for such kind of problem. With the assumptions that the nonlinear static mapping relationship has been identified and is invertible, and that the input disturbance has the specified covariance structures, the estimating equations are established based on the moment method and work well for the simulated Wiener dynamic process. This approach has led to stable and robust estimators that have reasonable estimation errors. The estimation of the dynamic parameter does not require many observed output data points and the estimate is close to the true value. For the covariance parameters,

a couple of sampled processes are needed in order to use the proposed estimation method. The more observed process paths, the more reliable the estimates can be obtained.

The most important advantage of this approach is that there is no need to measure the input noises or calculate the time derivative of the observed output variable, where the later one is hard to obtain accurately for the stochastic process with noise. Only the original process output observations are needed over time. The input disturbances or noises are always unobservable in practice. It is more feasible to work with a method that makes use of just the observed values and avoids the derivative calculation of a process with stochastic noises, where the noise accentuation problem has to be faced.

For estimating equations, stability and independence are two important requirements. The proposed method gives stable estimates according to our simulation. It never failed for thousands of simulations. Also, it is pretty robust, especially for estimating the dynamic parameter and the variance of the input noise. The dynamic parameter can be estimated satisfactorily without any problem with just one sampled path. Recall that the estimation is done in three stages. The variance, which is estimated last, can still be estimated satisfactorily even when the estimates of the previous two parameters are a little bit away from the true values. Though we did not work on the proof of the efficiency and the condition checks of the proposed methods; the proposed method has been shown to be a new and efficient application to the Wiener dynamic system with stochastic input noises.

This work considered the SISO Wiener dynamic process only and the dynamics is limited to be first order. The case would be much more complicated for processes with second order or higher order dynamics because of the complexity of the higher order stochastic differential equations. The situation for multiple-input, multiple -output (MIMO) process with more than one input variable having the stochastic input noises imposed on them, especially when the interactions of the variables exist is complicated too. As have been pointed out, the nonlinear

static mapping is assumed to be invertible in this work, so that the intermediate output, or the output of the dynamic block, can be obtained from the SISO Wiener dynamic process final output after the nonlinear static mapping relation has been identified. However, in the MIMO case, it is highly possible that we cannot obtain the intermediate output $v(t)$ especially when interactions exist. Or in other words, the "invertible" assumption of the nonlinear static mapping is usually not satisfied for MIMO Wiener dynamic process. More work has to be done in that case.

Work on the Hammerstein process is also necessary since the Hammerstein model can approximate some physical processes better than the Wiener dynamic model, where the Hammerstein model is very similar to the Wiener dynamic model except that the order of the two blocks is reversed.

The same investigation is necessary to be done on a physical process, such as the CSTR, in order to see the effects of noisy inputs on the parameter estimation and further predictions. However, this physical process has to be able to be approximated by a Wiener dynamic process with first order dynamics reasonably. Otherwise, the proposed estimating equations cannot be applied. The real data are not yet available to the researchers. So, what has been done was to test the proposed method on the simulated theoretical Wiener dynamic process.

Another limitation is that the input noise is assumed to have the specified correlation structure given in (4.5). Though this correlation structure is common and acceptable, it is a strong assumption. However, the estimating equation approach is a general method that could be employed for other type of input noise correlation structure once the analytical solutions are available. Different estimating equations have to be established.

To be incorporated into the W-BEST technique, where the sequence step input changes are designed, more work has to be done because only one step input change is considered in this work. We understand that there is a gap between this theoretical work and the practice.

References

Bai, Er-Wei, Frequency domain identification of Hammerstein models, *IEEE Transactions on Automatic Control*, **48**: 4, 530-542, 2003.

Bhandari, N. and Rollins, D.K., Continuous-time multi-input, multi-output Wiener modeling method, *Industrial & Engineering Chemistry Research,* **42**: 22, 5583-5595, 2003.

Gomez, Juan C. and Baeyens, Enrique, Identification of block-oriented nonlinear systems using orthonormal bases, *Journal of Process Control*, **14**: 6, 685-697, 2004.

Greblicki, W., Nonparametric identification of Wiener systems, *IEEE Transactions on Information Theory*, **38**: 1487-1493 (1992).

Greblicki, W., Nonparametric approach to Wiener system identification, *IEEE Transactions on Circuits Systems I*, **44**: 538-545 (1997).

Hagenblad, Anna, Aspects of the identification of Wiener models, Linkoping Studies in Science and Technology, Thesis No. 793, Linkopings universitet, SE-581 83, Linkoping, Sweden, 1999.

Henson, M.A. and Seborg, D.E., *Nonlinear process control*, Upper Saddle River, NJ; Prentice Hall PTR, 1997.

Huang, H.-P., Lee, M.-W., and Tang, Y.-T., Identification of Wiener model using relay feedback test, *Journal of Chemical Engineering of Japan*, **31**: 604-612 (1998).

Kalafatis, A., Arifin, N., Wang, L., and Cluett W.R., A new approach to the identification of pH process based on the Wiener model, *Chemical Engineering Science*, **50**, 3693-3701, 1995.

Nordsjo, A.E., Cramer-Rao bounds for a class of systems described by Wiener and Hammerstein models, *International Journal of Control*, **68**: 5, 1067-1083, 1997.

Nordsjo, A.E. and Wigren, T., On estimation of errors caused by non-linear undermodelling in system identification, *International Journal of Control*, **75**: 14, 1100-

1113, 2002.

Ochi, Michel K., *Applied probability and stochastic processes in engineering and physical sciences*, Wiley, New York, 1990.

Ripley, B.D., *Stochastic simulation*, John Wiley & Sons, New York, 1987.

Rollins, D.K. and Bhandari, N., Constrained MIMO dynamic discrete-time modeling exploiting optimal experimental design, *Journal of Process Control*, **14**: 6, 671-683, 2004.

Rollins, D.K., Bhandari, N., Bassily, A.M., Colver, G.M., and Chin, S.-T., A continuous-time nonlinear dynamic predictive modeling method for Hammerstein processes, *Industrial & Engineering Chemistry Research,* **42**: 4, 861-872, 2003.

Schoukens, J., Nemeth, J.G., Crama, P., Rolain Y., and Pintelon, R., Fast approximate identification of nonlinear systems, *Automatica*, **39**, 1267-1274, 2003.

Sobczyk, Kazimierz, *Stochastic differential equations: application in physics and engineering*, Kluwer Academic, Boston, 1991.

Vandersteen, Gerd, Rolain, Yves and Schoukens, Johan, Non-parametric estimation of the frequency-response functions of the linear blocks of a Wiener-Hammerstein model, *Automatica*, **33**: 7, 1351-1355, 1997.

Wigren, T., Recursive prediction error identification using the nonlinear Wiener model, *Automatica*, **29**: 1011-1025, 1993.

Chapter 5. Parameter Estimation of the Continuous-Time Block-Oriented Wiener Dynamic System With Stochastic Input Noises — A Second Approach

5.1 Introduction

In Chapter 4, a parameter estimation problem was considered for the continuous-time Wiener dynamic system with stochastic input noises. It is assumed that the nonlinear static relationship has been identified and is invertible. With the observed process output only, all the parameters were estimated successfully by using the estimating equations established. In this chapter, we will re-consider this problem, but with a second approach. All the related concepts have been explained in Chapter 4.

The dynamic block model that was focused on in Chapter 4 is first order and could be described mathematically as

$$\frac{dv(t)}{dt} + av(t) = a\eta(t) + a\varepsilon(t) \tag{5.1}$$

where $\eta(t)$ is the nominal value of the input variable, which is deterministic, and $\varepsilon(t)$ is a random noise, which is assumed to be a weakly stationary Gaussian process with

$$E[\,\varepsilon(t)\,] = 0 \text{ and } Cov[\,\varepsilon(t_1), \varepsilon(t_2)\,] = \sigma^2 e^{-\alpha|t_2 - t_1|}. \tag{5.2}$$

The $v(t)$ is the intermediate output of the Wiener dynamic process, and can be obtained by inversing the nonlinear static mapping relationship once the final process outputs $y(t)$ are observed and the nonlinear static mapping relationship is identified. Here, a is the dynamic parameter, which is the inverse of the time constant τ, or $a = 1/\tau$, and σ^2 and α are covariance parameters, where σ^2 is the variance of the input noise and α determines the speed by which the correlation between two time points decreases.

In Chapter 4, the above stochastic differential equation was treated as it is. A set of estimating equations based on the moment structure was established and it has been shown

by simulation that the dynamic and covariance parameters can be estimated efficiently. As have been mentioned, so far little work has been done on this estimation problem for the above model in the literature. However, Bellach (1983) considered an approximate model instead of the above one and presented the corresponding estimation methods. This provides a second approach to solve the estimation problem — making use of an approximate model to estimate the dynamic and covariance parameters. By shifting the original stochastic problem to the approximate model with a standard Wiener stochastic process, one can make use of the well-known properties of the standard Wiener stochastic process, whose parameter estimation problem has been widely investigated. It is also interested to see how the estimating equation approach works in this case. Comparisons of the estimating equation approach with other researcher's methods are also of interest.

5.2 The approximate model for the estimation problem

Bellach (1983) worked on a stochastic process with the same moment structure of the input noise as in this work. The process she considered was as follows, where the coefficient for a third variable *X(t)* was also unknown and of interest.

$$\frac{dY(t)}{dt} = a\,Y(t) + b\,X(t) + \varepsilon(t) \text{ with } Y(0) = 0, \tag{5.3}$$

where $E[\varepsilon(t)] = 0$, and $E[\varepsilon(t_1), \varepsilon(t_2)] = k\,e^{\gamma|t_1 - t_2|}$ (5.4)

It is obvious that our model is a special case of this model. The difference is that there is a third variable *X(t)* with an unknown coefficient in her model. However, she considered an approximate model instead of the original one described in (5.3) and (5.4) when she proposed her estimation method. The model she considered was

$$\begin{cases} \dfrac{dY(t)}{dt} = a\,Y(t) + b\,X(t) + \varepsilon(t) \text{ with } Y(0) = 0 \\ d\varepsilon(t) = \rho\,\varepsilon(t)\,dt + c\,dW(t) \end{cases} \tag{5.5}$$

and she stated that this model could approximate the original one as c and ρ went to infinity and $-c/\rho$ converged to a constant. Here, $\{W(t),\ t \in [0,T]\}$ is a standard Wiener stochastic process, which is also called the Brownian motion process. It has the following properties: $W(0) = 0$ with probability 1; $E[W(t)] = 0$ for all t; $W(t)$ has stationary independent increment; every independent increment is normally distributed. The covariance function of a Brownian motion process is $Cov_w(t_1,t_2) = \min(t_1,t_2)$.

In order to understand this approximation, it is worth to take a look at the following stochastic differential equation (SDE) first, which is also called diffusion process, Ornstein-Uhlenbeck process, or Ito equation,

$$d\varepsilon(t) = \rho\,\varepsilon(t)dt + c\,dW(t),\ \ \varepsilon(0) = \varepsilon_0,\ \ \rho < 0,\ c > 0 \tag{5.6}$$

where $\{W(t),\ t \in [0,T]\}$ is a standard Wiener stochastic process. Its analytical solution is (Sobczyk, 1991)

$$\varepsilon(t) = \varepsilon_0\, e^{\rho t} + c\, e^{\rho t} \int_0^t e^{-\rho s}\, dW(s). \tag{5.7}$$

The corresponding mean value function and covariance functions are

$$E[\varepsilon(t)] = \varepsilon_0\, e^{\rho t} \tag{5.8}$$

$$Cov_\varepsilon(t_1,t_2) = -\frac{c^2}{2\rho} e^{\rho|\tau|}\left(1 - e^{2\rho\cdot\min(t_1,t_2)}\right) = -\frac{c^2}{2\rho}\left(e^{\rho|\tau|} - e^{\rho(t_1+t_2)}\right) \tag{5.9}$$

$$Var_\varepsilon(t) = -\frac{c^2}{2\rho}\left(1 - e^{2\rho t}\right) \tag{5.10}$$

where $\tau = t_2 - t_1$. Note that the $\epsilon(t)$ process is not weakly stationary.

The stationary solution to $\epsilon(t)$ as $t_1 \to \infty$ and $t_2 \to \infty$ (with τ fixed) has the following moments

$$E[\varepsilon(t)] = 0 \text{ and } Cov_\varepsilon(t_1,t_2) = Cov_\varepsilon(\tau) = -\frac{c^2}{2\rho} e^{\rho|\tau|}. \tag{5.11}$$

When $-\rho$ and c tend to be large in such a way that $-\rho/c$ converges to a constant, the process $\{\varepsilon(t),\ t \in [0,T]\}$ tends to be a weakly stationary Gaussian process and has the moment structure described above in (5.4). Therefore, it is reasonable that Bellach (1983) stated that the above approximation was appropriate under these conditions.

By following this approximation, we consider the model described by the following two equations (5.12) and (5.13) instead of our original model described in (5.1) and (5.2),

$$\frac{dv(t)}{dt} + a\,v(t) = a\,\eta(t) + a\,\varepsilon(t), \text{ with } v(0) = v_0 \tag{5.12}$$

and $$d\varepsilon(t) = -\alpha\,\varepsilon(t)\,dt + \sigma\sqrt{2\alpha}\,dW(t) \tag{5.13}$$

where a, α, and σ are unknown parameters, and $a > 0$, $\alpha > 0$, $\sigma > 0$. The stochastic process $\{v(t), t \in [0,T]\}$ thus can be simulated based on this approximation.

It is still necessary to make sure that this approximation would give the appropriate final output process when the process $\epsilon(t)$ under (5.13) was introduced into (5.12). The moment structure of the output process $v(t)$ under the approximate model is derived and listed below:

$$E[v(t)] = v_0\,e^{-at} + \eta(t)\left(1 - e^{-at}\right) \tag{5.14}$$

$$Cov_v(t_1,t_2) = \frac{a^2\sigma^2}{a^2-\alpha^2}\left[e^{-\alpha|t_1-t_2|} - \frac{\alpha}{a}e^{-a|t_1-t_2|} + \frac{2\alpha}{a-\alpha}\left(e^{-at_1-\alpha t_2} + e^{-\alpha t_1-at_2}\right)\right.$$
$$\left. - \frac{a+\alpha}{a-\alpha}e^{-\alpha(t_1+t_2)} - \frac{\alpha(a+\alpha)}{a(a-\alpha)}e^{-a(t_1+t_2)}\right] \tag{5.15}$$

$$Var_v(t) = \frac{a^2\sigma^2}{a^2-\alpha^2}\left[1 - \frac{\alpha}{a} + \frac{4\alpha}{a-\alpha}e^{-(a+\alpha)t} - \frac{a+\alpha}{a-\alpha}e^{-2\alpha t} - \frac{\alpha(a+\alpha)}{a(a-\alpha)}e^{-2at}\right] \tag{5.16}$$

The mean value function of the process $v(t)$ is exactly the same as that for the original model, while the covariance structure looks quite different from that for the original model as given in Chapter 4. However, the stationary covariance structures are the same when t_1 and

t_2 go to large values. Based on these evaluations, this approximation of the original model is employed in this work.

5.3 The process simulation

Simulation is a good way to check if the approximation is appropriate. However, the attention has to be paid to the Wiener stochastic process simulation and to the stochastic integral when simulating the stochastic process $\epsilon(t)$ based on (5.7) due to the special properties of the standard Wiener stochastic process. Note that it is not correct to calculate the integration term in (5.7) using the numerical method for regular Riemann integration. The stochastic integral is different from Riemann integration.

According to the algorithms for numerical simulation of SDE by Higham (2001), a scalar standard Wiener stochastic process over [0, T] can be simulated as follows.

Set $\Delta t = T/N$ for some positive integer N, and let W_j denote $W(t_j)$ with $t_j = j\,\Delta t$, where $j = 1, 2, \cdots, N$. Generate random variable dW_j, which is of the form $\sqrt{\Delta t}\ Norm(0,1)$ independently. $Norm(0,1)$ denotes the standard normal distribution with zero mean and variance one. Note that $W(0) = 0$ as given in the definition. Then, $W_j = W_{j-1} + dW_j$ gives the discretized Brownian path.

As to the stochastic integral, let $\int_0^T h(t)\,dW(t)$ denote the integration of function h with respect to the Brownian motion. As mentioned before, the numerical values cannot be calculated directly based on the dW_j values. It can be approximated as $\sum_{j=0}^{N-1} h(t_j)\left(W(t_{j+1}) - W(t_j)\right)$ (the Ito integral) or $\sum_{j=0}^{N-1} h\left(\frac{t_j + t_{j+1}}{2}\right)\left(W(t_{j+1}) - W(t_j)\right)$ (the Stratonovich integral). The stochastic process $\epsilon(t)$ can be obtained by simulating the Brownian path first and then doing the stochastic integral.

The stochastic process $\epsilon(t)$ can also be obtained by using the Euler-Maruyama method (Higham, 2001). For example, a one-dimension SDE

$$dX(t) = f(X(t))dt + g(X(t))dW(t), \quad X(0) = X_0, \quad 0 \le t \le T$$

can be written in its integral form as

$$X(t) = X_0 + \int_0^t f(X(s))ds + \int_0^t g(X(s))dW(s), \quad 0 \le t \le T \tag{5.17}$$

Letting $\Delta t = T/N$ for some positive number N, $t_j = j\Delta t$, and $X_j = X(j\Delta t)$, the Euler-Maruyama method then gives

$$X_j = X_{j-1} + f(X_{j-1})\Delta t + g(X_{j-1})(W(t_j) - W(t_{j-1})), \quad j = 1, 2, \cdots, N. \tag{5.18}$$

In this work, for the SDE shown in (5.13), the stochastic process $\epsilon(t)$ can be simulated by making use of the Euler-Maruyama method as shown below

$$\varepsilon_j = \varepsilon_{j-1} - \alpha\, \varepsilon_{j-1}\Delta t + \sigma\sqrt{2\alpha}\,(W(t_j) - W(t_{j-1})), \quad j = 1, 2, \cdots, N. \tag{5.19}$$

After that, the stochastic process $v(t)$ can then be obtained based on the explicit solution to (5.12), which is

$$v(t) = v_0 e^{-at} + a\, e^{-at} \int_0^t e^{as}\, \varepsilon(s)ds + \eta(t)(1 - e^{-at}). \tag{5.20}$$

Since the stochastic process $\epsilon(t)$ is continuous in time, unlike dW_j, it is not necessary to worry about the integration with the process $\epsilon(t)$. This numerical integration can be done as the regular Riemann integral.

Both simulation approaches are employed as well as all available numerical methods. The simulated processes with the same seed based on these methods all agree with each other. The first two moments of each simulated process are computed and compared to the theoretical ones to make sure the moment structure is correct. Thus, the simulated output

process $v(t)$ is available. The estimation is based on these process outputs only; no stochastic input noises are needed.

5.4 The parameter estimation method

Only limited literature has been found on the estimation of the three parameters for the approximate model. Some papers (Bellach, 1983; Chen and Kozin, 1991) concentrated on estimating the dynamic parameter a, which is certainly of interest to engineers. Each method has its own assumptions and some of them are very strict. However, these papers did not consider the estimation of the covariance structure parameters. On the other hand, many papers (e.g., Pedersen, 1995; Sorensen, 1997) considered the estimation of the covariance parameters based on the diffusion type process (5.6). These methods could be used after some preliminary estimation though they were not specifically for the approximate model. That is one advantage to shift the original SDE to the Wiener stochastic process and consider the approximate model instead of the original one. These methods will be reviewed in this section first and the proposed method will then be presented. The proposed method and other methods will all be employed to estimate the parameters for the Wiener dynamic process later and the results will be presented in Section 5.5.

5.4.1 Dynamic parameter estimation — A review

To the best of my knowledge, Bellach (1983) is the only one who worked on a stochastic model with the same input noise moment structure as in this work and her model was listed in (5.3) and (5.4). The difference between her model and the one in this work is that there is a third variable $X(t)$ in her model and the coefficient for $X(t)$ is unknown and also of interest. Her objective was to estimate the parameters a and b at the same time. She considered the model in (5.5) instead of the original one in (5.3) and (5.4), where c and ρ went to infinity

and $-c/\rho$ converged to a constant. Based on this approximation, Bellach (1983) mentioned the least squares estimator (LSE) of the coefficients *a* and *b*, which had nothing to do with the covariance parameters. Also, note that *X(t)* is assumed to be a differentiable real function and its derivatives are measurable and bounded over [0, T]. The LSE she provided was

$$\begin{pmatrix}\hat{a}_T\\ \hat{b}_T\end{pmatrix}=\frac{\int_0^T \begin{pmatrix}Y(t)\\ X(t)\end{pmatrix}\frac{dY(t)}{dt}\,dt}{\int_0^T \begin{pmatrix}Y(t)\\ X(t)\end{pmatrix}\begin{pmatrix}Y(t) & X(t)\end{pmatrix}dt} \tag{5.21}$$

However, the LSE is biased for $T \to \infty$ as the author pointed out. Then she constructed an instrumental variable estimator, which was

$$\begin{pmatrix}\hat{a}_T\\ \hat{b}_T\end{pmatrix}=\min_{\theta \in R\times R}\left\|\frac{dY(\cdot)}{dt}-a\,\hat{Y}(\cdot)-b\,X(\cdot)\right\|_{[0,T]}=\frac{\int_0^T \begin{pmatrix}\hat{Y}(t)\\ X(t)\end{pmatrix}\frac{dY(t)}{dt}\,dt}{\int_0^T \begin{pmatrix}\hat{Y}(t)\\ X(t)\end{pmatrix}\begin{pmatrix}\hat{Y}(t) & X(t)\end{pmatrix}dt} \tag{5.22}$$

The predicted process $\hat{Y}(t)$ was employed instead of the observed $Y(t)$. The idea here was still to minimize the error term. The estimator (5.22) is not straightforward to apply in practice since the predicted process $\hat{Y}(t)$ is generally not available and have to be estimated after estimating the unknown parameters, though this estimator was proved to be consistent asymptotically. An iterative algorithm is necessary to make use of this estimation method.

In our case, where there is no such third variable as *X(t)*, the LSE according to Bellach is simplified to be

$$\hat{a}(T)=\frac{\int_0^T v(t)\,dv(t)}{\int_0^T v(t)^2\,dt}. \tag{5.23}$$

This estimation method will be employed in this work to compare with the proposed method.

Chen and Kozin (1991) presented a strong consistent estimator to the *n*th order physical excitation system by using a generalization of a lemma on the law of large numbers for stochastic integral proved by Khazminskii when they considered a general system

$$\begin{cases} \dfrac{dY_t}{dt} = Q(Y_t)H + \varepsilon_t \\ d\varepsilon_t = B\,\varepsilon_t\,dt + dW_t \end{cases} \tag{5.24}$$

where H was an unknown parameter; Q was a known function of Y_t, which could be nonlinear; Y_t was assumed to be observable; ε_t was generated by a linear diffusion type differential equation. When $Q(Y_t) = aY_t$, this system becomes the Bellach's model in (5.3) and (5.4) without the third variable *X(t)*. However, Chen and Kozin did not relate this equation set back to one single SDE with specified input moment structure as described in (5.1) and (5.2).

For the system described in (5.24), if the partial derivative of $Q(Y_t)$ with respect to Y_t existed, and Y_t was a stationary ergodic process, the following estimator

$$\hat{H} = \frac{\int_0^T \left(\dfrac{dQ(Y_t)}{dt} - BQ(Y_t)\right) \cdot d\left(\dfrac{dY_t}{dt} - BY_t\right)}{\int_0^T \left(\dfrac{dQ(Y_t)}{dt} - BQ(Y_t)\right)^2 dt} \tag{5.25}$$

was proved to be a strong consistent estimator of H in one dimensional case. Also, Chen and Kozin stated that the estimator proposed by Bellach was only weakly consistent.

For the dynamic block in the Wiener dynamic system described by (5.1) and (5.2), and approximated by (5.12) and (5.13), according to Chen and Kozin's method, the estimator of the dynamic parameter a is

$$\hat{a} = -\frac{\int_0^T \left(\frac{dv_t}{dt} + \alpha v_t\right) \cdot d\left(\frac{dv_t}{dt} + \alpha v_t\right)}{\int_0^T \left(\frac{dv_t}{dt} + \alpha v_t\right)^2 dt} \tag{5.26}$$

This estimator requires the iterative estimation of the covariance parameter α and the dynamic parameter a. However, as shown in (5.14) to (5.16), the mean value function, and variance and covariance functions of the output process for the Wiener dynamic process with stochastic input noises are all changing with time. Thus, the output stochastic process is not stationary and not ergodic. Hence, this estimator is not applicable to the approximate model in this work because the assumptions are not valid. This method was tested with the Wiener dynamic process data, by assuming that the parameter α is known exactly, to decide if it is reliable to use and if it is necessary to do any further iterative estimation.

5.4.2 Covariance parameter estimation — A review

The estimation of the covariance structure parameters, α and σ, based on the diffusion process (Ornstein-Uhlenbeck process) has been widely investigated and the estimation methods provided by the literatures can be employed in this work. These covariance parameter estimation methods were almost completely separated from the estimation of dynamic parameter a except that the stochastic input noise process has to be computed with the estimated dynamic parameter $\hat{a}$ as shown below:

$$\hat{\varepsilon}(t) = \frac{1}{\hat{a}} \cdot \frac{dv(t)}{dt} + v(t) - \eta(t) \tag{5.27}$$

Once the process $\epsilon(t)$ is computed based on the available process $v(t)$, it is possible to use the estimation methods for the diffusion process to get estimates of α and σ for the Wiener dynamic process.

In practice, it is difficult to have continuous observations of a stochastic process over a given time period. Usually, only discretely observed data are available. For the diffusion process, many parameter estimation methods have been reviewed by Rao (1999) in details for discretely observed data. Here, two of the papers are reviewed particularly, and their methods will be employed to compare with the proposed method described later.

For a general diffusion process that can be written as

$$dX(t) = \theta\, X(t)\,dt + \phi\, dW(t),\ X(0) = X_0, \text{ where } \theta \in R \text{ and } \phi > 0, \tag{5.28}$$

Sorensen (1997) provided the following estimators for the discretely observed X_t:

$$\hat{\theta} = \Delta^{-1}\left(\sqrt{2Q_n - 1} - 1\right) \text{ and } \hat{\phi}^2 = \frac{\frac{1}{n}\sum_{i=1}^{n}\left(X_{t_i} - X_{t_{i-1}} Q_n\right)}{\Delta + \hat{\theta}\,\Delta^2 + \frac{2}{3}\hat{\theta}^2\,\Delta^3} \tag{5.29}$$

provided that $Q_n = \dfrac{\sum_{i=1}^{n} X_{t_i} X_{t_{i-1}}}{\sum_{i=1}^{n} X_{t_{i-1}}^2} \geq \dfrac{1}{2}$ and Δ is the sample interval length.

The maximum likelihood estimators for a diffusion process shown in (5.28) were given by Pedersen (1995) as follows

$$\hat{\theta} = \frac{1}{\Delta}\log\left(\frac{\sum_{i=1}^{n} X_{t_i} X_{t_{i-1}}}{\sum_{i=1}^{n} X_{t_{i-1}}^2}\right) \text{ and } \hat{\phi}^2 = \frac{-2\hat{\theta}}{n\left(1 - \exp\left(2\Delta\hat{\theta}\right)\right)}\sum_{i=1}^{n}\left(X_{t_i} - X_{t_{i-1}}\exp\left(\Delta\hat{\theta}\right)\right)^2 \tag{5.30}$$

and they were proved to be consistent estimators (Pedersen, 1995). The approximate log-likelihood estimator $\tilde{\theta}$ and the quadratic variation-like estimator $\tilde{\phi}^2$, which are inconsistent, were also provided by Pederson (1995) as follows

$$\tilde{\theta} = \frac{1}{\Delta}\left(\frac{\sum_{i=1}^{n} X_{t_i} X_{t_{i-1}}}{\sum_{i=1}^{n} X_{t_{i-1}}^2} - 1\right) \text{ and } \tilde{\phi}^2 = \frac{1}{n\Delta}\sum_{i=1}^{n}\left(X_{t_i} - X_{t_{i-1}}\right)^2. \tag{5.31}$$

Although these methods are all for the diffusion process, they can also be employed in this work once the noise process $\varepsilon(t)$ can be computed for the approximate model shown in

(5.12) and (5.13). Note that (5.13) and (5.28) are identical by setting $X_t = \varepsilon(t)$, $\theta = -\alpha$, and $\phi = \sigma\sqrt{2\alpha}$. Therefore, the estimation methods of Sorensen and Pedersen can be applied to the approximate model.

5.4.3 The proposed parameter estimation method

The proposed method is based on estimating equations. The basic idea is that the first two moments of the observed outputs are supposed to approximate the theoretical ones. Based on the discretely available stochastic process $v(t_i)$ over the time scale, and the theoretical moments of the process, the estimating equations can be applied to the approximate model. Therefore, the estimating equation for the dynamic parameter a is:

$$\sum_{i=1}^{N} {}^{k}v(t_i) = \sum_{i=1}^{N} \left(v_0 e^{-a t_i} + \eta(t)\left(1 - e^{-a t_i}\right)\right). \tag{5.32}$$

The equations for estimating covariance parameters α and σ can be written as:

$$\begin{aligned}
&\sum_{d=1}^{m}\sum_{k=1}^{Nsiml}\sum_{i=1}^{N-d}\left({}^{k}v(t_{i+d}) - v_0 e^{-\hat{a}\,t_{i+d}} - \eta(t)\left(1 - e^{-\hat{a}\,t_{i+d}}\right)\right)\left({}^{k}v(t_i) - v_0 e^{-\hat{a}\,t_i} - \eta(t)\left(1 - e^{-\hat{a}\,t_i}\right)\right) \\
&= \sum_{d=1}^{m}\sum_{k=1}^{Nsiml}\sum_{i=1}^{N-d}\frac{\hat{a}^2\,\sigma_\varepsilon^{\,2}}{\hat{a}^2 - \alpha^2}\left[e^{-\alpha|t_{i+d}-t_i|} - \frac{\alpha}{\hat{a}}e^{-\hat{a}|t_{i+d}-t_i|} + \frac{2\alpha}{\hat{a}-\alpha}\left(e^{-\hat{a}\,t_{i+d}-\alpha\,t_i} + e^{-\alpha\,t_{i+d}-\hat{a}\,t_i}\right)\right. \\
&\qquad \left. - \frac{\hat{a}+\alpha}{\hat{a}-\alpha}e^{-\alpha(t_{i+d}+t_i)} - \frac{\alpha(\hat{a}+\alpha)}{\hat{a}(\hat{a}-\alpha)}e^{-\hat{a}(t_{i+d}+t_i)}\right]
\end{aligned} \tag{5.33}$$

$$\begin{aligned}
&\sum_{d=m+1}^{p}\sum_{k=1}^{Nsiml}\sum_{i=1}^{N-d}\left({}^{k}v(t_{i+d}) - v_0 e^{-\hat{a}\,t_{i+d}} - \eta(t)\left(1 - e^{-\hat{a}\,t_{i+d}}\right)\right)\left({}^{k}v(t_i) - v_0 e^{-\hat{a}\,t_i} - \eta(t)\left(1 - e^{-\hat{a}\,t_i}\right)\right) \\
&= \sum_{d=m+1}^{p}\sum_{k=1}^{Nsiml}\sum_{i=1}^{N-d}\frac{\hat{a}^2\,\sigma_\varepsilon^{\,2}}{\hat{a}^2 - \alpha^2}\left[e^{-\alpha|t_{i+d}-t_i|} - \frac{\alpha}{\hat{a}}e^{-\hat{a}|t_{i+d}-t_i|} + \frac{2\alpha}{\hat{a}-\alpha}\left(e^{-\hat{a}\,t_{i+d}-\alpha\,t_i} + e^{-\alpha\,t_{i+d}-\hat{a}\,t_i}\right)\right. \\
&\qquad \left. - \frac{\hat{a}+\alpha}{\hat{a}-\alpha}e^{-\alpha(t_{i+d}+t_i)} - \frac{\alpha(\hat{a}+\alpha)}{\hat{a}(\hat{a}-\alpha)}e^{-\hat{a}(t_{i+d}+t_i)}\right]
\end{aligned} \tag{5.34}$$

where i denotes the number of observations of the stochastic process $v(t)$ in one path, $i = 1,2,\ldots,N$, and N is the total number of sampled observations for each path; k denotes the number of paths, and $k = 1,2,\ldots,Nsiml$, where $Nsiml$ is the total number of the sampled paths; d is the distance between two time points over the sampling interval.

These estimating equations are different from those provided in Chapter 4 since the second moments of the outputs for the approximate and original models are different. Equation (5.32) can be solved first to obtain the estimate of a. Equations (5.33) and (5.34) are coupled, but some manipulation can be taken to simplify the root-finding procedure and make the procedure more stable. Canceling out σ^2 by dividing (5.33) by (5.34), we can find the estimate for α first. After this, the following estimating equation, which is more reliable, can be employed to estimate σ, where $\hat{a}$ and $\hat{\alpha}$ are estimated values from the precious steps.

$$\sum_{i=1}^{N}\left(v(t_i)-v_0\,e^{-\hat{a}t_i}-\eta(t)\left(1-e^{-\hat{a}t_i}\right)\right)^2 = \sum_{i=1}^{N}\frac{\hat{a}^2\,\sigma_\varepsilon^{\,2}}{\hat{a}^2-\hat{\alpha}^2}\left(1-\frac{\hat{\alpha}}{\hat{a}}+\frac{4\hat{\alpha}}{\hat{a}-\hat{\alpha}}e^{-(\hat{a}+\hat{\alpha})t}-\frac{\hat{a}+\hat{\alpha}}{\hat{a}-\hat{\alpha}}e^{-2\hat{\alpha}t}-\frac{\hat{\alpha}(\hat{a}+\hat{\alpha})}{\hat{a}(\hat{a}-\hat{\alpha})}e^{-2\hat{a}t}\right) \tag{5.35}$$

The reviewed methods, as well as the proposed method in this work, are applied to the Wiener dynamic process simulated under the approximate model. The estimation results are given in the next section.

5.5 Results and conclusions

5.5.1 The estimation results

A Wiener dynamic process with the first order dynamic parameter $\tau = 5.0$ ($a = 0.2$) and covariance parameters $\alpha = 0.6$ and $\sigma = 0.5$ was simulated by the approach discussed in Section 5.3. (It is not reasonable to have very large α and σ values in practice, especially when considering the physical meaning of those parameters. Thus, $\alpha = 0.6$ and $\sigma = 0.5$ are chosen as an example.) Stochastic processes were simulated and the mean and variance at each time point, as well as the covariance values of the simulated processes, were calculated and compared with the theoretical ones. In these simulations, the sampling instance was 0.1 time unit, and the sampling frequency is fixed. The good agreement between the simulated output moments and the theoretical ones ensured that there was no obvious deviation of the

simulation except for that caused by the numerical rounding.

Table 5.1. The parameter estimates for approximate model with different methods.

Dynamic parameter a (True value is $a = 0.2$)			
	The proposed method	Bellach's method	Chen and Kozin's method
Mean of $\hat{a}$	0.212	0.00107	-0.00519
Standard error of $\hat{a}$	0.0569	0.000373	0.00173
Approximate 95% C. I.	(0.100, 0.323)	(3.39e-4, 1.80e-3)	(-8.57e-3, -1.81e-3)

Covariance parameter α (True value is $\alpha = 0.6$)				
	The proposed method	Sorensen's method	Pedersen's MLE method	Pedersen's Quasi-MLE method
Mean of $\hat{\alpha}$	0.628	-0.235	-0.235	-0.232
Standard error of $\hat{\alpha}$	0.166	0.0171	0.0171	0.0167
Approximate 95% C. I.	(0.303, 0.953)	(-0.268, -0.202)	(-0.268, -0.202)	(-0.265, -0.199)

Covariance parameter σ (True value is $\sigma = 0.5$)				
	The proposed method	Sorensen's method	Pedersen's MLE method	Pedersen's Quasi-MLE method
Mean of $\hat{\sigma}$	0.490	0.470	1.798	1.777
Standard error of $\hat{\sigma}$	0.0324	0.0316	0.110	0.108
Approximate 95% C. I.	(0.426, 0.554)	(0.408, 0.532)	(1.581, 2.014)	(1.566, 1.988)

Only one observed output process or sampled path is needed to estimate the dynamic parameter for all these methods. As to this point, it is the same for the Sorensen and Pedersen's estimation methods for α and σ. However, the estimation of the parameters α and σ proposed in this work has to be done with several sample paths since the covariance of the stochastic process has to be calculated based on several sample paths. Thus, ten sample paths, as a group, were sampled in order to get one set of the estimated covariance parameters. More than one group of such simulated paths were sampled to get the variances

of the estimated parameters and their confidence intervals (C.I.) since the variance and C.I. are good indicators of the reliability of the estimator. Since the estimator based on the estimating equations is approximately normally distributed, the 95% C.I. of θ can be approximated by $\hat{\theta} \pm 1.96 \times s.e.(\hat{\theta})$ (*s.e.* stands for standard error). The estimates were obtained for the simulated Wiener dynamic process. Each of the simulated paths had 1000 sampled observations. For other researcher's methods, one set of dynamic or covariance parameters can be obtained from just one sampled path; while for the proposed method, again, the dynamic parameter was estimated for each sampled path; the covariance parameters were estimated based on groups of 10 sampled paths. Totally 500 estimates were obtained for each parameter and each method.

Then, the proposed estimating equations were applied to the stochastic processes in three stages. All the parameters were estimated successfully by the proposed method and the estimates were listed in Table 5.1. With the same data processes, the methods proposed by other researchers were also applied for parameter estimation. It is clear that the proposed estimating equation method works well for all three parameters, and the estimates are all close to the true value. The methods proposed by other researchers did not work here.

The reason why Chen and Kozin's method did not work is that the process *v(t)* of the Wiener dynamic process is not stationary or ergodic, and some of the assumptions under which their estimator was derived and proved do not hold here.

Bellach's method also did not work. One of the possible reasons was that her method required the value of the time derivative of the stochastic process, which was very difficult to estimate due to the variation of the process caused by the stochastic input noise. Our tests showed that Bellach's method worked well for the approximate model once the true values of the derivatives of the process generated in the simulation were employed. The confidence interval of the estimated a was 0.1994± 1.96*0.0095, which was (0.181, 0.218), for just 500

simulated processes and it was very accurate.

The same thing happened to the Sorensen's and Pedersen's methods. They worked well with the approximate model once the derivatives of the output variable could be obtained exactly. However, it is very difficult to know the time derivatives of the stochastic process exactly and directly in reality.

The proposed estimating equation method never failed to converge for all these of simulations. Thus we can say it is robust and stable. The estimates are all close to the corresponding true values satisfactorily. None of them is significantly different from the true value by t-test based on 500 estimates for each parameter. Considering that the derivative of the output process is not available in practice and difficult to estimate, those methods in the literature are basically not applicable. The proposed method does not require the derivatives of the outputs processes and it worked well for the simulated data. Also it can be applied in the real world since it only requires the output variable itself.

Again, when establishing the estimating equations for α and σ, the choice of p and m values is critical. The values of m cannot be too large since the estimated covariance is not reliable when the distance between the two points gets large. Therefore, m value has to be chosen reasonably, say $m = 50$ in our example. The estimator for σ is robust to the change of estimating equations (choice of p and m) and the estimated α. This was always seen in the simulation and estimation.

5.5.2 Conclusions

This work considered the parameter estimation problem of the continuous-time single-input, single-output Wiener dynamic process with stochastic input noises. We limited our model with first order dynamics and specific correlation structures of the stochastic input noises. It is also assumed that the nonlinear static relationship has been identified and is

invertible. The original model can be shifted to an approximate model under some conditions. This approximation is acceptable based on some analysis and derivation. The estimating equation methodology was shown to work well for the approximate model, while other existing methods do not work at all. All the estimates based on the estimating equations are close to the corresponding true values. The proposed estimating equation method gives stable estimates according to our simulation. It never failed for thousands of simulations. Also, it is pretty robust, especially for estimating the dynamic parameter and the variance of the input noises. The dynamic parameter can be estimated satisfactorily with just one sampled path. Recall that the estimation is done in three stages. The variance, which is estimated last, can still be estimated satisfactorily even when the estimates of the previous two parameters are a little bit away from the true values. Though we did not work on the proof of the efficiency and the condition checks of the proposed methods, the proposed method has been shown to be a new and efficient application to the Wiener dynamic system with stochastic input noises.

The most critical advantage of the estimating equation approach is that it is not necessary to compute the time derivative of the observed process, which is hard to obtain accurately for the stochastic process with noises. Only the original process observations are needed over time. It is more practical to work with a method that makes use of just the observed values and avoids the derivative calculation of a process with stochastic noises, where the noise accentuation problem has to be faced. The failure of other researcher's methods was ascribed to the inaccurate computation of the time derivatives of the stochastic output process based on the tests done. Difficulty in computing the time derivatives of the output process accurately is truly an obstacle to use those methods.

Till now, it has been shown that the estimating equation method works for either the original or the approximate model, and it is powerful. The estimates are all close to the true

values with these two approaches.

References

Bellach, B.; Parameter estimation in linear stochastic differential equations and their asymptotic properties, *Math. Operationsforsch. Statist., Ser. Statistics*, **14**: 1, 141-191, 1983.

Chen, X.-K.; Kozin, F.; Almost sure consistent estimates of parameters in continuous systems, *Control – Theory and Advanced Technology*, **7**: 1, 1-18, 1991.

Higham, Desmond J., An algorithm to numerical simulation of stochastic differential equations, *SIAM Review*, **43**: 3, 525-546, 2001.

Pedersen, Asger Roer; A new approach to maximum likelihood estimation for stochastic differential equations based on discrete observations, *Scandinavian Journal of Statistics*, **22**, 55-71, 1995.

Prakasa Rao, B.L.S., *Statistical inference for diffusion type process*, Arnold, a member of the Hodder Headline Group, London, 1999.

Sobczyk, Kazimierz, *Stochastic differential equations: application in physics and engineering*, Kluwer Academic, Boston, 1991.

Sorensen, Michael; Estimating functions for discretely observed diffusions: a review, *Selected proceedings of the symposium on estimating functions*, Instidute of Mathematical Statistics, Volume 32, edited by Ishwar V. Basawa, V.P. Godambe, and Robert L. Taylor, 305-325, 1997.

Chapter 6. General Conclusions and Future Work

6.1 General conclusions

The process dynamics analysis of the Hammerstein and Wiener systems when excited by sinusoidal input changes is done for the first-order, second-order overdamped, and second-order overdamped plus lead dynamics. The continuous-time closed-form algorithms to sinusoidal input changes are proposed and presented on single-input, single-output (SISO) Hammerstein and Wiener systems. By simulation on theoretical Hammerstein and Wiener systems, the predicted responses by these algorithms agree exactly with the true process responses. Only the most recent input change information and the output, and its derivative (for the second order dynamics) at the changing point are needed for the prediction. This is the property we call "compact." The algorithms to SISO Hammerstein and Wiener systems can be conveniently extended to the multiple-input, multiple-output (MIMO) systems as shown by the two-input, two-output examples and demonstrated by the simulated seven-input, five-output continuous stirred tank reactor (CSTR). The predictions and the simulated theoretical system responses agree exactly and the predicted multiple CSTR outputs are close to the true process outputs.

Comparison with the piece-wise step input approximation of the sinusoidal input changes are done on a simulated MIMO CSTR and it is shown that the continuous-time algorithms proposed in this work give smaller sum of squared prediction error. In addition, noting that the noisy process input could be decomposed as the summation of sinusoidal signals imposed on a step input change; the proposed algorithms can be employed to predict the process outputs for the noisy process inputs once the decomposition is done. The simulation work on the simulated CSTR has shown that the predicted noisy process outputs are close to the true ones, and are much better than the predictions based on the perfect filtering of the input

signals.

The system cannot reach its steady state once sinusoidal input changes are introduced. This is quite different from what happens to the step input changes, where the steady state can always be obtained by giving enough time. Thus, there are no ultimate gain value and no steady state for the sinusoidal input change. Correspondingly, the closed-form algorithms to sinusoidal input changes are quite different from that for the step input changes.

First order, second order overdamped, second order overdamped plus lead, and their corresponding dynamics plus dead time can model most process dynamics adequately. Also, the Hammerstein and Wiener models are popular and efficient in modeling nonlinear processes. The proposed closed-form compact algorithms can be used to predict the process responses in many cases.

For the Wiener dynamic process, process disturbances and noises, which are usually correlated, generally could cause significant drifts from the deterministic values of the output variables, and more critically, those outputs over time are highly correlated. The linear or nonlinear regression methods, which are applicable only to the independent observations, are not valid here for the parameter estimation any more. The estimating equations based on the moment method are proposed in this work and they work well for the simulated Wiener dynamic process with stochastic input noises. No one has ever proposed the estimating equation method for such kind of problem before to my best knowledge. This approach has led to stable and robust estimators that have reasonable estimation errors. The estimation of the dynamic parameter does not require many observed output data and the estimate is close to the true value. For the covariance parameters, a couple of sampled processes are needed to use the proposed estimation method. The more observed process paths included, the more reliable the estimates can be obtained.

The original model for the Wiener dynamic process with stochastic input noises can be

shifted to an approximate model under some conditions. This approximation is acceptable based on the analysis and derivation. The estimating equation methodology was shown to work well for the approximate model, while other existing methods do not work at all.

The most important advantage of the estimating equation approach is that there is no need to measure the input disturbances or noises, or to calculate the time derivative of the observed output variable, which is hard to obtain accurately for the stochastic process with noise. Only the original process output observations over time are needed. It is more feasible to work with a method that makes use of just the observed values and avoids the derivative calculation of a process with stochastic noises, where the noise accentuation problem has to be faced.

6.2 Future work

Application to the soil dynamics and earthquake engineering or physical processes

The proposed algorithms were applied to a simulated CSTR only. It is highly possible that there may be more problems involved, such as lack of fit of the Hammerstein or Wiener model and the uncertainty of the parameter estimation when these algorithms are used for a real physical system. It is valuable to apply the proposed algorithms to some physical processes and see how it works.

If we can approximate the soil dynamics by the Hammerstein or Wiener model or some other block-oriented models introduced in the literature review, the stochastic estimation of the nonlinear response of structures, such as earth dam and concrete building, to strong earthquake spectrum can be obtained. The ground excitation spectrum can be approximated by the high frequency sinusoidal input changes and the process is nonlinear. The algorithms derived in Chapters 2 and 3 are applicable. Also, the details of the ground excitation are random and no confidence can be achieved from the results of a single deterministic dynamic

analysis. It is reasonable to include a stochastic model in modeling the ground motion. The efficient parameterization and continuous-time prediction of the proposed algorithms would be preferred for the soil-structure interaction analysis.

Parameter estimation with complicated Wiener dynamic models

This work considered the SISO Wiener dynamic process only and the dynamics is limited to be first order. The case would be complicated for processes with second order or higher order dynamics because of the complexity of the higher order stochastic differential equations.

The situation is much more complicated for the MIMO process with more than one input variables having the stochastic input noises imposed on them, especially when the interactions of the variables exist. As have been pointed out, the nonlinear static mapping is assumed to be invertible in this work, so that the intermediate output, or the output of the dynamic block, can be obtained from the SISO Wiener dynamic process final output after the nonlinear static mapping relation has been identified. However, in the MIMO case, it is highly possible that we can not obtain the intermediate output $v(t)$ when interactions exist. Or in other words, the "invertible" assumption of the nonlinear static mapping is usually not satisfied for MIMO Wiener dynamic process. More work has to be done for this case.

Work on the Hammerstein process is also necessary since the Hammerstein model can approximate some physical nonlinear processes better than the Wiener dynamic model.

The same investigation is necessary to be done on a physical process, such as the CSTR, in order to see the effects of noisy inputs on the parameter estimation and further predictions. However, this physical process has to be able to be approximated by a Wiener dynamic process with first order dynamics reasonably. Otherwise, the proposed estimating equations cannot be applied. The real data are not yet available to the researchers. So, what has been

done was to test the proposed method on the simulated theoretical Wiener dynamic process.

Another limitation of this work is that the input noise is assumed to have the specified correlation structure given in (4.5). Though this correlation structure is common and acceptable, it is a strong assumption. However, the estimating equation approach is a general method that could be employed for other type of input noise correlation structure once the analytical solutions to the corresponding differential equations are available. Different estimating equations have to be established.

To be incorporated into the W-BEST technique, where the sequence step input changes are designed, more work has to be done because only one step input change is considered in this work. We understand that there is a gap between this theoretical work and the practice.

Appendix. Mathematical Derivation of the Closed-form Compact Algorithms to Hammerstein and Wiener Systems

The closed-form compact solutions to the Hammerstein and Wiener processes with various dynamics, including first order, second order overdamped, and second order overdamped plus lead, when they are excited by the sinusoidal input changes, have been presented in Chapters 2 and 3. The applications to theoretical Hammerstein and Wiener systems and simulated CSTR have demonstrated that the solutions are exact for the theoretical systems and predict the process responses well. This appendix will provide the mathematical derivations of the closed-form compact solutions in details. The derivations are based on the Laplace transforms and inverse Laplace transforms. The derivations are given for the Hammerstein and Wiener systems with first order, and second order overdamped dynamics, separately considering the following two types of input changes.

$$\textbf{Case I.}\quad u(t)=\begin{cases}0 & t\le 0\\ b_1+A_1\sin(\omega_1 t) & 0<t\le t_1\\ b_2+A_2\sin(\omega_2(t-t_1)) & t_1<t\le t_2\\ \quad\vdots & \quad\vdots\\ b_n+A_n\sin(\omega_n(t-t_{n-1})) & t_{n-1}<t\le t_n\end{cases} \tag{A.1}$$

$$\textbf{Case II.}\quad u(t)=\begin{cases}0 & t\le 0\\ A_1\sin(\omega_1 t+\phi_1) & 0<t\le t_1\\ A_2\sin(\omega_2(t-t_1)+\phi_2) & t_1<t\le t_2\\ \quad\vdots & \quad\vdots\\ A_n\sin(\omega_n(t-t_{n-1})+\phi_n) & t_{n-1}<t\le t_n\end{cases} \tag{A.2}$$

where, A_i is the amplitude, ω_i is the frequency, b_i is the step input change imposed on the sinusoidal change, ϕ_i is the phase angle. For the different dynamics introduced in the following sections, *u(t)* and *y(t)* are process input and output respectively and they are both deviation variables. It is assumed that the initial conditions for all cases at time zero is zero,

unless otherwise stated. But the initial conditions at other changing points except time zero are not necessarily zero depending on the specific time that the change is made. *v(t)* denotes the intermediate variable for either Hammerstein or Wiener system, which is unknown in physical process.

I. The Hammerstein system with first order dynamics

Mathematically, this system can be written as:

$$\tau \frac{dy(t)}{dt} + y(t) = v(t) \tag{A.3}$$

where $v(t) = f(u(t))$ gives the nonlinear static mapping relationship. τ is the time constant.

a. Case I

The sinusoidal input $u(t) = b_i + A_i \sin(\omega_i (t - t_{i-1}))$ starts at the changing point t_{i-1}. The initial condition for the output *y(t)* at the changing point t_{i-1} can be written as

$$y(t)\big|_{t_{i-1}} = y(t_{i-1}) \cdot \boldsymbol{S}(t - t_{i-1}) \tag{A.4}$$

where $\boldsymbol{S}(t - t_{i-1}) = \begin{cases} 0 & t < t_{i-1} \\ 1 & t \geq t_{i-1} \end{cases}$, is a unit step function.

and $v(t) = \left\{a_1 \cdot [b_i + A_i \sin(\omega_i (t - t_{i-1}))] + a_2 \cdot [b_i + A_i \sin(\omega_i (t - t_{i-1}))]^2 \right\} \cdot \boldsymbol{S}(t - t_{i-1})$

$$= \left\{\left(a_1 b_i + a_2 b_i^2 + a_2 A_i^2 / 2\right) + (a_1 A_i + 2 a_2 b_i A_i) \sin(\omega_i (t - t_{i-1})) - a_2 A_i^2 / 2 \cdot \cos(2\omega_i (t - t_{i-1}))\right\} \cdot \boldsymbol{S}(t - t_{i-1}) \tag{A.5}$$

for $f(u(t)) = a_1 u(t) + a_2 u^2(t)$. Simple linear relationship $f(u(t)) = a_1 u(t)$ is a special situation of this one with $a_2 = 0$.

The solution for the interval $t_{i-1} < t < \infty$ is given by Eqs. A.6 to A.9,

$$y(t)=\left(a_1b_i+a_2b_i^{\,2}+\frac{1}{2}a_2A_i^{\,2}\right)\cdot g_0(t-t_{i-1};\tau)+(a_1A_i+2a_2b_iA_i)\cdot g_s(t-t_{i-1};\omega_i,\tau)$$
$$-\frac{1}{2}a_2A_i^{\,2}\cdot g_c(t-t_{i-1};2\omega_i,\tau)+y(t_{i-1})\cdot e^{-(t-t_{i-1})/\tau} \tag{A.6}$$

where

$$g_0(t;\tau)=1-e^{-t/\tau} \tag{A.7}$$

$$g_s(t;\omega,\tau)=\frac{1}{1+(\omega t)^2}\left[\omega\tau\cdot e^{-t/\tau}-\omega\tau\cdot\cos(\omega t)+\sin(\omega t)\right] \tag{A.8}$$

$$g_c(t;\omega,\tau)=\frac{1}{1+(\omega t)^2}\left[-e^{-t/\tau}+\omega\tau\cdot\sin(\omega t)+\cos(\omega t)\right] \tag{A.9}$$

Since the Laplace transform is defined on the interval $(0,\infty)$, firstly, the following shift is introduced. Define $m=t-t_{i-1}$, which means $t=m+t_{i-1}$ and $m\in(0,\infty)$ for $t\in(t_{i-1},\infty)$, then the dynamic equation becomes

$$\tau\frac{dy(m+t_{i-1})}{dm}+y(m+t_{i-1})=v(m+t_{i-1}) \tag{A.10}$$

Let $x(m)=y(m+t_{i-1})$. Then

$$\tau\frac{dx(m)}{dm}+x(m)=v(m+t_{i-1})=\left\{a_1\cdot[b_i+A_i\sin(\omega_i m)]+a_2\cdot[b_i+A_i\sin(\omega_i m)]^2\right\}\cdot\boldsymbol{S}(0) \tag{A.11}$$

with $x(0)=y(t_{i-1})\cdot\boldsymbol{S}(0)$ as initial condition.

Taking the Laplace transform of Eq. A.11 gives

$$\tau[s\cdot X(s)-x(0)]+X(s)=V(s) \tag{A.12}$$

where

$$X(s)=\mathscr{L}\{x(m)\}=\int_0^\infty x(m)\cdot e^{-sm}dm, \tag{A.13}$$

$$V(s)=\left(a_1b_i+a_2b_i^{\,2}+a_2A_i^{\,2}/2\right)\cdot\frac{1}{s}+(a_1A_i+2a_2b_iA_i)\cdot\frac{\omega_i}{s^2+\omega_i^{\,2}}-\frac{a_2A_i^{\,2}}{2}\cdot\frac{s}{s^2+4\omega_i^{\,2}} \tag{A.14}$$

Rearranging terms in Eq.A.12 gives

$$X(s)=\frac{V(s)}{\tau s+1}+\frac{\tau\cdot x(0)}{\tau s+1} \tag{A.15}$$

Taking the inverse Laplace transform of Eq. A.15 after plugging Eq.A.14 into Eq. A.15 gives

$$\begin{aligned} x(m)=&\mathscr{L}^{-1}\left[\left(a_1b_i+a_2b_i^{\,2}+a_2A_i^{\,2}/2\right)\cdot\frac{1}{s(\tau s+1)}\right]\\ &+\mathscr{L}^{-1}\left[\left(a_1A_i+2a_2b_iA_i\right)\cdot\frac{\omega_i}{s^2+\omega_i^{\,2}}\cdot\frac{1}{\tau s+1}\right]\\ &+\mathscr{L}^{-1}\left[-\frac{a_2A_i^{\,2}}{2}\cdot\frac{s}{s^2+4\omega_i^{\,2}}\cdot\frac{1}{\tau s+1}\right]+\mathscr{L}^{-1}\left[x(0)\cdot\frac{\tau}{\tau s+1}\right] \end{aligned} \tag{A.16}$$

With the definitions of $g_0(t;\tau)$, $g_s(t;\omega,\tau)$, and $g_c(t;\omega,\tau)$, we have

$$\begin{aligned} x(m)=&\left(a_1b_i+a_2b_i^{\,2}+a_2A_i^{\,2}/2\right)\cdot g_0(m;\tau)+\left(a_1A_i+2a_2b_iA_i\right)\cdot g_s(m;\omega_i,\tau)\\ &-\frac{a_2A_i^{\,2}}{2}\cdot g_c(m;2\omega_i,\tau)+x(0)\cdot e^{-m/\tau} \end{aligned} \tag{A.17}$$

As defined before, $x(m)=y(m+t_{i-1})$, so, we can rewrite Eq. A.17 as,

$$\begin{aligned} y(m+t_{i-1})=&\left(a_1b_i+a_2b_i^{\,2}+a_2A_i^{\,2}/2\right)\cdot g_0(m;\tau)+\left(a_1A_i+2a_2b_iA_i\right)\cdot g_s(m;\omega_i,\tau)\\ &-\frac{a_2A_i^{\,2}}{2}\cdot g_c(m;2\omega_i,\tau)+x(0)\cdot e^{-m/\tau} \end{aligned} \tag{A.18}$$

Plugging the relation that $m+t_{i-1}=t$ and $m=t-t_{i-1}$ into Eq. A.18, we finally obtain

$$\begin{aligned} y(t)=&\left(a_1b_i+a_2b_i^{\,2}+a_2A_i^{\,2}/2\right)\cdot g_0(t-t_{i-1};\tau)+\left(a_1A_i+2a_2b_iA_i\right)\cdot g_s(t-t_{i-1};\omega_i,\tau)\\ &-\frac{1}{2}a_2A_i^{\,2}\cdot g_c(t-t_{i-1};2\omega_i,\tau)+y(t_{i-1})\cdot e^{-(t-t_{i-1})/\tau} \end{aligned} \tag{A.19}$$

Eq. A.19 gives the solution to the Hammerstein system with first order dynamics and quadratic nonlinear static mapping for input sequence Case I.

b. Case II

The sinusoidal input starting at changing point t_{i-1} is given by $u(t)=A_i\sin(\omega_i(t-t_{i-1})+\phi_i)$.

The initial condition for the output at the changing time point t_{i-1} is the same as Eq. A.4 and

$$v(t)\big|_{t_{i-1}\le t<t_i} = \left(a_1 \cdot A_i \sin(\omega_i(t-t_{i-1})+\phi_i)+a_2 \cdot (A_i \sin(\omega_i(t-t_{i-1})+\phi_i))^2\right)\cdot \boldsymbol{S}(t-t_{i-1})$$

$$= \left[a_2 A_i^{\,2}/2 + a_1 A_i \cos(\phi_i)\sin(\omega_i(t-t_{i-1})) + a_1 A_i \sin(\phi_i)\cos(\omega_i(t-t_{i-1}))\right.$$
$$\left. - a_2 A_i^{\,2}/2 \cdot (\cos(2\phi_i)\cos(2\omega_i(t-t_{i-1})) - \sin(2\phi_i)\sin(2\omega_i(t-t_{i-1})))\right]\cdot \boldsymbol{S}(t-t_{i-1}) \quad \text{(A.20)}$$

for quadratic nonlinear mapping $f(u(t)) = a_1 u(t) + a_2 u^2(t)$.

The solution for the time points between the interval $t_{i-1} < t < \infty$ is given by Eq. A.21

$$y(t) = a_2/2 \cdot g_0(t-t_{i-1};\tau) + a_1[\cos\phi_i \cdot g_s(t-t_{i-1};\omega_i,\tau) + \sin\phi_i \cdot g_c(t-t_{i-1};\omega_n,\tau)]$$
$$- a_2/2 \cdot [\cos(2\phi_i)\cdot g_c(t-t_{i-1};2\omega_i,\tau) - \sin(2\phi_i)\cdot g_s(t-t_{i-1};2\omega_i,\tau)] + y(t_{i-1})\cdot e^{-(t-t_{i-1})/\tau} \quad \text{(A.21)}$$

Similarly, define $m = t - t_{i-1}$, which means $t = m + t_{i-1}$ and $m \in (0,\infty)$ for $t \in (t_{i-1},\infty)$. Then the dynamic equation Eq. A.3 turns out to be

$$\tau \frac{dy(m+t_{i-1})}{dm} + y(m+t_{i-1}) = v(m+t_{i-1}) \quad \text{(A.22)}$$

Let $x(m) = y(m+t_{i-1})$. Then

$$\tau \frac{dx(m)}{dm} + x(m) = v(m+t_{i-1}) = \left(a_1 \cdot A_i \sin(\omega_i m+\phi_i)+a_2 \cdot (A_i \sin(\omega_i m+\phi_i))^2\right)\cdot \boldsymbol{S}(0) \quad \text{(A.23)}$$

with $x(0) = y(t_{i-1})\cdot \boldsymbol{S}(0)$ as initial condition.

Taking the Laplace transform of Eq. A.23 gives

$$\tau[s\cdot X(s) - x(0)] + X(s) = V(s) \quad \text{(A.24)}$$

where $X(s)$ was defined previously in Eq. A.13 and

$$V(s) = \frac{a_2 A_i^{\,2}}{2}\cdot\frac{1}{s} + a_1 A_i \cos(\phi_i)\frac{\omega_i}{s^2+\omega_i^{\,2}} + a_1 A_i \sin(\phi_i)\frac{s}{s^2+\omega_i^{\,2}}$$
$$- \frac{a_2 A_i^{\,2}}{2}\cdot\left(\cos(2\phi_i)\frac{s}{s^2+4\omega_i^{\,2}} - \sin(2\phi_i)\frac{2\omega_i}{s^2+4\omega_i^{\,2}}\right) \quad \text{(A.25)}$$

Rearranging terms in Eq. A.24 as before, taking the inverse Laplace transform after plugging Eq. A.25 into it gives

$$x(m)=\mathcal{L}^{-1}\left[\frac{a_2A_i^{\,2}}{2}\cdot\frac{1}{s(\tau s+1)}\right]+\mathcal{L}^{-1}\left[a_1A_i\cos(\phi_i)\cdot\frac{\omega_i}{s^2+\omega_i^{\,2}}\cdot\frac{1}{\tau s+1}\right]$$
$$+\mathcal{L}^{-1}\left[a_1A_i\sin(\phi_i)\cdot\frac{s}{s^2+\omega_i^{\,2}}\cdot\frac{1}{\tau s+1}\right]-\mathcal{L}^{-1}\left[\frac{a_2A_i^{\,2}}{2}\cos(2\phi_i)\cdot\frac{s}{s^2+4\omega_i^{\,2}}\cdot\frac{1}{\tau s+1}\right] \quad \text{(A.26)}$$
$$+\mathcal{L}^{-1}\left[\frac{a_2A_i^{\,2}}{2}\sin(2\phi_i)\frac{2\omega_i}{s^2+4\omega_i^{\,2}}\cdot\frac{1}{\tau s+1}\right]+\mathcal{L}^{-1}\left[x(0)\cdot\frac{\tau}{\tau s+1}\right]$$

With the definitions of $g_0(t;\tau)$, $g_s(t;\omega,\tau)$, and $g_c(t;\omega,\tau)$, we have

$$x(m)=\frac{a_2A_i^{\,2}}{2}\cdot g_0(m;\tau)+a_1A_i\cdot[\cos\phi_i\cdot g_s(m;\omega_i,\tau)+\sin\phi_i\cdot g_c(m;\omega_n,\tau)]$$
$$-\frac{a_2A_i^{\,2}}{2}\cdot[\cos(2\phi_i)\cdot g_c(m;2\omega_i,\tau)-\sin(2\phi_i)\cdot g_s(m;2\omega_i,\tau)]+x(0)\cdot e^{-m/\tau} \quad \text{(A.27)}$$

Since $x(m)=y(m+t_{i-1})$, and $m=t-t_{i-1}$, we finally get

$$y(t)=\frac{a_2A_i^{\,2}}{2}\cdot g_0(t-t_{i-1};\tau)+a_1A_i\cdot[\cos\phi_i\cdot g_s(t-t_{i-1};\omega_i,\tau)+\sin\phi_i\cdot g_c(t-t_{i-1};\omega_n,\tau)]$$

$$-\frac{a_2A_i^{\,2}}{2}\cdot[\cos(2\phi_i)\cdot g_c(t-t_{i-1};2\omega_i,\tau)-\sin(2\phi_i)\cdot g_s(t-t_{i-1};2\omega_i,\tau)]+y(t_{i-1})\cdot e^{-(t-t_{i-1})/\tau} \quad \text{(A.28)}$$

This gives the solution to the Hammerstein system with first order dynamics and quadratic nonlinear mapping for input sequence Case II.

II. The Wiener system with first order dynamics

This Wiener system can be written as

$$\tau\frac{dv(t)}{dt}+v(t)=u(t) \quad \text{(A.29)}$$

with $v(t)\big|_{t_{i-1}}=v(t_{i-1})\cdot S(t-t_{i-1})$ (A.30)

and $y(t) = f(v(t))$ (A.31)

where $f(v(t))$ can be any nonlinear static mapping relationship. τ is the time constant.

a. Case I

The sinusoidal input starting at any given changing point t_{i-1} can be written as $u(t) = [b_i + A_i \sin(\omega_i (t - t_{i-1}))] \cdot \boldsymbol{S}(t - t_{i-1})$. The initial condition for the intermediate output *v(t)* at the time of input change t_{i-1} is given in Eq. A.30.

The solution to *v(t)* for the interval $t_{i-1} < t < \infty$ is given by the following:

$$v(t) = b_i \cdot g_0(t - t_{i-1}; \tau) + A_i \cdot g_s(t - t_{i-1}; \omega_i, \tau) + v(t_{i-1}) \cdot e^{-(t-t_{i-1})/\tau} \quad \text{(A.32)}$$

where $g_0(t;\tau)$, and $g_s(t;\omega,\tau)$ are defined in Eqs. A.7 and A.8.

We use the same time shift to Eq. A.29 as that for the Hammerstein system with first order dynamics in order to use the Laplace transform more conveniently. Let $m = t - t_{i-1}$, which means that $t = m + t_{i-1}$ and $m \in (0, \infty)$ for $t \in (t_{i-1}, \infty)$. Then the dynamic equation becomes

$$\tau \frac{dv(m + t_{i-1})}{dm} + v(m + t_{i-1}) = u(m + t_{i-1}) \quad \text{(A.33)}$$

Let $x(m) = v(m + t_{i-1})$. Then

$$\tau \frac{dx(m)}{dm} + x(m) = u(m + t_{i-1}) = [b_i + A_i \sin(\omega_i m)] \cdot S(0) \quad \text{(A.34)}$$

with $x(0) = v(t_{i-1}) \cdot S(0)$ as initial condition.

Taking the Laplace transform of Eq. A.34 gives

$$\tau[s \cdot X(s) - x(0)] + X(s) = U(s) \quad \text{(A.35)}$$

where

$$X(s) = \mathcal{L}\{x(m)\} = \int_0^\infty x(m) \cdot e^{-sm} dm \tag{A.36}$$

$$U(s) = b_i \cdot \frac{1}{s} + A_i \cdot \frac{\omega_i}{s^2 + \omega_i^2} \tag{A.37}$$

Rearranging terms in Eq.A.35 gives

$$X(s) = \frac{U(s)}{\tau s + 1} + \frac{\tau \cdot x(0)}{\tau s + 1} \tag{A.38}$$

Taking the inverse Laplace transform of Eq. A.38 after plugging Eq. A.37 into Eq. A.38 gives

$$x(m) = \mathcal{L}^{-1}\left[b_i \cdot \frac{1}{s} \cdot \frac{1}{\tau s + 1} \right] + \mathcal{L}^{-1}\left[A_i \cdot \frac{\omega_i}{s^2 + \omega_i^2} \cdot \frac{1}{\tau s + 1} \right] + x(0) \cdot e^{-m/\tau} \tag{A.39}$$

With the definitions of $g_0(t;\tau)$ and $g_s(t;\omega,\tau)$, we have

$$x(m) = b_i \cdot g_0(m;\tau) + A_i \cdot g_s(m;\omega_i,\tau) + x(0) \cdot e^{-m/\tau} \tag{A.40}$$

As defined, $x(m) = v(m + t_{i-1})$, and $x(0) = v(t_{i-1}) \cdot S(0)$. Thus,

$$v(m + t_{i-1}) = b_i \cdot g_0(m;\tau) + A_i \cdot g_s(m;\omega_i,\tau) + v(t_{i-1}) \cdot e^{-m/\tau} \tag{A.41}$$

Since $m = t - t_{i-1}$, the solution in the time domain can thus be written as

$$v(t) = b_i \cdot g_0(t - t_{i-1};\tau) + A_i \cdot g_s(t - t_{i-1};\omega_i,\tau) + v(t_{i-1}) \cdot e^{-(t-t_{i-1})/\tau} \tag{A.42}$$

This gives the solution to *v(t)* of this Wiener system with first order dynamics and quadratic nonlinear static mapping for input sequence Case I. Then, the response *y(t)* can be obtained by following different nonlinear static mapping relationships.

b. Case II

The sinusoidal input starting at changing point t_{i-1} can be written as

$$\begin{aligned} u(t) &= A_i \sin(\omega_i(t - t_{i-1}) + \phi_i) \cdot S(t - t_{i-1}) \\ &= [A_i \cos(\phi_i)\sin(\omega_i(t - t_{i-1})) + A_i \sin(\phi_i)\cos(\omega_i(t - t_{i-1}))] \cdot S(t - t_{i-1}) \end{aligned} \tag{A.43}$$

The initial condition for the intermediate output at the time of input change t_{i-1} can be written as Eq. A.30. The solution to *v(t)* for the interval $t_{i-1} < t < \infty$ is given by Eq. A.44,

$$v(t) = A_i \sin\phi_i \cdot g_c(t - t_{i-1}; \omega_i, \tau) + A_i \cos\phi_i \cdot g_s(t - t_{i-1}; \omega_i, \tau) + v(t_{i-1}) \cdot e^{-(t-t_{i-1})/\tau} \quad \text{(A.44)}$$

where $g_s(t; \omega, \tau)$ and $g_c(t; \omega, \tau)$ were defined by Eqs. A.8 and A.9.

The same time shift is applied to the dynamic equation as that for the Wiener system with first order dynamics Case I. Let $m = t - t_{i-1}$. Then the dynamic equation becomes

$$\tau \frac{dv(m + t_{i-1})}{dm} + v(m + t_{i-1}) = u(m + t_{i-1}) \quad \text{(A.45)}$$

Let $x(m) = v(m + t_{i-1})$. Then

$$\tau \frac{dx(m)}{dm} + x(m) = u(m + t_{i-1}) = [b_i + A_i \sin(\omega_i m)] \cdot \boldsymbol{S}(0) \quad \text{(A.46)}$$

with $x(0) = v(t_{i-1}) \cdot \boldsymbol{S}(0)$ as initial condition.

Taking the Laplace transform of Eq. A.46 gives

$$\tau[s \cdot X(s) - x(0)] + X(s) = U(s) \quad \text{(A.47)}$$

where $X(s)$ was defined as before and

$$U(s) = A_i \cos(\phi_i) \frac{\omega_i}{s^2 + \omega_i^2} + A_i \sin(\phi_i) \frac{s}{s^2 + \omega_i^2}. \quad \text{(A.48)}$$

Plugging Eq.A.48 into Eq. A.47, rearranging terms in Eq. A.47, and taking the inverse Laplace transform gives

$$v(t) = \mathcal{L}^{-1}\left[A_i \cos(\phi_i) \cdot \frac{\omega_i}{s^2 + \omega_i^2} \cdot \frac{1}{\tau s + 1}\right] + \mathcal{L}^{-1}\left[A_i \sin(\phi_i) \cdot \frac{s}{s^2 + \omega_i^2} \cdot \frac{1}{\tau s + 1}\right] + x(0) \cdot e^{-m/\tau} \quad \text{(A.49)}$$

With the definitions of $g_s(t; \omega, \tau)$, and $g_c(t; \omega, \tau)$ in Eqs. A.8 and A.9, we have

$$x(m) = A_i \cdot [\cos\phi_i \cdot g_s(m; \omega_i, \tau) + \sin\phi_i \cdot g_c(m; \omega_n, \tau)] + x(0) \cdot e^{-m/\tau} \quad \text{(A.50)}$$

As defined, $x(m) = v(m + t_{i-1})$, and realizing that $x(0) = v(t_{i-1}) \cdot S(0)$, we have

$$v(m + t_{i-1}) = A_i \cdot [\cos\phi_i \cdot g_s(m; \omega_i, \tau) + \sin\phi_i \cdot g_c(m; \omega_n, \tau)] + v(t_{i-1}) \cdot e^{-m/\tau} \quad \text{(A.51)}$$

Since $m = t - t_{i-1}$, the solution in the time domain can thus be rewritten as,

$$v(t) = A_i \cdot [\cos\phi_i \cdot g_s(t - t_{i-1}; \omega_i, \tau) + \sin\phi_i \cdot g_c(t - t_{i-1}; \omega_n, \tau)] + v(t_{i-1}) \cdot e^{-(t-t_{i-1})} \quad \text{(A.52)}$$

This gives the solution to *v(t)* of this Wiener system when the phase, amplitude and frequency of the input sequence all change at each changing point. Then, the response *y(t)* can be obtained by following different nonlinear static mapping relationships.

III. The Hammerstein system with second-order overdamped dynamics

This Hammerstein system can be written as

$$\tau_1\tau_2 \frac{d^2y(t)}{dt^2} + (\tau_1 + \tau_2) \cdot \frac{dy(t)}{dt} + y(t) = v(t) \quad \text{(A.53)}$$

where $v(t) = f(u(t))$ can be any nonlinear static mapping relationship. τ_1 and τ_2 are the time constants.

a. Case I

The sinusoidal input starting at any changing point t_{i-1} can be written as $u(t) = [b_i + A_i \sin(\omega_i(t - t_{i-1}))] \cdot S(t - t_{i-1})$. The initial conditions for the output at the time of input change t_{i-1} is $y(t)|_{t_{i-1}} = y(t_{i-1}) \cdot S(t - t_{i-1})$ and $y'(t)|_{t_{i-1}} = y'(t_{i-1}) \cdot S(t - t_{i-1})$. For the case $f(u(t)) = a_1u(t) + a_2u^2(t)$, we have

$$\begin{aligned} v(t) &= \left(a_1 \cdot (b_i + A_i \sin(\omega_i(t - t_{i-1}))) + a_2 \cdot (b_i + A_i \sin(\omega_i(t - t_{i-1})))^2\right) \cdot S(t - t_{i-1}) \\ &= \left\{\left(a_1b_i + a_2b_i^2 + a_2A_i^2/2\right) + (a_1A_i + 2a_2b_iA_i)\sin(\omega_i(t - t_{i-1})) \right. \\ &\quad \left. - a_2A_i^2/2 \cdot \cos(2\omega_i(t - t_{i-1}))\right\} \cdot S(t - t_{i-1}) \end{aligned} \quad \text{(A.53)}$$

The solution in the interval $t_{i-1} < t < \infty$ is given by Eqs. A.54 to A.59.

$$y(t)=\left(a_1 b_i + a_2 b_i^{\,2} + \frac{1}{2}a_2 A_i^{\,2}\right)\cdot g_{20}(t-t_{i-1};\tau_1,\tau_2)$$
$$+(a_1 A_i + 2a_2 b_i A_i)\cdot g_{2s}(t-t_{i-1};\omega_i,\tau_1,\tau_2) - \frac{1}{2}a_2 A_i^{\,2}\cdot g_{2c}(t-t_{i-1};2\omega_i,\tau_1,\tau_2) \quad \text{(A.54)}$$
$$+ y(t_{i-1})\cdot g_{02}(t-t_{i-1};\tau_1,\tau_2) + y'(t_{i-1})\cdot g_{12}(t-t_{i-1};\tau_1,\tau_2)$$

where

$$g_{20}(t;\tau_1,\tau_2)=1+\frac{\tau_1}{\tau_2-\tau_1}e^{-t/\tau_1}-\frac{\tau_2}{\tau_2-\tau_1}e^{-t/\tau_2} \quad \text{(A.55)}$$

$$g_{2s}(t;\omega,\tau_1,\tau_2)$$
$$=\frac{\omega\tau_1^2\cdot e^{-t/\tau_1}}{(\tau_1-\tau_2)(1+\omega^2\tau_1^2)}+\frac{\omega\tau_2^2\cdot e^{-t/\tau_2}}{(\tau_2-\tau_1)(1+\omega^2\tau_2^2)}+\frac{(1-\omega^2\tau_1\tau_2)\sin(\omega t)-\omega(\tau_1+\tau_2)\cdot\cos(\omega t)}{(1+\omega^2\tau_1^2)(1+\omega^2\tau_2^2)} \quad \text{(A.56)}$$

$$g_{2c}(t;\omega,\tau_1,\tau_2)$$
$$=\frac{-\tau_1\cdot e^{-t/\tau_1}}{(\tau_1-\tau_2)(1+\omega^2\tau_1^2)}+\frac{-\tau_2\cdot e^{-t/\tau_2}}{(\tau_2-\tau_1)(1+\omega^2\tau_2^2)}+\frac{(1-\omega^2\tau_1\tau_2)\cos(\omega t)-\omega(\tau_1+\tau_2)\cdot\sin(\omega t)}{(1+\omega^2\tau_1^2)(1+\omega^2\tau_2^2)} \quad \text{(A.57)}$$

$$g_{02}(t;\tau_1,\tau_2)=\frac{\tau_1 e^{-t/\tau_1}-\tau_2 e^{-t/\tau_2}}{\tau_1-\tau_2} \quad \text{(A.58)}$$

$$g_{12}(t;\tau_1,\tau_2)=\frac{\tau_1\tau_2\cdot e^{-t/\tau_1}-\tau_1\tau_2 e^{-t/\tau_2}}{\tau_1-\tau_2} \quad \text{(A.59)}$$

Define $m=t-t_{i-1}$. Then, $m\in(0,\infty)$ for $t\in(t_{i-1},\infty)$, and the dynamic equation A.53 becomes

$$\tau_1\tau_2\frac{d^2y(m+t_{i-1})}{dm^2}+(\tau_1+\tau_2)\cdot\frac{dy(m+t_{i-1})}{dm}+y(m+t_{i-1})=v(m+t_{i-1}) \quad \text{(A.60)}$$

Let $x(m)=y(m+t_{i-1})$. Then

$$\tau_1\tau_2\frac{d^2x(m)}{dm^2}+(\tau_1+\tau_2)\cdot\frac{dx(m)}{dm}+x(m)=v(m+t_{i-1})$$
$$=\left\{a_1\cdot[b_i+A_i\sin(\omega_i m)]+a_2\cdot[b_i+A_i\sin(\omega_i m)]^2\right\}\cdot\boldsymbol{S}(0) \quad \text{(A.61)}$$

with $x(0)=y(t_{i-1})\cdot\boldsymbol{S}(0)$ and $x'(0)=y'(t_{i-1})\cdot\boldsymbol{S}(0)$ as initial conditions.

Taking the Laplace transform of Eq. A.61 gives

$$\tau_1\tau_2\cdot\left[s^2\cdot X(s)-s\cdot x(0)-x'(0)\right]+(\tau_1+\tau_2)\cdot\left[s\cdot X(s)-x(0)\right]+X(s)=V(s) \tag{A.62}$$

where *X(s)* was defined as before, and

$$V(s)=\left(a_1b_i+a_2b_i^{\,2}+a_2A_i^{\,2}/2\right)\cdot\frac{1}{s}+\left(a_1A_i+2a_2b_iA_i\right)\cdot\frac{\omega_i}{s^2+\omega_i^{\,2}}-\frac{a_2A_i^{\,2}}{2}\cdot\frac{s}{s^2+4\omega_i^{\,2}} \tag{A.63}$$

Rearranging terms in Eq. A.62 gives

$$X(s)=\frac{V(s)}{(\tau_1s+1)(\tau_2s+1)}+\frac{(\tau_1+\tau_2+\tau_1\tau_2\cdot s)\cdot x(0)}{(\tau_1s+1)(\tau_2s+1)}+\frac{\tau_1\tau_2\cdot x'(0)}{(\tau_1s+1)(\tau_2s+1)} \tag{A.64}$$

Taking the inverse Laplace transform of Eq. A.64 after plugging Eq. A.63 into it gives

$$\begin{aligned}x(m)=&\mathcal{L}^{-1}\left[\left(a_1b_i+a_2b_i^{\,2}+a_2A_i^{\,2}/2\right)\cdot\frac{1}{s}\cdot\frac{1}{(\tau_1s+1)(\tau_2s+1)}\right]\\&+\mathcal{L}^{-1}\left[\left(a_1A_i+2a_2b_iA_i\right)\cdot\frac{\omega_i}{s^2+\omega_i^{\,2}}\cdot\frac{1}{(\tau_1s+1)(\tau_2s+1)}\right]\\&+\mathcal{L}^{-1}\left[-\frac{a_2A_i^{\,2}}{2}\cdot\frac{s}{s^2+4\omega_i^{\,2}}\cdot\frac{1}{(\tau_1s+1)(\tau_2s+1)}\right]\\&+x(0)\cdot\mathcal{L}^{-1}\left[\frac{(\tau_1+\tau_2+\tau_1\tau_2\cdot s)}{(\tau_1s+1)(\tau_2s+1)}\right]+x'(0)\cdot\mathcal{L}^{-1}\left[\frac{\tau_1\tau_2}{(\tau_1s+1)(\tau_2s+1)}\right]\end{aligned} \tag{A.65}$$

With the definitions of $g_{20}(t;\tau_1,\tau_2)$, $g_{2s}(t;\omega,\tau_1,\tau_2)$, $g_{2c}(t;\omega,\tau_1,\tau_2)$, $g_{02}(t;\tau_1,\tau_2)$, and $g_{12}(t;\tau_1,\tau_2)$, we have,

$$\begin{aligned}x(m)=&\left(a_1b_i+a_2b_i^{\,2}+\frac{1}{2}a_2A_i^{\,2}\right)\cdot g_{20}(m;\tau_1,\tau_2)+\left(a_1A_i+2a_2b_iA_i\right)\cdot g_{2s}(m;\omega_i,\tau_1,\tau_2)\\&-\frac{1}{2}a_2A_i^{\,2}\cdot g_{2c}(m;2\omega_i,\tau_1,\tau_2)+x(0)\cdot g_{02}(m;\tau_1,\tau_2)+x'(0)\cdot g_{12}(m;\tau_1,\tau_2)\end{aligned} \tag{A.66}$$

Thus,

$$\begin{aligned}y(t)=y(m+t_{i-1})=&\left(a_1b_i+a_2b_i^{\,2}+\frac{1}{2}a_2A_i^{\,2}\right)\cdot g_{20}(t-t_{i-1};\tau_1,\tau_2)\\&+\left(a_1A_i+2a_2b_iA_i\right)\cdot g_{2s}(t-t_{i-1};\omega_i,\tau_1,\tau_2)-\frac{1}{2}a_2A_i^{\,2}\cdot g_{2c}(t-t_{i-1};2\omega_i,\tau_1,\tau_2)\\&+y(t_{i-1})\cdot g_{02}(t-t_{i-1};\tau_1,\tau_2)+y'(t_{i-1})\cdot g_{12}(t-t_{i-1};\tau_1,\tau_2)\end{aligned} \tag{A.67}$$

This gives the solution to the Hammerstein system with second order overdamped dynamics

and quadratic nonlinear static gain for input sequence Case I.

b. Case II

The sinusoidal input starting at any changing point t_{i-1} is given by

$u(t) = A_i \sin(\omega_i(t-t_{i-1})+\phi_i)\cdot \boldsymbol{S}(t-t_{i-1})$, and the initial conditions for the output at the time of input change t_{i-1} are $y(t)\big|_{t_{i-1}} = y(t_{i-1})\cdot \boldsymbol{S}(t-t_{i-1})$, $y'(t)\big|_{t_{i-1}} = y'(t_{i-1})\cdot \boldsymbol{S}(t-t_{i-1})$, and

$$\begin{aligned} v(t) = \big[&a_2 A_i^{\,2}/2 + a_1 A_i \cos(\phi_i)\sin(\omega_i(t-t_{i-1})) + a_1 A_i \sin(\phi_i)\cos(\omega_i(t-t_{i-1})) \\ &- a_2 A_i^{\,2}/2\cdot(\cos(2\phi_i)\cos(2\omega_i(t-t_{i-1})) - \sin(2\phi_i)\sin(2\omega_i(t-t_{i-1})))\big]\cdot \boldsymbol{S}(t-t_{i-1}) \end{aligned} \tag{A.68}$$

for the quadratic nonlinear static mapping $f(u(t)) = a_1 u(t) + a_2 u^2(t)$. The solution for the interval $t_{i-1} < t < \infty$ is given by Eq. A.69.

$$\begin{aligned} y(t) = &\frac{1}{2} a_2 A_i^{\,2}\cdot g_{20}(t-t_{i-1};\tau_1,\tau_2) + a_1 A_i \cos\phi_i \cdot g_{2s}(t-t_{i-1};\omega_i,\tau_1,\tau_2) \\ &+ a_1 A_i \sin\phi_i \cdot g_{2c}(t-t_{i-1};\omega_i,\tau_1,\tau_2) + \frac{a_2 A_i^{\,2}}{2}\sin 2\phi_i \cdot g_{2s}(t-t_{i-1};2\omega_i,\tau_1,\tau_2) \\ &- \frac{1}{2} a_2 A_i^{\,2}\cos 2\phi_i \cdot g_{2c}(t-t_{i-1};2\omega_i,\tau_1,\tau_2) + y(t_{i-1})\cdot g_{02}(t-t_{i-1};\tau_1,\tau_2) \\ &+ y'(t_{i-1})\cdot g_{12}(t-t_{i-1};\tau_1,\tau_2) \end{aligned} \tag{A.69}$$

Define $m = t - t_{i-1}$. Then $m \in (0,\infty)$ for $t \in (t_{i-1},\infty)$, and Eq. A.53 turns out to be

$$\tau_1\tau_2 \frac{d^2 y(m+t_{i-1})}{dm^2} + (\tau_1+\tau_2)\cdot\frac{dy(m+t_{i-1})}{dm} + y(m+t_{i-1}) = v(m+t_{i-1}) \tag{A.70}$$

Let $x(m) = y(m+t_{i-1})$. Then

$$\begin{aligned} \tau_1\tau_2 \frac{d^2 x(m)}{dm^2} + (\tau_1+\tau_2)\cdot\frac{dx(m)}{dm} + x(m) &= v(m+t_{i-1}) \\ &= \left\{a_1\cdot A_i \sin(\omega_i m+\phi_i) + a_2\cdot[A_i\sin(\omega_i m+\phi_i)]^2\right\}\cdot \boldsymbol{S}(0) \end{aligned} \tag{A.71}$$

with $x(0) = y(t_{i-1})\cdot \boldsymbol{S}(0)$ and $x'(0) = y'(t_{i-1})\cdot \boldsymbol{S}(0)$ as initial conditions.

Taking the Laplace transform of Eq. A.71 and rearranging terms gives

$$X(s)=\frac{V(s)}{(\tau_1 s+1)(\tau_2 s+1)}+\frac{(\tau_1+\tau_2+\tau_1\tau_2\cdot s)\cdot x(0)}{(\tau_1 s+1)(\tau_2 s+1)}+\frac{\tau_1\tau_2\cdot x'(0)}{(\tau_1 s+1)(\tau_2 s+1)} \tag{A.72}$$

where $X(s)$ was defined as before, and

$$\begin{aligned} V(s)=&\frac{a_2 A_i^{\,2}}{2}\cdot\frac{1}{s}+a_1 A_i\cos(\phi_i)\frac{\omega_i}{s^2+\omega_i^{\,2}}+a_1 A_i\sin(\phi_i)\frac{s}{s^2+\omega_i^{\,2}} \\ &-\frac{a_2 A_i^{\,2}}{2}\cdot\left(\cos(2\phi_i)\frac{s}{s^2+4\omega_i^{\,2}}-\sin(2\phi_i)\frac{2\omega_i}{s^2+4\omega_i^{\,2}}\right) \end{aligned} \tag{A.73}$$

Taking the inverse Laplace transform of Eq. A.72 after plugging Eq. A.73 into it gives

$$\begin{aligned} x(m)=&\mathscr{L}^{-1}\left[\frac{a_2 A_i^{\,2}}{2}\cdot\frac{1}{s}\cdot\frac{1}{(\tau_1 s+1)(\tau_2 s+1)}\right]+\mathscr{L}^{-1}\left[a_1 A_i\cos(\phi_i)\cdot\frac{\omega_i}{s^2+\omega_i^{\,2}}\cdot\frac{1}{(\tau_1 s+1)(\tau_2 s+1)}\right] \\ &+\mathscr{L}^{-1}\left[a_1 A_i\sin(\phi_i)\cdot\frac{s}{s^2+\omega_i^{\,2}}\cdot\frac{1}{(\tau_1 s+1)(\tau_2 s+1)}\right] \\ &-\mathscr{L}^{-1}\left[\frac{a_2 A_i^{\,2}}{2}\cos(2\phi_i)\cdot\frac{s}{s^2+4\omega_i^{\,2}}\cdot\frac{1}{(\tau_1 s+1)(\tau_2 s+1)}\right] \\ &+\mathscr{L}^{-1}\left[\frac{a_2 A_i^{\,2}}{2}\sin(2\phi_i)\frac{2\omega_i}{s^2+4\omega_i^{\,2}}\cdot\frac{1}{(\tau_1 s+1)(\tau_2 s+1)}\right] \\ &+x(0)\cdot\mathscr{L}^{-1}\left[\frac{(\tau_1+\tau_2+\tau_1\tau_2\cdot s)}{(\tau_1 s+1)(\tau_2 s+1)}\right]+x'(0)\cdot\mathscr{L}^{-1}\left[\frac{\tau_1\tau_2}{(\tau_1 s+1)(\tau_2 s+1)}\right] \end{aligned} \tag{A.74}$$

With the definitions of $g_{20}(t;\tau_1,\tau_2)$, $g_{2s}(t;\omega,\tau_1,\tau_2)$, $g_{2c}(t;\omega,\tau_1,\tau_2)$, $g_{02}(t;\tau_1,\tau_2)$, and $g_{12}(t;\tau_1,\tau_2)$ in Eqs. A.55 to A.59, we have,

$$\begin{aligned} x(m)=&\frac{1}{2}a_2 A_i^{\,2}\cdot g_{20}(m;\tau_1,\tau_2)+a_1 A_i\cos\phi_i\cdot g_{2s}(m;\omega_i,\tau_1,\tau_2)+a_1 A_i\sin\phi_i\cdot g_{2c}(m;\omega_i,\tau_1,\tau_2) \\ &+\frac{a_2 A_i^{\,2}}{2}\sin 2\phi_i\cdot g_{2s}(m;2\omega_i,\tau_1,\tau_2)-\frac{1}{2}a_2 A_i^{\,2}\cos 2\phi_i\cdot g_{2c}(m;2\omega_i,\tau_1,\tau_2) \\ &+x(0)\cdot g_{02}(m;\tau_1,\tau_2)+x'(0)\cdot g_{12}(m;\tau_1,\tau_2) \end{aligned} \tag{A.75}$$

Realizing that $x(m)=y(m+t_{i-1})$ and $t=m+t_{i-1}$, we have,

$$
\begin{aligned}
y(t) = y(m + t_{i-1}) = \frac{1}{2} a_2 A_i^{\,2} \cdot g_{20}(t - t_{i-1}; \tau_1, \tau_2) + a_1 A_i \cos\phi_i \cdot g_{2s}(t - t_{i-1}; \omega_i, \tau_1, \tau_2) \\
+ a_1 A_i \sin\phi_i \cdot g_{2c}(t - t_{i-1}; \omega_i, \tau_1, \tau_2) + \frac{a_2 A_i^{\,2}}{2} \sin 2\phi_i \cdot g_{2s}(t - t_{i-1}; 2\omega_i, \tau_1, \tau_2) \\
- \frac{1}{2} a_2 A_i^{\,2} \cos 2\phi_i \cdot g_{2c}(t - t_{i-1}; 2\omega_i, \tau_1, \tau_2) \\
+ y(t_{i-1}) \cdot g_{02}(t - t_{i-1}; \tau_1, \tau_2) + y'(t_{i-1}) \cdot g_{12}(t - t_{i-1}; \tau_1, \tau_2)
\end{aligned}
\tag{A.76}
$$

This gives the solution to the Hammerstein system with second order overdamped dynamics and quadratic nonlinear static gain for input sequence Case II.

IV. The Wiener system with second-order overdamped dynamics

This Wiener system can be written as

$$
\tau_1 \tau_2 \frac{d^2 v(t)}{dt^2} + (\tau_1 + \tau_2) \cdot \frac{dv(t)}{dt} + v(t) = u(t) \tag{A.77}
$$

and $y(t) = f(v(t))$, where, $f(v(t))$ can be any nonlinear static mapping relationship, and τ_1 and τ_2 are the time constants.

a. Case I

The sinusoidal input starting at any time changing point t_{i-1} can be written as $u(t) = [b_i + A_i \sin(\omega_i (t - t_{i-1}))] \cdot S(t - t_{i-1})$. The initial conditions for the intermediate output $v(t)$ at time t_{i-1} are $v(t)\big|_{t_{i-1}} = v(t_{i-1}) \cdot S(t - t_{i-1})$, and $v'(t)\big|_{t_{i-1}} = v'(t_{i-1}) \cdot S(t - t_{i-1})$.

The solution for $v(t)$ in the interval $t_{i-1} < t < \infty$ is given by Eq. A.78.

$$
\begin{aligned}
v(t) = b_i \cdot g_{20}(t - t_{i-1}; \tau_1, \tau_2) + A_i \cdot g_{2s}(t - t_{i-1}; \omega_i, \tau_1, \tau_2) \\
+ v(t_{i-1}) \cdot g_{02}(t - t_{i-1}; \tau_1, \tau_2) + v'(t_{i-1}) \cdot g_{12}(t - t_{i-1}; \tau_1, \tau_2)
\end{aligned}
\tag{A.78}
$$

where $g_{20}(t; \tau_1, \tau_2)$, $g_{2s}(t; \omega, \tau_1, \tau_2)$, $g_{02}(t; \tau_1, \tau_2)$, and $g_{12}(t; \tau_1, \tau_2)$ were defined in Eqs. A.55 to A.59.

After defining $m = t - t_{i-1}$, $m \in (0,\infty)$ for $t \in (t_{i-1},\infty)$. Then Eq. A.77 becomes

$$\tau_1\tau_2 \frac{d^2v(m+t_{i-1})}{dm^2} + (\tau_1+\tau_2)\cdot\frac{dv(m+t_{i-1})}{dm} + v(m+t_{i-1}) = u(m+t_{i-1}) \tag{A.79}$$

Let $x(m) = v(m+t_{i-1})$. Then

$$\tau_1\tau_2 \frac{d^2x(m)}{dm^2} + (\tau_1+\tau_2)\cdot\frac{dx(m)}{dm} + x(m) = v(m+t_{i-1}) = [b_i + A_i\sin(\omega_i m+\phi_i)]\cdot \boldsymbol{S}(0) \tag{A.80}$$

with $x(0) = v(t_{i-1})\cdot \boldsymbol{S}(0)$ and $x'(0) = v'(t_{i-1})\cdot \boldsymbol{S}(0)$ as initial condition.

Taking the Laplace transform of Eq. A.80 and rearranging terms gives

$$X(s) = \frac{U(s)}{(\tau_1 s+1)(\tau_2 s+1)} + \frac{(\tau_1+\tau_2+\tau_1\tau_2\cdot s)\cdot x(0)}{(\tau_1 s+1)(\tau_2 s+1)} + \frac{\tau_1\tau_2\cdot x'(0)}{(\tau_1 s+1)(\tau_2 s+1)} \tag{A.81}$$

where

$$X(s) = \mathscr{L}\{x(m)\} = \int_0^\infty x(m)\cdot e^{-sm}dm \tag{A.82}$$

$$U(s) = b_i\cdot\frac{1}{s} + A_i\cdot\frac{\omega_i}{s^2+\omega_i^{\,2}} \tag{A.83}$$

Taking the inverse Laplace transform of Eq. A.81 after plugging Eq. A.83 into it gives

$$\begin{aligned} x(m) = {} & \mathscr{L}^{-1}\left[b_i\cdot\frac{1}{s}\cdot\frac{1}{(\tau_1 s+1)(\tau_2 s+1)}\right] + \mathscr{L}^{-1}\left[A_i\cdot\frac{\omega_i}{s^2+\omega_i^{\,2}}\cdot\frac{1}{(\tau_1 s+1)(\tau_2 s+1)}\right] \\ & + x(0)\cdot\mathscr{L}^{-1}\left[\frac{(\tau_1+\tau_2+\tau_1\tau_2\cdot s)}{(\tau_1 s+1)(\tau_2 s+1)}\right] + x'(0)\cdot\mathscr{L}^{-1}\left[\frac{\tau_1\tau_2}{(\tau_1 s+1)(\tau_2 s+1)}\right] \end{aligned} \tag{A.84}$$

With the definitions of $g_{20}(t;\tau_1,\tau_2)$, $g_{2s}(t;\omega,\tau_1,\tau_2)$, $g_{02}(t;\tau_1,\tau_2)$, and $g_{12}(t;\tau_1,\tau_2)$ in Eqs. A.55 to A.59, we have,

$$\begin{aligned} x(m) = {} & b_i\cdot g_{20}(m;\tau_1,\tau_2) + A_i\cdot g_{2s}(m;\omega_i,\tau_1,\tau_2) \\ & + x(0)\cdot g_{02}(m;\tau_1,\tau_2) + x'(0)\cdot g_{12}(m;\tau_1,\tau_2) \end{aligned} \tag{A.85}$$

Since $x(m) = v(m+t_{i-1})$ and $m = t - t_{i-1}$

$$v(t) = v(m + t_{i-1}) = b_i \cdot g_{20}(t - t_{i-1}; \tau_1, \tau_2) + A_i \cdot g_{2s}(t - t_{i-1}; \omega_i, \tau_1, \tau_2) + v(t_{i-1}) \cdot g_{02}(t - t_{i-1}; \tau_1, \tau_2) + v'(t_{i-1}) \cdot g_{12}(t - t_{i-1}; \tau_1, \tau_2) \quad \text{(A.86)}$$

This gives the solution to the Wiener system with second order overdamped dynamics and quadratic nonlinear static mapping for input sequence Case I. Then, the response *y(t)* can be obtained by following different nonlinear static mapping relationships.

b. Case II

The sinusoidal input in any given interval $t_{i-1} \le t < t_i$ is given by

$$u(t) = A_i \sin(\omega_i \cdot (t - t_{i-1}) + \phi_i) \cdot \boldsymbol{S}(t - t_{i-1}) = [A_i \cos(\phi_i)\sin(\omega_i (t - t_{i-1})) + A_i \sin(\phi_i)\cos(\omega_i (t - t_{i-1}))] \cdot \boldsymbol{S}(t - t_{i-1}) \quad \text{(A.87)}$$

The initial conditions for the intermediate output at the time t_{i-1} are

$v(t)\big|_{t_{i-1}^+} = v(t_{i-1}) \cdot \boldsymbol{S}(t - t_{i-1})$ and $v'(t)\big|_{t_{i-1}^+} = v'(t_{i-1}) \cdot \boldsymbol{S}(t - t_{i-1})$.

The solution to *v(t)* for the interval $t_{i-1} < t < \infty$ is given by Eq. A.88,

$$v(t) = A_i \cos\phi_i \cdot g_{2s}(t - t_{i-1}; \omega_i, \tau_1, \tau_2) + A_i \sin\phi_i \cdot g_{2c}(t - t_{i-1}; \omega_i, \tau_1, \tau_2) + v(t_{i-1}) \cdot g_{02}(t - t_{i-1}; \tau_1, \tau_2) + v'(t_{i-1}) \cdot g_{12}(t - t_{i-1}; \tau_1, \tau_2) \quad \text{(A.88)}$$

where $g_{2s}(t; \omega, \tau)$, $g_{2c}(t; \omega, \tau_1, \tau_2)$, $g_{02}(t; \tau_1, \tau_2)$ and $g_{12}(t; \tau_1, \tau_2)$ were defined before. After defining $m = t - t_{i-1}$, $m \in (0, \infty)$ for $t \in (t_{i-1}, \infty)$, and $x(m) = v(m + t_{i-1})$, taking the Laplace transform, and rearranging the terms in the equation, we have

$$X(s) = \frac{U(s)}{(\tau_1 s + 1)(\tau_2 s + 1)} + \frac{(\tau_1 + \tau_2 + \tau_1\tau_2 \cdot s) \cdot x(0)}{(\tau_1 s + 1)(\tau_2 s + 1)} + \frac{\tau_1\tau_2 \cdot x'(0)}{(\tau_1 s + 1)(\tau_2 s + 1)} \quad \text{(A.89)}$$

where *X(s)* was defined as before,

$$U(s) = A_i \cos(\phi_i)\frac{\omega_i}{s^2 + \omega_i^2} + A_i \sin(\phi_i)\frac{s}{s^2 + \omega_i^2} \quad \text{(A.90)}$$

and $x(0) = v(t_{i-1}) \cdot S(0)$ and $x'(0) = v'(t_{i-1}) \cdot S(0)$.

Taking the inverse Laplace transform of Eq. A.89 after plugging Eq.A.90 into it gives

$$\begin{aligned} x(m) = {} & \mathcal{L}^{-1}\left[A_i \cos(\phi_i) \cdot \frac{\omega_i}{s^2 + \omega_i^2} \cdot \frac{1}{(\tau_1 s + 1)(\tau_2 s + 1)} \right] \\ & + \mathcal{L}^{-1}\left[A_i \sin(\phi_i) \cdot \frac{s}{s^2 + \omega_i^2} \cdot \frac{1}{(\tau_1 s + 1)(\tau_2 s + 1)} \right] \\ & + x(0) \cdot \mathcal{L}^{-1}\left[\frac{(\tau_1 + \tau_2 + \tau_1 \tau_2 \cdot s)}{(\tau_1 s + 1)(\tau_2 s + 1)} \right] + x'(0) \cdot \mathcal{L}^{-1}\left[\frac{\tau_1 \tau_2}{(\tau_1 s + 1)(\tau_2 s + 1)} \right] \end{aligned} \tag{A.91}$$

With the definitions of $g_{2s}(t;\omega,\tau_1,\tau_2)$, $g_{2c}(t;\omega,\tau_1,\tau_2)$, $g_{02}(t;\tau_1,\tau_2)$, and $g_{12}(t;\tau_1,\tau_2)$, we have

$$\begin{aligned} x(m) = {} & A_i \cos\phi_i \cdot g_{2s}(m;\omega_i,\tau_1,\tau_2) + A_i \sin\phi_i \cdot g_{2c}(m;\omega_i,\tau_1,\tau_2) \\ & + x(0) \cdot g_{02}(m;\tau_1,\tau_2) + x'(0) \cdot g_{12}(m;\tau_1,\tau_2) \end{aligned} \tag{A.92}$$

Since $x(m) = v(m + t_{i-1})$ and $m = t - t_{i-1}$,

$$\begin{aligned} v(t) = v(m + t_{i-1}) = {} & A_i \cos\phi_i \cdot g_{2s}(t - t_{i-1};\omega_i,\tau_1,\tau_2) + A_i \sin\phi_i \cdot g_{2c}(t - t_{i-1};\omega_i,\tau_1,\tau_2) \\ & + v(t_{i-1}) \cdot g_{02}(t - t_{i-1};\tau_1,\tau_2) + v'(t_{i-1}) \cdot g_{12}(t - t_{i-1};\tau_1,\tau_2) \end{aligned} \tag{A.93}$$

This gives the solution to the Wiener system with second order overdamped dynamics and quadratic nonlinear static mapping for input sequence Case II. Then, the response *y(t)* can be obtained by following different nonlinear static mapping relationships.

Acknowledgements

First and foremost, I would like to express my sincere thanks to my major professors; Dr. Huaiqing Wu and Dr. Derrick K. Rollins, Sr., for your understanding, encouragement, guidance, and support over my study and research in Statistics and Chemical Engineering at Iowa State University.

To my committee members, Dr. Morris, Dr. Gonzalez and Dr. Colver, I thank you for your help and services.

Special thanks go to Dr. Wolfgang H Kliemann in Department of Mathematics, Iowa State University for his helpful suggestions as to the simulation of the Brownian motion.

I acknowledge Nidhi, and Swee-Teng, for your help and insightful discussions. I would also like to thank my other group members; Stephanie, Aulia, Brie, Liza, and Sandra. Spending time with you is such a wonderful thing for me.

Finally, I am deeply grateful to my parents, my husband, Weihua, and my daughter, Victoria, without whose love and support, I could not have done this study. Also, thanks to all my friends who helped me these years.